COMMITTEE CERTIFICATION OF APPROVED VERSION

The committee for William Harrison Boylston, III certifies that this is the approved version of the following dissertation:

INVESTIGATING THE MOLECULAR BIOLOGY OF AGING AND EXTENDED LONGEVITY: PROTEOMIC AND GENOMIC ANALYSIS OF MOUSE LIVER

Committee:

_____
John Papaconstantinou, Ph.D., Chair

_____
Jeffrey P. Rabek, Ph.D.

_____
Giulio Taglialatela, Ph.D.

_____
Steven G.Widen, Ph.D.

_____
Philip T. Palade, Ph.D.

_____
Pamela L. Larsen, Ph.D.

_____
Cary Cooper, Ph.D.
Dean, Graduate School

INVESTIGATING THE MOLECULAR BIOLOGY OF AGING AND EXTENDED LONGEVITY: PROTEOMIC AND GENOMIC ANALYSIS OF MOUSE LIVER

by

William Harrison Boylston, III, B.A., B.S.

Dissertation
Presented to the Faculty of the University of Texas Graduate School of
Biomedical Sciences at Galveston
in Partial Fulfillment of the Requirements
for the Degree of

Doctor of Philosophy

Approved by the Supervisory Committee

Dr. John Papaconstantinou, Chair
Dr. Philip T. Palade
Dr. Pamela L. Larsen
Dr. Jeffrey P. Rabek
Dr. Giulio Taglialatela
Dr. Steven G. Widen

December 2004
Galveston, Texas

Key words: ER stress, SREBP, LXR, PPAR, CoQ, Obesity, Diabetes

To my fine parents, my dear brother, and my lovely wife.

ACKNOWLEDGEMENTS

I am also indebted to the members of the Papaconstantinou lab, both past and present, who have invested their time and patience in the interest of providing quality training and sound advice vital for my development as a research scientist. In particular, Dr. Jeffrey P. Rabek, over the years, has been both an insightful mentor and a trusted friend, and has guided and instructed me in acquiring essential laboratory techniques. I would also like to acknowledge Dr. Ching-Chyuan "Winston" Hsieh who devoted many hours educating me in protein analysis and provided insightful guidance through several projects. Dr. James DeFord was responsible for the initial generation of the microarray data, and provided much helpful insight into the statistical treatment and design of microarrays. Dr. Arpad Gerstner has been a supportive colleague and contributed through many discussions regarding the statistical and quantitative analysis of RT-PCR data. In addition, my good friend, Kash Choksi, is responsible for introducing me to the isolation and investigation of mitochondria, and will certainly continue to be a valued collaborator. Diane Strain provided expert clerical and administrative assistance in the preparation of manuscripts and the acquisition of laboratory supplies. Of course, my deepest gratitude extends to Dr. John Papaconstantinou who is directly responsible for my academic advancement through his constant support both intellectually and financially. More importantly, he has always been a magnificent mentor and an invaluable colleague, and has truly become a respected friend.

Finally, I would also like to acknowledge the remaining members of my exceptional doctoral committee, Drs. Giulio Taglialatela, Philip Palade, Steve Widen, and Pam Larsen, who have each contributed considerably to my development in soundly counseling me along the way. I am also indebted to them for their guidance and suggestions in the preparation this text. Their constant support and assistance has made all the difference at UTMB, and has helped establish the foundations for my future as a research scientist.

INVESTIGATING THE MOLECULAR BIOLOGY OF AGING AND EXTENDED LONGEVITY: PROTEOMIC AND GENOMIC ANALYSIS OF MOUSE LIVER

William Harrison Boylston, III, Ph.D.

The University of Texas Graduate School of Biomedical Sciences at Galveston, 2004

Supervisor: John Papaconstantinou

Recent advances in molecular gerontology have provided important clues about the fundamental biology of the aging process including the role of oxidative stress and the genetic basis of longevity. Progressive accumulation of oxidative damage to macromolecules is thought to underlie the aging-associated decline in physiologic function characteristic of the senescent phenotype. Mitochondria are a major intracellular source of reactive oxygen species (ROS); however, other organelles are also endogenous sources of oxyradicals and oxidants that can damage macromolecules. This investigation examines the relationship between aging and oxidative damage to ER resident proteins, which exist in a strongly oxidizing environment necessary for disulfide bond formation. In these studies, young and aged mouse liver homogenates were separated into enriched sub-cellular fractions, and the ER/mitochondrial fraction was resolved by 2-dimensional gel electrophoresis and then assayed for oxidative damage as indicated by protein carbonylation. MALDI/TOF analysis and N-terminal sequencing of these proteins identified BiP/Grp78, protein disulfide isomerase (PDI), and calreticulin as exhibiting a specific age-associated increase in carbonyl content. This increase in oxidative damage to critical ER proteins in aged liver strongly indicates an impairment in protein folding, disulfide cross-linking, and glycosylation which may significantly contribute to the functional decline observed in aging liver.

Providing evidence for the genetic basis of aging, several murine models demonstrate that longevity can be increased by mutations affecting endocrine signaling, particularly via the GH/IGF-1 axis. In this investigation of long-lived GH/IGF-1-

deficient mice, characteristic patterns of hepatic gene expression in $Pit1^{dw/dwJ}$ dwarf mice were revealed. Comparative microarray analysis of young and aged male livers was utilized to identify specific genes differentially expressed in $Pit1^{dw/dwJ}$ mice. Further examination of both male and female livers by real-time RT-PCR demonstrated striking transcriptional differences in $Pit1^{dw/dwJ}$ mice comprised of genes regulating cholesterol biosynthesis, fatty acid utilization, and lipoprotein metabolism. Affecting global energy homeostasis, this programmatic shift in hepatic expression may contribute to longevity by influencing bioenergetic and oxidative reactions occurring within mitochondria, ER, and peroxisomes. Intriguingly, these long-term patterns in metabolic gene expression in $Pit1^{dw/dwJ}$ livers mirror many transcriptional changes induced by caloric restriction and fasting, further implicating energy metabolism in longevity.

TABLE OF CONTENTS

LIST OF TABLES

LIST OF FIGURES

LIST OF ABBREVIATIONS

Apo A-IV	Apolipoprotein A-IV
β3AR	Beta-3 adrenergic receptor
BiP	Glucose-regulated protein 78
CoA	Coenzyme A
CoQ	Coenzyme Q
Cyp	Cytochrome P450
Daf	Dauer formation
ER	Endoplasmic reticulum
FAS	Fatty acid synthase
Fdps	Farnesyl diphosphate synthetase
G6P	Glucose-6-phosphate
G6Pase	Glucose-6-phosphatase
HMG-CoA	β-hydroxy-β-methylglutaryl Coenzyme A
HMGCR	HMG-CoA reductase
HMGCS	HMG-CoA synthase
IGF-1	Insulin-like growth factor 1
IGF-1R	Insulin-like growth factor 1 receptor
InRβ	Insulin receptor, beta subunit
Idi1	Isopentenyl-diphosphate delta isomerase
LXR	Liver X receptor
Mvd	Mevalonate diphosphate decarboxylase
PDI	Protein disulfide isomerase
PEPCK	Phosphoenolpyrophosphate carboxykinase
PGC-1α	Peroxisome proliferator-activated receptor gamma coactivator alpha
Pit1	Pituitary–specific transcription factor 1
PPAR	Peroxisome proliferator-activated receptor
Prop1	Prophet of Pit1
RXR	Retinoid X receptor
Sqle	Squalene epoxidase
SREBP	Sterol regulatory element binding protein
UPR	Unfolded protein response

CHAPTER I

INTRODUCTION

As I approve of a youth that has something of the old man in him, so I am no less pleased with an old man that has something of the youth. He that follows this rule, may be old in body, but can never be so in mind. Cicero

As a biological process which afflicts virtually all living organisms, aging is marked by a gradual physical and functional decline over time at the tissue, cellular, and molecular levels. Nevertheless, our scientific understanding of the fundamental basis of aging and senescence is still astoundingly vague and incomplete. With the recent advent of functional genomics and proteomics, however, the field of biogerontology has matured from a predominately descriptive, population-based endeavor to a far more molecular and mechanistic science. Distinguishing between the aged phenotype and aging-related pathologies has been a critical step in the advancement of our knowledge about aging as a biological process *per se*. In particular, the phenotypic traits of aging are exhibited by the population as a whole, whereas age-related disorders and diseases affect only a subset of the larger population (Kirkwood, 2002; Johnson et al., 1999). Research in molecular gerontology over the last decades has revealed that the aging process at the sub-cellular level is characterized by intrinsic deterioration and an accumulation of macromolecular damage which are reflected in the senescent population by declines in offspring production, physiological function, and survival rate with advancing age (Johnson et al., 1999). In light of these recent discoveries, one of the principal aims of modern gerontology is therefore to identify the primary genetic and epigenetic mechanisms which underlie the molecular biology of aging and predispose elderly individuals to be more susceptible to aging-related pathologies.

1

Over the past 25 years, a new era of gerontology has been ushered in by the discovery of long-lived genetic mutants in model organisms including *S. cerevisiae, C. elegans* and *D. melanogaster*, which have provided the first critical insights into the molecular basis of senescence and life-span determination (Nemoto and Finkel, 2004; Guarente and Kenyon, 2000). These model organisms are remarkably adaptable to research on aging based on their relative simplicity, short life-spans, fully-sequenced genomes, and well-characterized biology (Partridge and Gems, 2002a; Martin et al., 1996). These landmark discoveries demonstrated not only that genetic mutations can extend life-span, but can also modulate the biological and physiological processes underlying aging (Hasty et al., 2003).

The unveiling of genetic factors regulating aging and life-span also re-kindled a long-standing question among evolutionary biologists regarding the selective advantage of genes which regulate a biological process that typically occurs in the post-replicative phase of an organism's life (Hekimi and Guarente, 2003; Martin, 2000). Under the laws of natural selection, genes which diminish an organism's survival and reproductive fitness should be selected against, while those which extend life-span beyond reproductive fitness should have little selection pressure to remove them from the gene pool, as natural selection exerts its effects through the successful production of offspring.

In an attempt to explain these phenomena, there are three prevailing and complementary theories concerning the origins of aging and senescence which have been put forth by evolutionary biologists in the 20th century: the disposable soma, mutation accumulation, and antagonistic pleiotropy theories (Partridge and Gems, 2002b; Kirkwood and Austad, 2000). The 'disposable soma' theory centers on the distinction between germ-line and somatic cell maintenance, and an organism's distribution of resources for the preservation and surveillance of these cell types, as only germ-line mutations are passed on to successive generations (Kirkwood, 1977). In contrast, the 'antagonistic pleiotropy' theory asserts that genes conferring a selective advantage early in life while causing deleterious effects late in life will be maintained over evolutionary time as a result of successful reproduction occurring prior to the harmful effects imparted

2

by the pleiotropic allele. (Kirkwood and Austad, 2000; Williams, 1957). Similarly, the 'mutation accumulation' theory predicts that alleles with late-acting deleterious effects are subject to diminished selection pressure, since they have little effect on progeny production. Consequently, these deleterious alleles will be preserved randomly over evolutionary time, and thus appear polymorphically throughout the general population (Martin et al., 1996). Although evolutionary theories may help to explain the preservation and survival value of particular traits in the senescent population, and may also help to explain the existence of longevity-promoting genes, these theories do not directly address the molecular genetic mechanisms which underlie the biological and physiological processes of aging.

THE MOLECULAR BASIS OF AGING

While there is probably no single explanation for why organisms age, substantial and mounting evidence indicates that cumulative damage to multiple physiological systems serves as a primary causative factor in the biology of aging (Melov, 2000). It is widely accepted today that the accumulation of damage in somatic tissues is a principal factor leading to the age-related declines exhibited by a wide variety of living organisms including yeast, worms, flies, mice, and humans (Hasty et al., 2003). The intrinsic and extrinsic sources of this damage have been a central focus of research on aging in the 20th century. In 1956, Harman proposed a revolutionary theory on aging asserting that oxidative damage caused by free radicals is the primary cause of the degeneration associated with aging (Harman, 1956). Over the past decades, numerous studies have demonstrated age-associated damage to key macromolecules which ultimately leads to age-associated pathophysiologies (Finkel and Holbrook, 2000; Berlett and Stadtman, 1997; Ames et al., 1993). Presently, it is well established that oxidative damage to macromolecules including proteins, lipids, and nucleic acids serves as a fundamental basis for many of the age-associated declines observed at the cellular and organ levels (Levine and Stadtman, 2001). Reactive oxygen species (ROS) are inherently generated as a by-product of normal metabolism, and cells have consequently developed a number

of anti-oxidant defenses to combat these toxic radicals, as well as repair mechanisms aimed at reversing damage, and degradation pathways which eliminate damaged molecules from the cell (Johnson et al., 2000; Friguet et al., 2000; Cottrell et al., 2000). As a major source of intracellular ROS generation, mitochondria have taken center stage in the current interpretation of Harman's original 'free radical theory' of aging; consequently, the genetics, physiology, and biochemistry of this organelle have been the focus of much recent research. Today it is widely believed that alterations in metabolic rate and electron transport efficiency can lead to age-related physical declines and mortality by influencing mitochondrial production of free radicals and the consequent accumulation of damage to macromolecules (Barja, 2004; Hekimi and Guarente, 2003; Jazwinski, 2002; Gems et al., 2002; Barja, 2002; Osiewacz, 2002).

Notwithstanding the great importance of this theory, aging is an extremely complex and multi-factorial process, and there is substantial evidence to support other related, and equally plausible mechanisms underlying the molecular biology of aging. One clearly evident cause of aging results from the accumulation of mitochondrial and nuclear DNA mutations resulting from both environmental and intracellular sources (Golden and Melov, 2001; Kirkwood, 2000; Johnson et al., 1999). Characteristic changes in endocrine function and hormone production are also thought to be central to the development of the aged-phenotype (Tatar et al., 2003; Pedersen et al., 2001; Lamberts et al., 1997). Substantiating the proposed link between aging and metabolism, caloric restriction of widely diverse organisms including mammals is well established to extend life-span and slow the aging process (Dhahbi et al., 2004; Barja, 2004; Barger et al., 2003; Merry, 2002; Sohal, 2002).

The recent elucidation of evolutionarily conserved pathways which regulate life-span across diverse species has provided vast insight into the genetic and cellular mechanism which control aging (Partridge and Gems, 2002b; Kenyon, 2001; Guarente and Kenyon, 2000). Many of these genes are involved in endocrine pathways regulate metabolism, reproduction, and stress resistance (Tatar et al., 2003; Larsen et al., 1995; Larsen, 1993). First discovered in *C. elegans*, mutations in a conserved, insulin/IGF-1

4

like signaling pathway and its orthologs have been demonstrated to extend lifespan in diverse model organisms (Richardson et al., 2004; Hwangbo et al., 2004; Holzenberger et al., 2003; Bluher et al., 2003; Aigaki et al., 2002; Dominici et al., 2002; Dozmorov et al., 2002; Clancy et al., 2001; Flurkey et al., 2001; Lee et al., 2001; Barsyte et al., 2001; Kenyon, 2001; Larsen, 2001) . In mammals, GH regulates the hepatic production of IGF-1, and mutations affecting the pituitary production and release of GH has been shown to extend life-span in laboratory mice (Coschigano et al., 2003; Liang et al., 2003; Hauck et al., 2002; Flurkey et al., 2001; Coschigano et al., 2000). Two strains of hypopituitary mice with naturally occurring mutations affecting the GH/IGF-1 axis have also been reported to have extended longevity (Longo and Finch, 2003; Dominici et al., 2002; Dozmorov et al., 2002; Flurkey et al., 2001; Bartke et al., 2001; Asa et al., 2000).

In the past several years, great interest among molecular gerontologists has centered on investigating the mechanism by which GH and IGF-1 modulate mammalian life-span in these mice. With the advent of new technologies including DNA microarrays and proteomics, the dissection of the pleiotropic effects of aging and hypopituitarism has now begun to be accomplished on a genomic scale (Gems and McElwee, 2003; Weindruch et al., 2001). Consequently, the studies described herein utilize a discovery-based approach to explore the complex processes of aging and the molecular mechanism of longevity extension using mouse models, and provide new insights into the selective oxidative damage to proteins with aging, and support a metabolic model for the regulation of mammalian life-span.

CHAPTER II

CARBONYLATION OF ENDOPLASMIC RETICULUM CHAPERONE PROTEINS IN AGED MOUSE LIVER†

SUMMARY

Progressive accumulation of oxidative damage to macromolecules in aged tissues is thought to contribute to the decline in tissue function characteristic of the aged phenotype. Mitochondria are a major intracellular source of reactive oxygen species (ROS); however, other organelles are also endogenous sources of oxyradicals and oxidants which can damage macromolecules. We therefore sought to examine the relationship between aging and oxidative damage to ER resident proteins, which exist in a strongly oxidizing environment necessary for disulfide bond formation. In these studies, we have fractionated young and aged liver homogenates, resolved the proteins by 2-dimensional gel electrophoresis, assayed for oxidative damage as indicated by protein carbonylation, and identified BiP/Grp78, protein disulfide isomerase (PDI), and calreticulin as exhibiting an age-associated increase in oxidative damage. Increased carbonylation of these key proteins in aged liver suggests an age-associated impairment in protein folding, disulfide cross-linking, and glycosylation in the aged mouse liver.

INTRODUCTION

Increased oxidative damage to cellular macromolecules, particularly to DNA and proteins, has been demonstrated in normal aging and age-related diseases (Mandavilli et al., 2002; Golden et al., 2002; Hamilton et al., 2001; Finkel and Holbrook, 2000; Stadtman, 1992). Progressive accumulation of oxidative damage to macromolecules in aged tissues is thought to contribute to the decline in tissue function, characteristic of the aged phenotype (Beal, 2002; Sohal, 2002; Stadtman, 2001). An age-associated increase in oxidative damage to proteins has been reported in several model organisms in which

specific proteins have been shown to be particularly susceptible to these modifications (Beal, 2002; Sohal, 2002).

Mitochondria are a major source of reactive oxygen species (ROS) including superoxide anions, hydroxyl radicals, and hydrogen peroxide. Mitochondria isolated from aged rat livers have been shown to produce greater amounts of ROS (Barja, 2002; Barja, 1999). Several reports have linked the production of ROS and oxidative damage to the mitochondrial proteins aconitase and adenine nucleotide transporter (ANT) in aging Drosophila (Yan and Sohal, 1998; Yan et al., 1997). Other organelles, including lysosomes, peroxisomes, and the endoplasmic reticulum (ER) are also endogenous sources of oxyradicals and powerful oxidants which can damage macromolecules (Tu and Weissman, 2002; Mueller et al., 2002; Fewell et al., 2001; Tu et al., 2000). An age-associated accumulation of oxidative damage should therefore be seen not only in mitochondrial proteins, but also in resident proteins of other organelles and sub-cellular compartments.

Oxidative damage to proteins results in a variety of covalent modifications including the formation of lipid peroxidation adducts and disulfide cross-links, nitration of tyrosine residues, and carbonylation (Berlett and Stadtman, 1997). Protein carbonylation has been widely used as a measure of oxidative damage to tissues in a variety of organisms, and has been shown to increase in aged tissues and in age-associated diseases (Mandavilli et al., 2002) However, few proteins that are oxidized during the mammalian aging process have yet to be specifically identified. In these studies, we have isolated an ER/mitochondrial fraction from young and aged mouse liver homogenates, resolved the proteins by 2-dimensional gel electrophoresis, and identified several ER-resident proteins which exhibit an age-associated increase in oxidative damage, *i.e.*, carbonylation.

EXPERIMENTAL PROCEDURES

Animals and Tissue Harvest.

Young (3 month) and aged (24 month) male C57BL/6 mice from the National Institute on Aging colonies (Bethesda, MD) were obtained through the Charles River Laboratories (Wilmington, MA), maintained with a 12 hr. light/dark cycle and fed *ad libitum* on a standard chow diet for at least one week before use. The animals were sacrificed by decapitation, and the livers were harvested immediately, rinsed in ice-cold PBS, and then prepared for sub-cellular fractionation.

Sub-Cellular Fractionation.

All procedures were performed at 4° C. Livers were minced on ice and then homogenized in Buffer M (10 mM Tris-HCl, pH 7.4, 250 mM sucrose, 2 mM EDTA, 0.5 mM EGTA, 10 mM DTT) using a Potter-Elvehjem homogenizer. Nuclei and cellular debris were removed by centrifugation at $800 \times g$, three times for 20 min each. An ER/mitochondria enriched pellet was obtained by centrifugation of this clarified supernatant at $8000 \times g$ for 20 min, and then washed twice with Buffer M. Mitochondria were isolated from this pellet by ultracentrifugation using a modification of the technique described by Rajapakse. (Rajapakse et al., 2001). An ER enriched fraction was prepared from the post-mitochondrial supernatant by sedimentation at $30,000 \times g$ for 30 min. Shown below in Figure 1 is the differential centrifugation scheme utilized for the sub-cellular fractionation of mouse livers.

Protein Quantification and Electrophoresis.

The ER/mitochondrial pellets were solubilized in chilled 8 M urea, 4% CHAPS, 100 mM DTT. The protein content of all sub-cellular fractions was determined by the Bradford method (Bio-Rad) using BSA as standard. For single dimension SDS-PAGE analysis, proteins were mixed with 2X loading buffer (2% SDS, 5% beta-mercaptoethanol, 20 mM Tris-HCl, pH 8.8) [19], and analyzed on 4-20% polyacrylamide

Whole Tissue Homogenate

↓

(800 x *g*, 20 min, 4°C) 3x

Crude Nuclei & Cell Debris ←

(8000 x *g*, 20 min, 4°C) 3x

Crude Mitochondria

Supernatant   *Pellet*

30,000 x *g*, 30 min, 4°C   **30-60% Percoll Step Gradient**

Cytoplasm ←

Endoplasmic Reticulum   **Enriched Mitochondria**
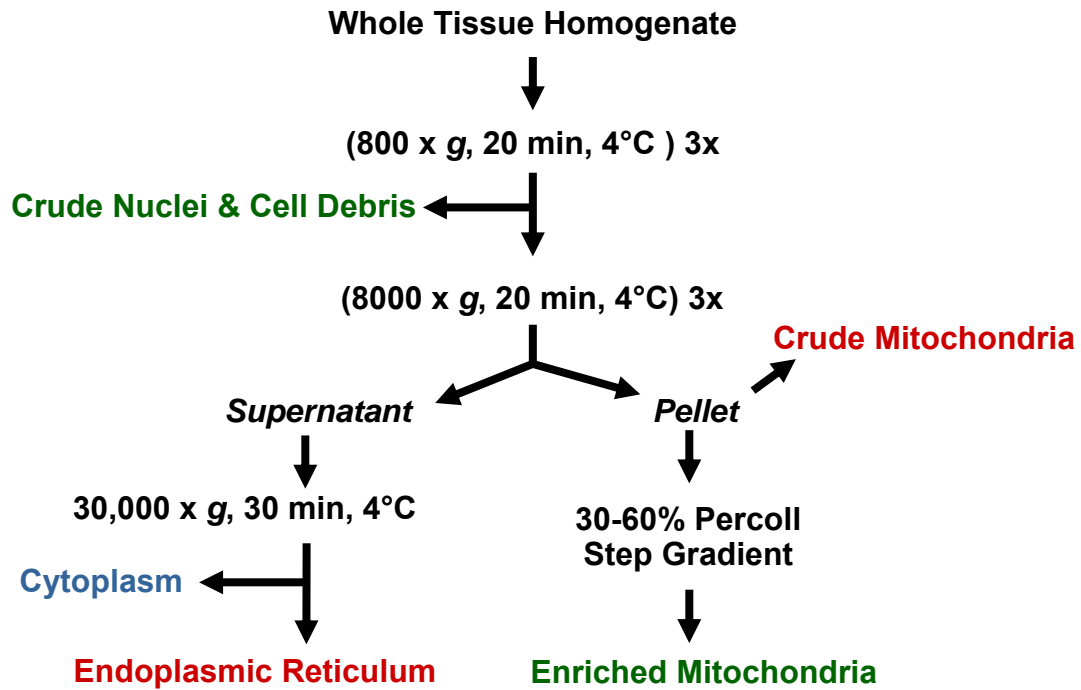
Figure 1: Sub-cellular Fractionation Method

gradient Tris-Glycine gels (Cambrex). For 2D gel analysis, protein samples were mixed with rehydration buffer (8 M urea, 2% CHAPS, 0.5% IPG buffer, 100 mM DTT) and applied to immobilized pH gradient strips (IPG strip, Amersham Biosciences) per manufacturer's recommendations. The sample and pH 3-10 IPG strips were rehydrated for 14 hours and then focused for 16,000 V-hr. Following isoelectric focusing, IPG strips were washed in SDS equilibration buffer (50 mM Tris-HCl, pH 8.8, 6 M urea, 30% glycerol, 2% SDS, 10 mg/ml DTT) and then resolved by SDS-PAGE on 4-20% gradient Tris-Glycine gels as above. After electrophoresis, gels were stained with SYPRO® Ruby for visualization of proteins. Alternatively, the gels were transferred electrophoretically to PVDF membranes (Immobilon P, Millipore), stained with SYPRO® Ruby and then analyzed by immunoblotting.

Detection of Oxidized Proteins.

Carbonylated proteins were labeled by derivatization of carbonyl groups with 2,4-dinitrophenylhydrazone by reaction with 2,4-dinitrophenylhydrazine, and then detected using an antibody specific to the DNP moiety (OxyBlot, Intergen Co., Purchase, NY). (Levine and Stadtman, 2001; Levine et al., 2000). For visualization, DNP-derivatized proteins were resolved by either one or two-dimensional SDS-PAGE, transferred to PVDF membranes, and identified by immunoblot analysis using specific antisera.

Immunoblot Analysis.

Western analysis was performed as described previously (An et al., 1996). Specific antibodies were obtained commercially; calnexin, cytochrome C, p38α, BiP/GRP78, and calreticulin (Santa Cruz Biotechnology); 70-kDa subunit of complex II (succinate dehydrogenase (SDH)/flavoprotein) (Molecular Probes); and protein disulfide isomerase (PDI) (Accurate Chemical and Scientific). Horseradish peroxidase conjugated secondary antibodies (Chemicon, Santa Cruz) were used for detection in conjunction with SuperSignal chemiluminescent substrate (Pierce), and Kodak X-Omat AR film was used to visualize specific antibody binding. Exposed films of immunoblots were digitized by using a MultiImage imaging system (Alpha Innnotech) and quantified by densitometry using AlphaEase software.

Identification of Oxidized Proteins

Electroblotted membranes or 2D gels were stained with Coomassie G-250. Proteins were excised, and submitted to the UTMB Protein Core Facility for either Edman sequencing or MALDI-TOF analysis. Protein identification was determined by submission of tryptic digest peptide masses obtained by mass spectrometry to the ProFound and ProSite databases. For protein identification following N-terminal sequence analysis, the first 10 amino acids were submitted to NCBI protein BLAST.

RESULTS

Characterization of ER/Mitochondrial Fraction.

Solubilized 8000 x g pellets were resolved by single dimension, gradient SDS-PAGE, and immunoblotting was used to detect organelle-specific (ER/mitochondrial) protein markers to assess the relative enrichment of these sub-cellular compartments. The relative immunoreactivity of calnexin (ER) and cytochrome C (mitochondria) demonstrates the enrichment of these marker proteins in the 8000 x g pellet, with very little cytoplasmic contamination (p38 MAPK). Additional fractionation of the ER/mitochondrial pellet produced further enrichment of PDI, calnexin and BiP/GRP78 in the 30,000 x g ER pellet, and of the 70 kDa subunit of succinate dehydrogenase in the Percoll-purified mitochondrial fraction (Fig. 2B). The 8000 x g ER/mitochondrial fraction obtained from young and aged mouse livers was assayed for oxidative damage, *i.e.,* protein carbonylation. By immunoblot analysis of derivatized total hepatic proteins (Fig 3), a significant increase in the carbonylation of ER/mitochondrial resident proteins was observed in aged liver.
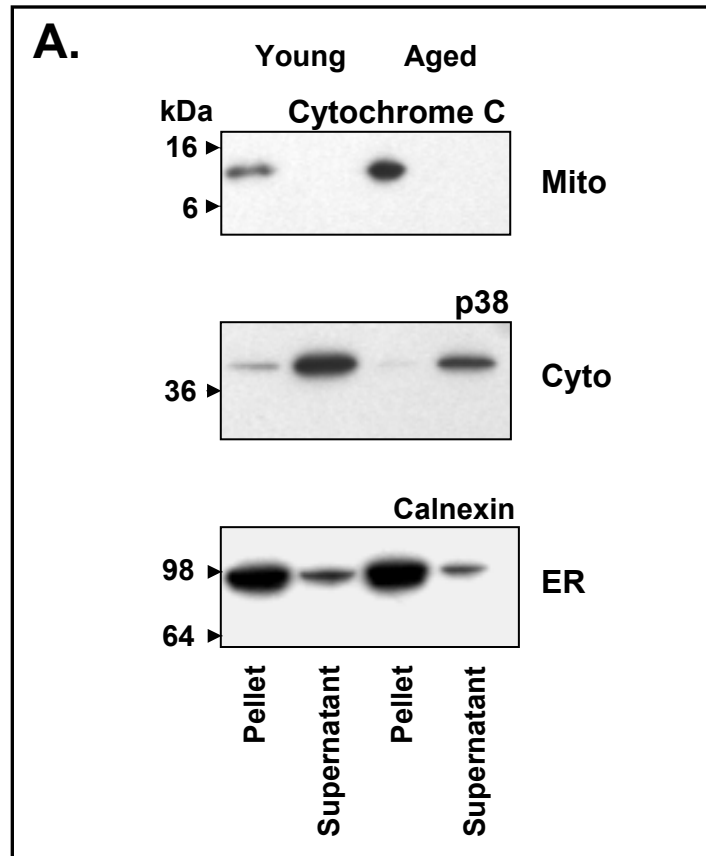
Figure 2A: Immunoblot Analysis of Organelle Marker Proteins from Livers of Young and Aged Male C57BL/6 Mice

Cytoplasmic (8000 x g supernatant) and ER/mitochondrial (pellet) proteins (15 μg) from young and aged mouse liver were electrophoresed on 4-20% SDS-PAGE gels. Immunoblot analysis was performed with antisera specific for cytochrome C (mitochondrial), p38 MAPK (cytoplasmic), and calnexin (ER). Molecular weight markers are indicated on the left side of each panel.
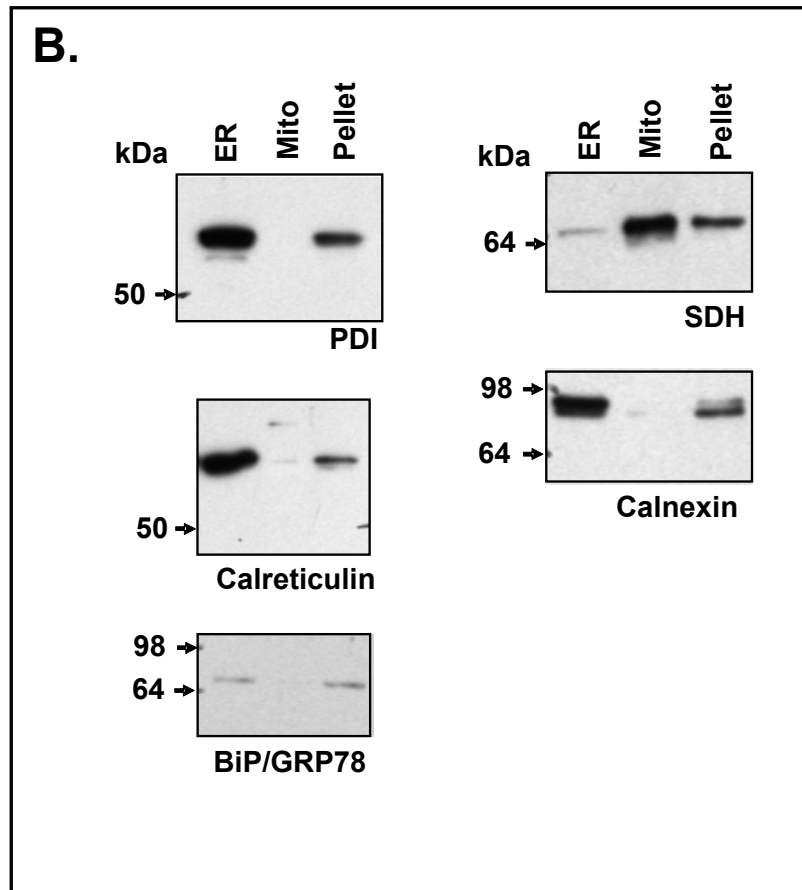
Figure 2B: Carbonylated Proteins Are Localized to the Endoplasmic Reticulum.

Mixed ER/mitochondrial pellet, ER, and mitochondrial (see Experimental Procedures) fractions (15μg) from young mouse liver were electrophoresed on 4-20% SDS-PAGE gels. Immunoblot analysis was performed with antibodies specific for additional mitochondrial (70-kDa SDH subunit) and ER (calnexin) marker proteins, and also with BiP/Grp78, calreticulin, and PDI antibodies. The relevant molecular weight markers are indicated by arrowheads.
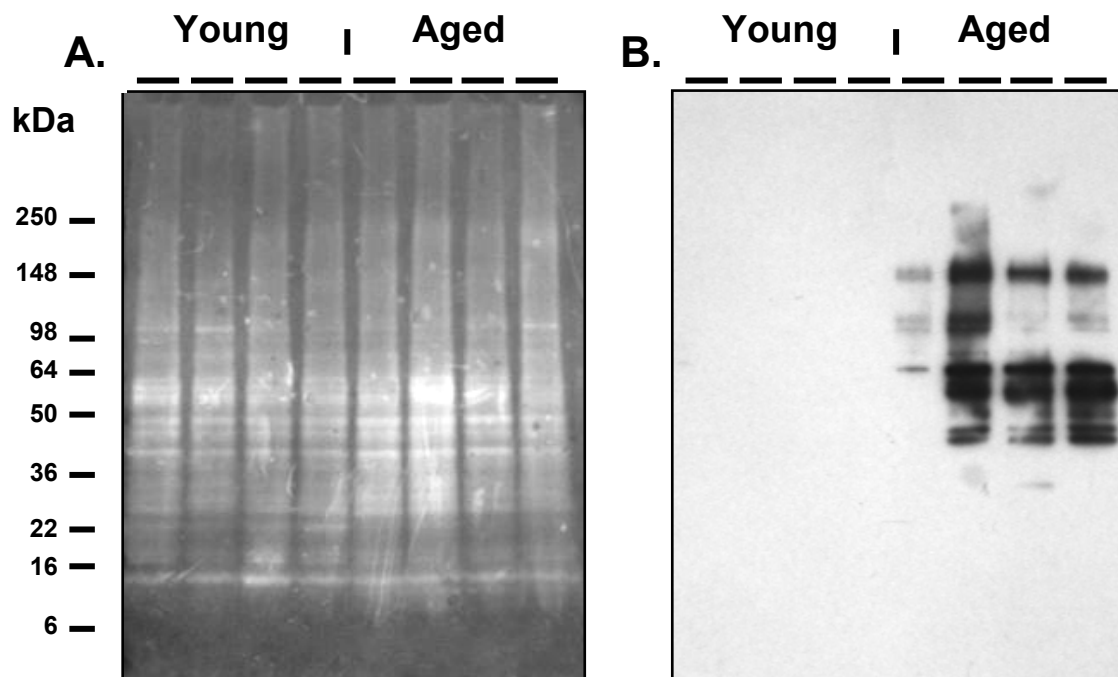
Figure 3: Detection of Carbonylated Proteins of the ER/Mitochondrial Fraction of Livers from Young and Aged Male C57BL/6 Mice.

ER/mitochondrial proteins (15µg) were derivatized with DNP, resolved by electrophoresis on 4-20% SDS-PAGE gels and electrotransferred to PVDF membranes. The membranes were stained with Sypro Ruby for total protein (Panel A), and then used for immunoblot analysis with DNP-specific primary antisera (Panel B).

Analysis of oxidative damage to ER/mitochondrial proteins.

To analyze the increased oxidative damage to aged liver proteins, we compared the pool levels of total proteins with the pattern of carbonylated proteins in young and aged mouse livers by 2D gel electrophoresis and Western blot analysis. Figure 4 depicts a representative example of the 2D pattern of total proteins (SYPRO Ruby) and of carbonylated proteins detected by the anti-DNP antibody. Within the detection limits of the assay, the 2D analyses show only a single carbonylated protein (BiP/Grp78) in livers of young mice, and also show a significant increase in the number of carbonylated

14

proteins in aged livers. Direct comparison of the SYPRO Ruby staining pattern (total
protein) with the Western (anti-DNP) pattern allows correlation of the encircled
immunoreactive proteins (carbonylated) with specific protein spots visible on the SYPRO
Ruby stained membranes (Fig 4).
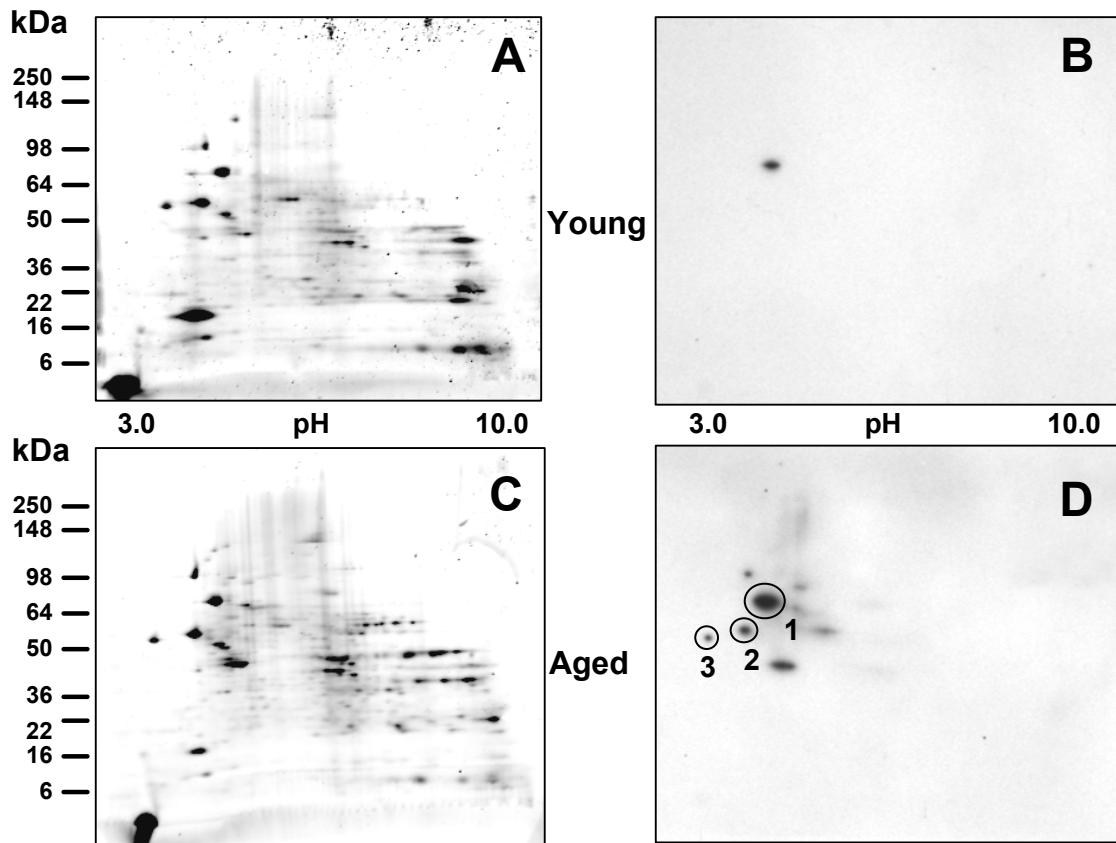
**Figure 4: Two-Dimensional Gel Analysis of Carbonylated Proteins from Liver
ER/Mitochondria of Young and Aged Mice.**

Solubilized ER/mitochondrial proteins from young (A, B) and aged (C, D) were
derivatized with DNP. Following 2-D gel electrophoresis and transfer to PVDF
membranes, total protein was visualized by fluorescent staining (Sypro Ruby), and the
derivatized proteins were detected using an anti-DNP specific antibody. The left panels
(A, C) show the total protein; while the right panels (B, D) indicate the
immunoreactive/carbonylated proteins on the same membrane.

Identification and Analysis of Carbonylated Proteins.

At least three proteins (Fig. 4D) were consistently observed to show increased carbonylation in aged mouse livers (N=3). These proteins were excised from ER/mitochondrial protein 2D gels, and Edman degradation of the 10 N-terminal amino acids yielded sequences with 100% identity to the published sequences of murine BiP, protein disulfide isomerase (PDI), and calreticulin proteins (Table 1). These proteins are ER-resident proteins which play critical roles in the proper folding, glycosylation, and transmembrane transport of nascent ER proteins. Additionally, these ER-resident proteins are central to the Unfolded Protein Response (UPR) of the ER, which activates cellular stress signaling pathways and protein degradation (Ma and Hendershot, 2001). The alignment of our amino-terminal peptides with the full-length proteins is consistent with proteolytic processing of an N-terminal localization sequence on ER-targeted precursor proteins following import into the ER. The identities of BiP, PDI and calreticulin were also confirmed by MALDI/TOF analysis (data not shown).

Table 1: Identification of Age-Specific Carbonylated Proteins

Spot*	Protein	Alignment	Accession Number[†]
1	Bip/GRP-78	MMKFTVVAALLLLGAVRAEEEDKKEDVGTWG EEEDKKEDVG	P20029
2	PDI	MLSRALLCLALAWAARVGADALEEEDNVLVLK DALEEEDVVL	P09103
3	Calreticulin	MLLSVPLLLGLLGLAAADPAIYFKEQFLDGDAW DPAIYFKEQF	NP_031617.1

* Number corresponds to spot marked in Figure 4D
[†] SwissProt or NCBI Accession Number

Since oxidatively modified proteins are targeted for degradation, we examined the protein abundance of each of these carbonylated proteins in young and aged mouse livers.

The immunoblot results (Figure 5) confirm that BiP, PDI and calreticulin are indeed present in the ER/mitochondrial fraction, and that there is no significant change in the protein pool of calreticulin or PDI with aging. However, the abundance of BiP was shown to decrease significantly with aging. These results suggest that the rate of either degradation or replacement of carbonylated ER chaperone proteins may not be sufficient to remove these damaged proteins from the pool.
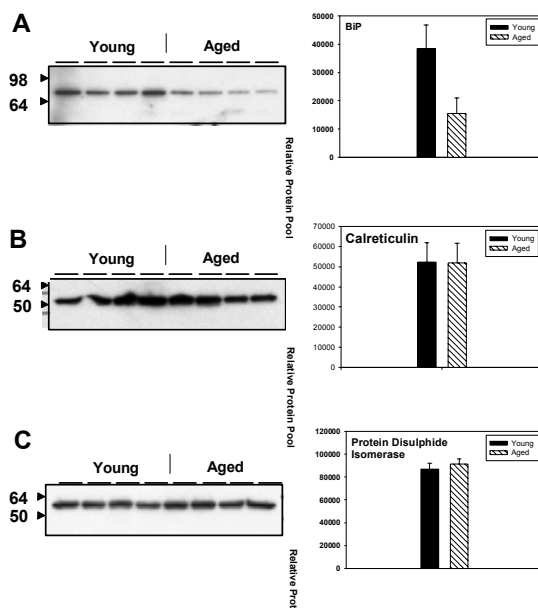
Figure 5: Protein Abundance of Bip, PDI and Calreticulin in Young and Aged Mouse Liver ER

ER/mitochondrial protein fractions (15 μg) from four young and four aged mouse livers were resolved by SDS-PAGE on 4-20% gradient gels and transferred to PVDF membranes. The relative abundance of the three proteins identified N-terminal sequencing was determined by immunoblotting using specific antisera: (A) BiP; (B) calreticulin, and (C) protein disulfide isomerase. The relevant molecular weight markers are indicated on the left side of each figure. The data are presented in the graphs to the left of each Western (mean ± S.D.).

As an additional confirmation of the identity of these proteins, ER/mitochondrial proteins from aged liver were derivatized with DNP, resolved by 2D electrophoresis, and then transferred to PVDF membranes. The same membrane was stained with SYPRO Ruby for total protein, and then used for immunoblotting with both anti-DNP and anti-PDI anti-sera. The results shown in Figure 6 confirm that the spot identified as PDI (arrow head) in the stained gel (Panel A) corresponds exactly to the spot identified as PDI by Western analysis (Panel C) and shown to be carbonylated (Panel B).
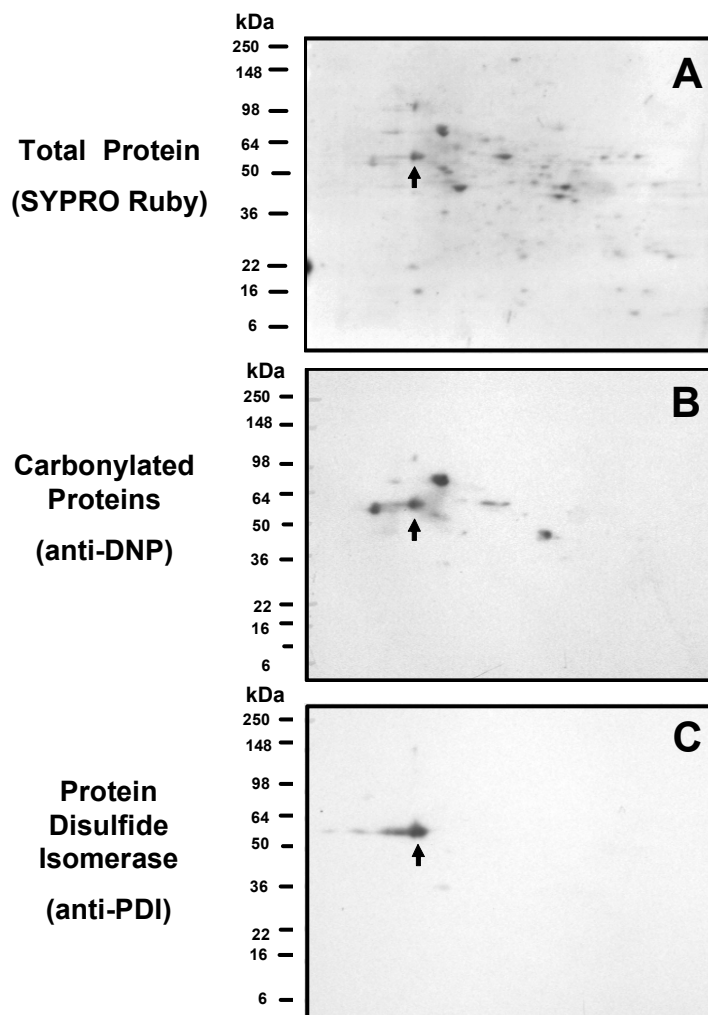
Figure 6: Two-dimensional Immunoblot Confirmation of Carbonylated PDI

     ER/mitochondrial proteins from an aged mouse liver were derivatized with DNP to identify carbonylated proteins, resolved by 2D gel electrophoresis, and transferred to PVDF membranes. The membrane was first stained with SYPRO Ruby blot stain to detect total protein (A), subjected to Western analysis using DNP-specific antisera to detect carbonylated proteins (B), and finally probed by Western analysis using PDI-specific antisera to detect PDI (C). The arrowhead indicates the location of PDI in each panel. Molecular weight standards are shown to the left.

The oxidized proteins identified from the ER/mitochondria pellet are all resident proteins of the ER. To demonstrate their localization in the ER, rather than the mitochondria, purified ER and mitochondrial fractions were subjected to immunoblot analysis using BiP, calreticulin, and PDI specific antibodies, and also antibodies specific for calnexin (ER marker) and the 70-kD subunit of succinate dehydrogenase/Complex II (mitochondrial marker). The analysis using calnexin and the 70-kD subunit demonstrate a high degree of enrichment for the ER and mitochondrial fractions, respectively (Figure 2B). Immunoblot analysis of the fractions using BiP, calreticulin, and PDI antibodies illustrates that these proteins are indeed enriched in the ER fraction.

DISCUSSION

We have shown by protein carbonyl assay that oxidative damage to critical ER proteins increases in the aged mouse liver. Carbonylated proteins have been reported to be indicators of oxidative damage, to increase with age, and to significantly impair the function of such oxidized proteins (Beal, 2002; Sohal, 2002; Barja, 2002; Barja, 1999; Tien et al., 1999; Berlett and Stadtman, 1997). For example, the selective carbonylation of aconitase and ANT in aged muscle mitochondria affects their enzymatic and functional activities, and thereby may contribute to the development of mitochondrial dysfunction in aged tissue (Yan and Sohal, 1998; Yan et al., 1997). Similarly, the age-associated increase in carbonylation of specific ER resident proteins, BiP, PDI, and calreticulin (observed in the present study) suggests that protein folding, disulfide bond formation and glycosylation may be compromised in aged mouse liver. Our results also suggest that ER-chaperone proteins may be more susceptible to age-associated oxidative damage, and that protein carbonylation in the aged ER may affect a specific subpopulation of ER proteins. This accumulation of oxidative damage to ER chaperones could result in organellar (ER) dysfunction, and thus contribute to the age-associated decline in tissue function. Carbonylated proteins cannot be repaired; they are either removed by proteolytic degradation or accumulate as damaged or unfolded proteins (Stadtman and Levine, 2000). An inability to target oxidized proteins for proteolysis would increase the

19

cellular content of oxidatively modified proteins whose activities may be diminished or even abolished. (Esposito et al., 1999). We propose that oxidative damage to the chaperone proteins such as BiP, PDI and calreticulin may accelerate the accumulation of misfolded proteins, and thus play a key role in age-associated decline in tissue function. This increase in oxidative damage to chaperones may induce age-related dysfunction of the protein folding processes associated with these proteins. Protein misfolding has been linked to the pathogenesis of many age-associated, neurodegenerative disorders, including Parkinson's, Alzheimer's, Huntington's and amyotrophic lateral sclerosis (Rakhit et al., 2002; Mouradian, 2002). The oxidative modification of proteins is also implicated in the etiology and progression of aging itself (Sohal et al., 2002; Sohal, 2002; Drew and Leeuwenburgh, 2002; Cadenas and Packer, 1999; Melov et al., 1999; Tien et al., 1999). An important factor in the generation of biochemical stress processes, organellar dysfunction, and diseases of protein misfolding may be the consequence of impaired quality control mediated by ER chaperone proteins (Ma and Hendershot, 2002; Ma and Hendershot, 2001).

The expression of ER chaperone proteins is generally up-regulated under conditions of cellular stress. This response to stress is especially relevant to the aging process in which tissues exhibit characteristics of chronic stress. Our studies show that increased carbonylation of BiP, PDI, and calreticulin is endogenous in aged mouse liver. Previous studies have shown that aging tissues develop a state of chronic stress even in the absence of an external/environmental challenge (Hsieh et al., 1998). The age-related elevation in oxidative damage to critical ER proteins may contribute to the state of chronic oxidative stress in aged mouse liver through activation of the UPR.

Approximately one-third of all proteins are translocated into the ER where they undergo post-translational modifications, folding and oligomerization (Gething, 2004). The ER is the site where nascent membrane and secretory proteins fold, assemble and form disulfide bonds. Thus, any age-associated effects on the structure and function of ER-resident chaperones could affect protein processing efficiency (quality control) and result in a decline in tissue function.

The proper conformational maturation of nascent proteins is a complex process mediated by ER chaperones, and is termed ER quality control (Gething, 2004; Kopito, 1997). Protein misfolding is a factor in aging, and this study clearly demonstrates an age-associated oxidation of ER chaperones which may adversely affect their quality control. Only proteins that attain their native conformation are transported through the ER membrane; those that fail to fold or assemble properly are translocated to the cytosol for proteasomal destruction or they accumulate as misfolded proteins (Ma and Hendershot, 2002; Ma et al., 2002; Parodi, 2000). Our studies have shown that the major ER chaperones BiP, PDI and calreticulin accumulate as carbonylated proteins in aged mouse liver. Furthermore, Western analyses show that the BiP protein levels are decreased by ~50% while PDI and calreticulin levels do not change. These data are consistent with an age-associated decline in ER protein folding and surveillance.

It has been shown that life span-extending dietary restriction significantly decreases the BiP mRNA and protein levels by 50-70% in livers of long-lived female hybrid C3B10RF1 mice (Dhahbi et al., 1997). In young and aged energy-restricted mice, hepatic expression of Erp57 (37%), GRP170 (51%), ERp72 (43%), calreticulin (54%) and calnexin (23%) was significantly and specifically decreased. These studies link the life span extension mechanisms activated by caloric restriction to the chaperone activity of the ER, and strongly suggest that the misfolded protein syndromes of aging tissues might be caused by the failure of the ER-chaperone machinery. Our studies, then, suggest that the level of protein carbonylation may be associated with the physiological decline associated with aged liver.

ACKNOWLEDGEMENTS

CHAPTER III

ALTERED CHOLESTEROLOGENIC AND LIPOGENIC TRANSCRIPTIONAL PROFILES IN AGING SNELL DWARF (*PIT1$^{DW/DWJ}$*) LIVER†

SUMMARY

Several murine models demonstrate that mammalian longevity can be increased by single gene mutations affecting endocrine signaling, particularly via the GH/IGF-1 axis. In this study of long-lived GH-deficient mice, age-related patterns in hepatic gene expression characteristic of Snell (*Pit1$^{dw/dwJ}$*) dwarf mice are identified. Comparative microarray analysis of young and aged male livers was performed to discover specific genes differentially expressed between *Pit1$^{dw/dwJ}$* and control mice. Further examination by real-time RT-PCR of both male and female animals confirmed that transcripts encoding HMG-CoA synthase-1, HMG-CoA reductase, farnesyl diphosphate synthase, isopentenyl pyrophosphate isomerase, mevalonate decarboxylase, squalene epoxidase, lanosterol demethylase, malic enzyme, and apolipoprotein A-IV were significantly decreased in *Pit1$^{dw/dwJ}$* livers at both 3-5 and 24-28 months of age. In contrast, transcripts encoding the β3-adrenergic receptor, lipoprotein lipase, PPARγ and the very low-density lipoprotein receptor (homolog) were increased significantly and persistently in dwarf livers relative to age- and gender-matched controls. These studies reveal enduring transcriptional differences characteristic of *Pit1$^{dw/dwJ}$* dwarf mice involving genes which regulate cholesterol biosynthesis, fatty acid metabolism, and lipoprotein homeostasis. Linked to global energy metabolism, this stable shift in hepatic gene expression may contribute to longevity determination by influencing particular metabolic functions often compartmentalized within the mitochondrion and peroxisome; further this metabolic shift may also parallel many transcriptional changes induced by caloric restriction.

INTRODUCTION

Genetic mutations which influence adult longevity in distantly related species have revealed striking parallels in the molecular basis of life-span determination. Recently, mutations in a conserved IGF-1/insulin-like endocrine pathway have been demonstrated to increase life-span in yeast, worms, flies, and mice (Hekimi and Guarente, 2003; Aigaki et al., 2002; Clancy et al., 2001; Guarente and Kenyon, 2000). The extension of adult life-span by single gene mutations in orthologous signaling pathways strongly indicates that evolutionarily conserved mechanisms may regulate longevity.

Similar to long-lived *C. elegans* and *Drosophila* mutants with decreased IGF-1/insulin-like signaling, a number of mouse models with GH/IGF-1/insulin deficiencies also exhibit significant increases in life-span. With maximum life-spans 40-65% longer than wild-type mice, homozygous *Pit-1* (Snell) and *Prop-1* (Ames) mutants are hypopituitary dwarf mice with combined anterior pituitary hormone deficiencies in growth hormone (GH), thyroid stimulating hormone (TSH), and prolactin (Tatar et al., 2003; Parks et al., 1999). Secondary to the GH and TSH deficiencies, these long-lived mice have decreased circulating IGF-1 and insulin levels, and serve as important genetic models of extended longevity in mammals (Tatar et al., 2003; Flurkey et al., 2001). Diminished GH/IGF-1/insulin signaling is also thought to underlie the endocrine regulation of longevity in growth hormone receptor/binding protein (GHR/BP) knockout mice which live longer than either heterozygote or wild-type mice (Coschigano et al., 2003; Miller et al., 2002; Coschigano et al., 2000). Complete inactivation of the IGF-1 receptor in mice results in embryonic lethality; and interestingly, only female heterozygous IGF-1 receptor knockout mice demonstrate a statistically significant increase in life-span, living 33% longer than wild-type mice (Holzenberger et al., 2003). Similarly, tissue-specific disruption of the insulin receptor in adipocytes extends life-span in mice by 18% (Bluher et al., 2003). While several mechanisms have been implicated, including enhanced stress resistance and changes in energy metabolism, the fundamental molecular endocrinology underlying the increased longevity of murine models with

23

diminished GH/IGF-1/insulin signaling is still little understood (Tatar et al., 2003; Longo and Finch, 2003; Johnson et al., 1999).

Gene expression profiling now allows genomic insight into the complex molecular biology of aging and senescence, and has provided an essential foundation for better understanding the genetic mechanisms regulating longevity (Anisimov and Boheler, 2003; Prolla, 2002; Tollet-Egnell et al., 2001). A number of transcriptional profiling studies of the aging process have linked changes in energy metabolism, anti-oxidant defense, and stress resistance to both delayed aging and increased longevity (Sreekumar et al., 2002; Clancy et al., 2002; Kayo et al., 2001; Weindruch et al., 2001). In contrast to genetic manipulation, extrinsic factors such as caloric restriction (CR) also extend life-span and delay aging in distantly related model organisms (Knauf et al., 2002; Furuyama et al., 2002; Lee et al., 2002; Merry, 2002; Miller et al., 2002; Pletcher et al., 2002; Rogina et al., 2002; Roth et al., 2002; Lin et al., 2001; Kayo et al., 2001; Weindruch et al., 2001; Cao et al., 2001). Recent microarray analysis of cardiac muscle in aging mice demonstrated a metabolic shift in gene expression from fatty acid to carbohydrate utilization in the aged heart, however, caloric restriction (CR) initiated during middle age prevented many of these transcriptional changes, and preserved a pattern of cardiac gene expression which favors fatty acid oxidation (Lee et al., 2002). New evidence suggests that life-span extending mutations and extrinsic factors influencing longevity may share common molecular mechanisms through the regulation of parallel genes and pathways (Tatar et al., 2003; Longo and Finch, 2003; Jaenisch and Bird, 2003). Diminished insulin/IGF-1 signaling is thought to mimic caloric restriction via altering energy metabolism and enhancing stress resistance; however, the particular genetic and epigenetic mechanisms which collectively interact to modulate chronological life-span are currently unknown.

Genomic approaches applied to long-lived mutants have been invaluable in identifying and characterizing the genetic pathways regulating life-span in *C. elegans* via an orthologous IGF-1/insulin-like pathway (Murphy et al., 2003; Gems and McElwee, 2003). Similarly, microarray analyses of hepatic gene expression using several murine

longevity models with deficiencies in GH/IGF-1/insulin signaling have begun to reveal transcriptional changes which may be involved in evolutionarily-conserved genetic programs regulating mammalian life-span (Murakami et al., 2003; Miller et al., 2002; Dozmorov et al., 2002; Dozmorov et al., 2001). However, these initial studies were designed to generate limited transcriptional profiles for these GH-deficient dwarf mice, screening only a relatively small number of candidate genes. With over 30,000 unique murine transcripts currently recognized, many thousands of genes specifically affected by GH/IGF-1/insulin deficiency and potentially involved in the extended longevity of these mice have yet to be examined.

The liver is the principal organ regulating the synthesis, availability, and storage of essential metabolic intermediates for use by brain, heart, muscle, and adipose tissue. GH, insulin/IGF-1, and glucagon are the primary hormones regulating long-term carbohydrate and fatty acid metabolism in the liver. The integrated control of hepatic glucose and lipid metabolism plays a central physiological role in whole-body energy metabolism. These coordinated biosynthetic and metabolic pathways are regulated at several levels, but transcriptional activation of specific target genes serves as the primary mechanism for long-term control of hepatic energy metabolism (Foufelle and Ferre, 2002). Genes now known to be regulated at the transcriptional level by GH action include the GH receptor, IGF-1, cytochrome P450 enzymes, the pheromone-binding major urinary proteins (MUPs), serine protease inhibitor 2.1, and the prolactin receptor (Olsson et al., 2003). Administration of GH to hypophysectomized rodents is known to exert profound effects on hepatic lipoprotein production, LDL receptor expression, and lipoprotein lipase activity (Frick et al., 2001). Similarly, chronic over-expression of bovine growth hormone (bGH) in transgenic mice results in elevated serum cholesterol, diminished serum triglycerides, decreased hepatic fatty acid production, hyperinsulinemia, and insulin resistance with relatively normal glucose tolerance. (Olsson et al., 2003; Frick et al., 2001).

In this study, specific patterns of hepatic gene expression associated with aging and decreased GH/insulin/IGF-1 signaling in long-lived Snell dwarf mice are identified.

25

To characterize hepatic gene expression in young and aged $Pit1^{dw/dwJ}$ mice, microarray analysis of 12,422 murine transcripts was performed using total RNA isolated from young and aged livers of male control and $Pit1^{dw/dwJ}$ dwarf mice. To more closely examine age-independent differences indicated by microarray, real-time RT-PCR amplification was used to quantify selected transcripts from individual hepatic cDNA libraries constructed from both male and female livers. These studies provide a greatly expanded survey of hepatic gene expression in both young and aged $Pit1^{dw/dwJ}$ mice, reveal specific transcriptional differences associated with both the 'normal' aging process and with the combined pituitary hormone deficiencies of long-lived dwarf mice, and are corroborated by real-time RT-PCR amplification of RNA isolated from over thirty individual mice. The identification of age- and gender-independent patterns of gene expression in young and aged $Pit1^{dw/dwJ}$ livers provides new insight into the complex alterations in hepatic gene expression induced by the hypopituitarism of these long-lived mammals, and may serve to further elucidate the complex molecular endocrinology underlying longevity extension in GH/IGF-1/insulin-deficient animal models.

EXPERIMENTAL PROCEDURES

Animals

Figure 1: Male $Pit1^{dw/dwJ}$ **Snell dwarf (right) and wild-type littermate control at 6 months of age.**

Snell dwarf mice used in this study consisted of $Pit1^{dw/dwJ}$ compound heterozygotes bred and housed at The Jackson Laboratory. These mice are the F1 progeny of bidirectional mating of C3H/HeJ-$Pit1^{dwJ/+}$ and DW/J-$Pit1^{dw/+}$ mice, designated C3H/HeJ × DW/J F1, or C3DW mice. Non-dwarf mice produced by this cross (+/+, +/dw, and +/dw^J) are indistinguishable by either gross phenotype or lifespan, and were therefore used interchangeably as control animals and are designated as $Pit1^{+/?}$ (Flurkey et al., 2001).

To provide warmth, both male and female F1 hybrid C3DW-$Pit1^{dw/dwJ}$ mice were always housed with normal female

26

littermates. Dwarf and control mice were reared in a specific pathogen-free limited-access animal colony under positive air pressure with filtered air at 27 ± 1°C and 45-55% humidity on a 14-h light/10-h dark cycle. All mice were housed in filter-hooded plastic cages and fed *ad libitum* with autoclaved NIH-31 low-fat chow (Purina), 4% fat by weight, and provided chlorinated water, acidified to prevent the growth of *Pseudomonas*. Quarterly, sentinel mice from this colony were used for animal health assessment by The Jackson Laboratory's diagnostic laboratory.

Care and treatment practices of all mice were in accordance with institutional guidelines, and all procedures were in accordance with IACUC-approved protocols at The University of Texas Medical Branch (UTMB) and The Jackson Laboratory.

Tissues

Pit1$^{dw/dwJ}$ and wild-type control *Pit1$^{+/?}$* mice of both sexes ranging in age from 3-6 and 20-28 months were sacrificed by cervical dislocation and decapitation. The abdomen was rinsed briefly with 70% ethanol, the livers were harvested and gall bladders were removed. The livers were rinsed in ice-cold PBS, placed in cryovials, snap-frozen in liquid nitrogen, shipped on dry ice, and kept at -120°C until use.

Microarray Analyses

Transcriptional profiling of young (3-6 month, n=4 per group) and aged (22-24 months, n=3 per group) male C3DW control (*Pit1 $^{+/?}$*) and dwarf (*Pit1$^{dw/dwJ}$*) livers was performed for 12, 488 target probe sets using Affymetrix MG U74Av.2 chips (Affymetrix, Santa Clara, CA). Pit1$^{dw/dwj}$ mice have a mean lifespan of 1100 days while control C3DW mice have a mean lifespan of 800 days. At 25 months of age, approximately 80% and 90% of control and dwarf animals, respectively, are still alive.

RNA Isolation

Total RNA used for microarray analysis was prepared from frozen livers by gentle homogenization with a plastic pestle on ice in RNAqueous™-4PCR lysis/binding solution, and column-purified per the manufacturer's protocol (Ambion, Austin, TX).

For cDNA synthesis and subsequent real-time PCR analysis, total hepatic RNA was isolated using TriZol Reagent (Invitrogen/Gibco), isopropanol precipitated, ethanol washed, and resuspended in DEPC-treated distilled water. All hepatic RNA preparations were treated with RNase-free DNase (Ambion) for 30 min, quantified by absorbance spectroscopy at $\lambda = 260$nm, and the relative RNA purity determined by A $_{260/280}$ ratios. The structural integrity of each RNA sample was examined both by capillary electrophoresis using a Bioanalyzer 2100 (Agilent Technologies), and also by 28S and 18S rRNA ratios measured by densitometry (Alpha Image, Alpha Innotech) of ethidium bromide stained, formaldehyde/1.8% agarose gels.

RNA Target Preparation and Hybridization

In vitro transcription, hybridization, washing, staining, and scanning of the microarrays was performed by the Molecular Genomics Core Facility at the University of Texas Medical Branch (UTMB), according to standard protocols from Affymetrix, Inc (Santa Clara, CA). All guidelines for assessing sample and array quality were performed per the manufacturer's recommendations. Briefly, DNase-treated, total hepatic RNA from each animal (N=14) was reverse transcribed, biotin-labeled by *in vitro* transcription, and hybridized to individual Affymetrix MG U74Av.2 microarray chips with 12,488 probe sets representing 12,422 murine transcripts and ESTs. Each probe set corresponds to a single reference sequence and is comprised of an average of 16 pairs of perfect match (PM) and mismatch (MM) 25-mer oligonucleotides. Complete probe set design information and probe set listings for the MG U74Av.2 chip are available at http://www.affymetrix.com.

Data Analysis

Using default parameters for expression analysis, each scanned dataset from 14 individual MG U74Av.2 microarray hybridizations was globally scaled and normalized by Micro Array Suite 5.0 (MAS 5.0) software (Affymetrix) to obtain corrected signal intensities and 'Detection' *p*-value statistics for all probe sets on the array. For single array analysis, MAS 5.0 uses two separate algorithms in comparing fluorescent hybridization signals generated by the PM and MM probe pairs of each probe set in order

to calculate 1) a scaled fluorescent signal intensity value calculated by One-step Tukey's Biweight Estimate, representative of the relative expression level of a probe set, and 2) a detection *p*-value calculated using the Wilcoxon's Signed Rank test, reflecting the reliability of detecting and discriminating the target transcript. A complete description of probe set design and of statistical algorithms used by MAS 5.0 is provided in Affymetrix technical bulletins available through the web address listed above (Affymetrix, 2002a; Affymetrix, 2002b).

To identify transcriptional differences between dwarf and control mice, pair-wise, age-matched comparisons of mean signal intensities of each probe set were made between $Pit1^{dw/dwJ}$ and $Pit1^{+/?}$ mice. Within each experimental group (young male dwarf, n = 4; young male control, n = 4; aged male dwarf, n = 3; and aged control, n =3), the mean signal intensity and corresponding standard deviation was calculated for each probe set contained on the U74Av.2 chip from the scaled and normalized hybridization signal intensity values generated by each MAS 5.0 single array analysis. For group-wise array comparisons, the ratio of mean signal intensities for each probe set was used to estimate the relative fold change for each transcript. Using the probe set signal intensities obtained for individual mice from each group, the following grouped comparisons were made: young dwarf *vs.* young control (N=4 per group), and aged dwarf *vs.* aged control (N=3 per group). As a measure of the statistical significance of each change in expression, a 2-tailed Student's *t* test was performed using the more conservative assumption of unequal variance between dwarf and control populations (Microsoft Excel). Integrating bioinformatics, statistical, and array data, a comprehensive database was constructed using Microsoft Access to identify transcripts meeting the statistical significance criteria of $p \leq 0.05$ (Students *t*) and a mean signal intensity ratio ≤ 0.5 or $\geq$ 2.0 (2-fold decrease or increase). Similar statistical methods, selection strategies and thresholds have been successfully used for analysis of Affymetrix MGU74Av.2 microarrays (Maxwell et al., 2003; Horton et al., 2003). For further classification and analysis, such as identification of ESTs/cDNA clones on the array, sequence alignments, biological and molecular function, and corresponding protein sequence annotations,

additional information regarding Affymetrix probe sets was obtained through the NetAffx bioinformatics center (Liu et al., 2003).

Real Time RT-PCR

DNase-treated, total RNA was prepared from male and female control and dwarf livers harvested at 3-6 months and 20-28 months of age as described above. To synthesize cDNA libraries, 2.5 µg of total RNA from each liver (N=32) was reverse transcribed by SuperScript II RNase H- (Invitrogen) according to the manufacturer's instructions using oligo dT_{16-18} primers (Ambion), followed by RNase H treatment of resulting cDNA/RNA heteroduplexes. Hepatic cDNA libraries were diluted 1:10 in nuclease-free water (Qiagen). For real-time PCR amplification, 2 µl of diluted cDNA was used as template per 25 µl reaction.

Primers for selected target transcripts were designed from reference mRNA sequences obtained through GenBank using Primer 3 software (MIT/Whitehead Institute; http://www-genome.wi.mit.edu). To ensure specificity of the selected primer pairs, and prevent the amplification of multiple products, primer pairs with significant sequence identity to non-specific target sequences were excluded by alignment analysis (BLAST/NCBI; http://ncbi.nlm.nih.gov). To maximize PCR efficiencies, amplicons were designed if possible to be fewer than 250 base pairs in length with a common melting temperature of 60°C for all primers. Oligonucleotide primers were synthesized, purified, and desalted commercially (Genosys, Woodlands, TX). Prior to real-time RT-PCR analysis, confirmation of correct amplicon sizes for all primer pairs was determined by agarose gel electrophoresis of real-time RT-PCR products amplified from hepatic cDNA templates. Primer pair sequences, expected amplicon sizes, and GenBank accession numbers for reference sequences are provided below in Table 1.

Table 1: PCR Primer Summary

　　　　Oligonucleotide primer sequences, amplicon size, and GenBank reference sequences are listed. For array validation and gene verification purposes, amplicons were designed to include regions contained in the published sequence and regions corresponding to the Affymetrix probe sets.

Gene Name	Primer Sequence	Oligo Length (bp)	Amplicon Length (bp)	GenBank Reference
Apo-A4 L	CTCCAGACCAAGGTCTCTGC	20	465	M64248
Apo-A4 R	AGGTGTCTGCTGCTGTGATG	20		
β3AR L	TCCTTGTGATGCTCTTCGTCT	21	331	NM_013462
β3AR R	ACTCCGCTGGGAACTAGAGAG	21		
CYP 51 R	TTTTATTTTGGGGAGTGTGTTAGTC	25	151	BC031813
CYP 51 L	TGCCCTTAATCTGTGTTAGGAGTA	24		
FAS R	ACCCAAGCATCATTTTCGTC	20	168	NM_007988
FAS L	ATATGGAGAGGGCTGGTTCC	20		
Fdps L	ATGGAGATGGGCGAGTTCTT	20	376	NM_134469
Fdps R	AATTCCGGGGTCACTTTCTC	20		
GAPDH R	TGTGAGGGAGATGCTCAGTG	20	397	M32599
GAPDH L	GTGTTCCTACCCCCAATGTG	20		
G6Pase R	ACCGGCTTCAGTTGTGTCTGCG	22	445	U00445
G6Pase L	TGGCTTGGGCTAGGGAAAGGAG	22		
HMGCR R	GCGCTTCAGTTCAGTGTCAG	20	105	M62766
HMGCR L	TCAGAAGTCACATGGTTCACAAC	23		
HMGCS1 R	TTAACGCTCCGTGCCAGTA	19	152	NM_145942
HMGCS1 L	GGGGAGATGGTGCATGTAAT	20		
HMGCS2 R	GCTGTGGGTGGGATTTTAAG	20	113	BC024744
HMGCS2 L	AGGAAGTATGCCCGGTGTC	19		
IPP-Iso R	CATAGTCATATCCCCAATGATAAA	24	425	BC004801
IPP-Iso L	AGAGATCCACCTTCCTCTGAC	21		
LDLR R	TGTTGGATTTTTACAGAAGAGACA	24	102	AK036010
LDLR L	TGCTGGTTTCTTGGGATGA	19		
Lipoprotein Lipase L	CTAGGAGAAAGCTGGTTGTGC	21	300	M63335
Lipoprotein Lipase R	GGATGGAGACGGACACAAAG	20		
Malic Enzyme L	CAAACCCACACAGGCTTTA	19	146	AK004980

31

Gene Name	Primer Sequence	Oligo Length (bp)	Amplicon Length (bp)	GenBank Reference
Malic Enzyme R	GCCTTTCCCAGGTGGTATTA	20		
Mvd L	AACGGGACCTTTGACCTCTT	20	185	NM_138656
Mvd R	GAGGCACTTGAGAGGGGTTC	20		
PEPCK L	GGATGTTCGGGCGGATTGAAG	21	211	AF 009605
PEPCK R	TCAATTTCGTAAGGGAGGTCGGTG	24		
PPARγ L	GGAAGCCCTTTGGTGACTTT	20	211	U10374
PPARγ R	TCTGGGTGATTCAGCTTGAG	20		
SAA-1/2 L	GCGAGCCTACACTGACATGA	20	249	U60438
SAA-1/2 R	GGCAGTCCAGGAGGTCTGTA	20		
SqEpx L	CAGCTTCCTTCCTCCTTCCT	20	250	NM_009270
SqEpx R	CAAGGCCTGAGCCAATACAT	20		
SREBP-1 L	AGATGCAGGAGCCACCGTGAAG	22	324	NM_011480
SREBP-1 R	GCGCAAGACAGCAGATTTATTCAGC	25		
SREBP-2 R	TCCACCACACCCTGTTTATG	20	166	BC048071
SREBP-2 L	TCCCAGCCACTTTGAGTAAA	20		

For each target gene, real-time PCR master mixes were prepared to the following final concentrations: 500 nM forward and reverse primers, and 1X iCycler–Hot Start DNA Master SYBR Green I (Bio-Rad, Hercules, CA). Twenty-three microliters of master-mix were added per well in an optical 96-well plate, and 2 µl of diluted hepatic cDNA (~40 ng input RNA) were added as PCR template. Plates were sealed with optical tape, centrifuged briefly, and placed into the thermal cycler. For amplification, quantification, and melt curve analysis, the following protocol was performed by an iCycler iQ thermal cycler (Bio-Rad): initial denaturation (5 min at 95°C); PCR amplification and quantification cycle repeated 50 times (30 sec at 95°C; 30 sec at 55°C; 45 sec at 72°C with a single fluorescence measurement); final extension (1 min, 72°C); and finally, a melt curve analysis (60–95°C) using a heating rate of 0.5°C per 10 sec with a continuous fluorescence measurement. To determine the presence of residual DNA, control reverse transcription reactions using pooled RNA samples from male and female

mice were performed with no reverse transcriptase added. A no template control reaction was also run in parallel with all amplifications to detect contaminating DNA or the formation of secondary products generated by primer interactions.

To control for variation in input RNA quantities and differences in reverse transcription efficiencies, three separate housekeeping genes were used for normalization, *i.e.*, hypoxanthine/guanine phosphoribosyl transferase (HGPRT), glyceraldehyde 3-phosphate dehydrogenase (GAPDH), and phospholipase A2 (PLA2). Multiple housekeeping genes were used in this study to reduce experimental error caused by normalizing to a single 'invariant' control gene which may itself be affected by aging and/or multiple hormone deficiencies (Vandesompele et al., 2002). The geometric mean of the threshold cycle (C_t) values for the three housekeeping genes was calculated per cDNA sample, and a composite normalization factor for each sample was then calculated by correcting to the median value (Pfaffl et al., 2002). Amplification efficiencies were determined for each primer pair using 2-fold serial dilution of cDNAs pooled from all 32 samples as template in PCR reactions performed under the conditions described above. Standard curves were generated by plotting C_t values against the $\log_{10}$ of the template concentration with the slope of the linear regression defined as the amplification efficiency (Pfaffl, 2001). The PCR Base Line Subtracted Curve Fit mode with automatic threshold assignment was applied for C_t determination using iCycler iQ software, version 3.0a (Bio-Rad).

For determining the relative expression of target genes, the threshold cycle value (C_t) obtained for each cDNA sample was adjusted by the corresponding normalization

A. cDNA Amplification

B. Melt Curve

C. PCR Efficiency Determination

R²=0.994 E_{PCR} = 87.0%

Pit1$^{dw/dwJ}$; N=15
Pit1$^{+/?}$;   N=16
-RT & NT Controls
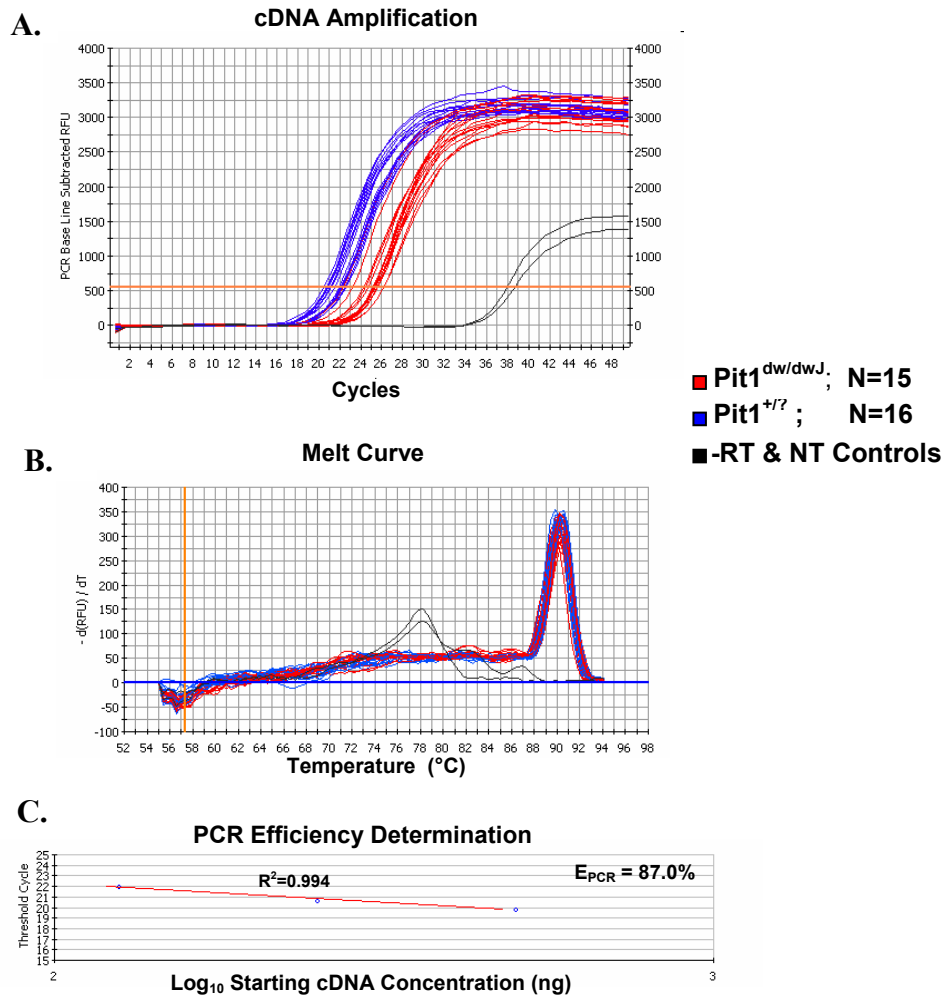
Figure 2: Determination of Amplification Efficiency, Amplicon Melting Temperature, and Threshold Cycle (C$_t$) for Apolipoprotein A-IV

The procedures utilized for determination of transcript levels are demonstrated above by the representative real-time RT-PCR analysis for apolipoprotein A-IV in dwarf and control livers. Thermal cycling trace with fluorescence threshold shown (A); PCR efficiencies (C) were determined using C$_t$ values from two-fold serial dilutions of pooled cDNA templates from all 32 samples. No template and minus RT control reactions were also run in parallel. Melt curve analysis (B) illustrates that a single amplicon is generated by the experimental samples, and the non-specific products formed in the control reactions are substantially smaller in size, *i.e.*, lower melting temperature, and are perhaps thus generated by non-specific amplification of primer dimers in extended cycles.

34

factor derived from the three reference genes listed above. After normalization of individual C_t values for each experimental gene, the mean C_t and standard error (SEM) within each experimental group was then calculated. The difference in mean C_t values between two groups ($\Delta C_{t\,mean}$) was used to estimate the relative expression of particular transcripts using the formula, fold change $= 2^{\Delta Ct}_{mean}$ which assumes optimal PCR efficiency (Pfaffl et al., 2002). Since nearly all primer pairs were found to have amplification efficiencies much greater than 85%, fold changes were determined from normalized mean C_t differences without PCR efficiency correction. To establish the statistical significance of each comparison, 2-tailed student's *t*-tests assuming unequal variance were performed using normalized C_t values obtained for individual animals in each group.

Plasma Lipids Analysis

Mice were fed ad lib on low-fat chow removed 1 hr prior to bleeding. Blood was collected from the retro-orbital sinus into heparinized tubes, placed on ice, centrifuged briefly, and the supernatant plasma collected and frozen in liquid nitrogen. Plasma lipid profiles were obtained by liquid chromatography/mass spectrometric analysis of plasma profiles of triglycerides, total cholesterol, lipase activity, HDL cholesterol, LDL cholesterol.

RESULTS

Microarray Analysis:

Assessment of Variation between Microarray Data Sets:

As microarray experiments comprise thousands of individual measurements each representing the abundance of particular mRNA, it is imperative to rule out experimental error as the source of observed differences in signal intensity. To evaluate the relative influence of systematic error and individual biological variation on the normalized microarray datasets, regression analysis was performed by generating XY scatter plots of hybridization signal intensities for all probe sets in each pair wise comparison. The correlation *within* age-matched experimental groups of the same phenotype (young

dwarf, young control, aged dwarf, and aged control) and the correlation *between* groups of different phenotype and age (young dwarf *vs.* young control, aged dwarf *vs.* aged control) were examined by linear regression analysis of probe set signal intensity values. Scatter plots comparing $\log_{10}$-transformed signal intensity values for all 12,422 non-control probe sets contained on each microarray were used to derive coefficients of determination (r^2) for all possible pair-wise comparisons, and the mean r^2 for each group of comparisons was then calculated. Although these paired regression analyses do not directly assess the reproducibility of each microarray *per se*, the stronger correlation observed within groups suggests that the variability inherent in each microarray experiment is less than the apparent individual biological variability. Therefore, transcriptional changes detected by these microarray experiments are not likely due to systematic error or individual biological variation within a given phenotypic group. Since the statistical method using all possible pair-wise comparisons can be strongly influenced by outliers in a given experimental group, the correlation between datasets was also examined using group-wise averages to minimize this potential bias (Figure 4). The mean signals derived for each experimental group were also log-transformed and then plotted per each comparison to determine the relative correlation *within* and *between* age- and phenotype-based comparisons.

Figure 3: Assessment of Systematic and Biological Variation: Linear Regression Analysis of Microarray Fluorescent Signals.

Representative scatter plots of individual pair-wise comparisons. These plots demonstrate that the biological variation within both dwarf and control groups (Panels A-D) is smaller than the inter-group (dwarf *versus* control) variation at both ages investigated (Panels E-F). For each probe set, the "detection call" provided by MAS 5.0 is indicated by separate colors with $p \leq 0.04$, present (green); $0.04 < p \leq 0.06$, marginal (yellow), and $p > 0.06$ called as absent (red).

A.

Intra-group Signal Comparison: Young *Pit1* [+/?]

B.

Intra-group Signal Comparison: Young *Pit1* [dw/dwJ]

37

C.

Intra-group Signal Comparison: Aged *Pit1* [+/?]

D.

Intra-group Signal Comparison: Aged *Pit1* [dw/dwJ]

38

E.

Inter-group Signal Comparison: Young *Pit1* $^{+/?}$ vs. Young *Pit1* $^{dw/dwJ}$

F.

Inter-group Signal Comparison: Aged *Pit1* $^{+/?}$ vs. Aged *Pit1* $^{dw/dwJ}$
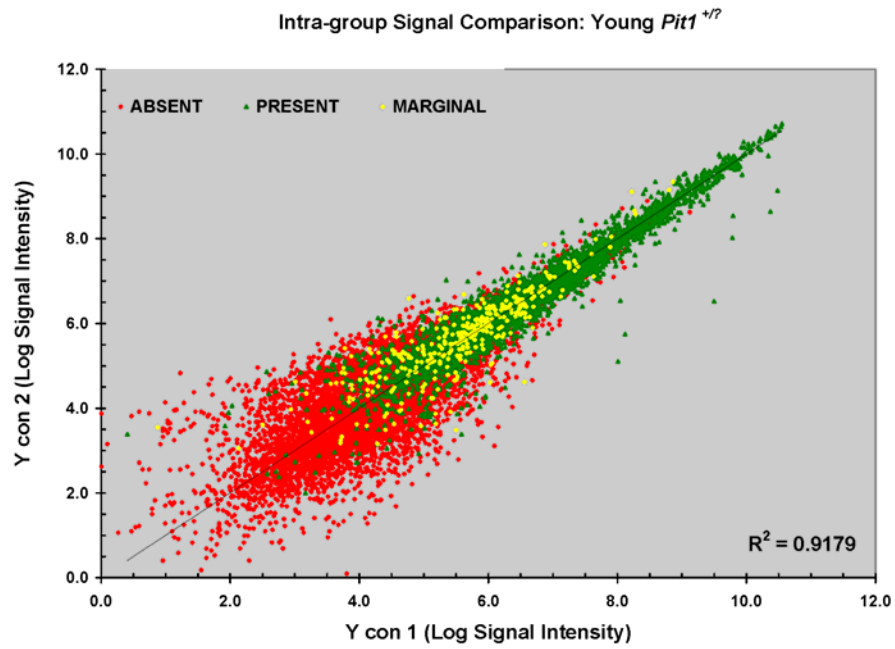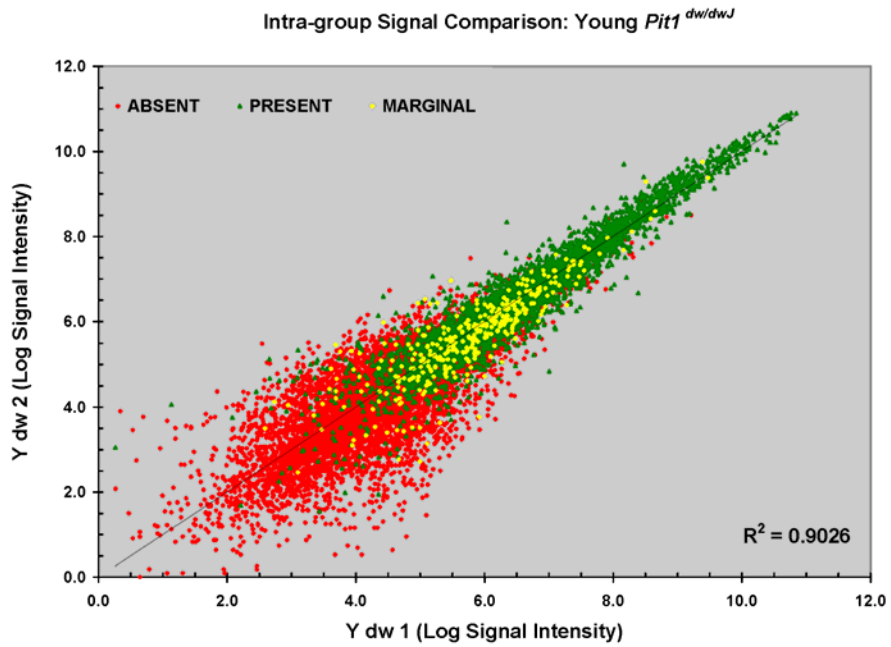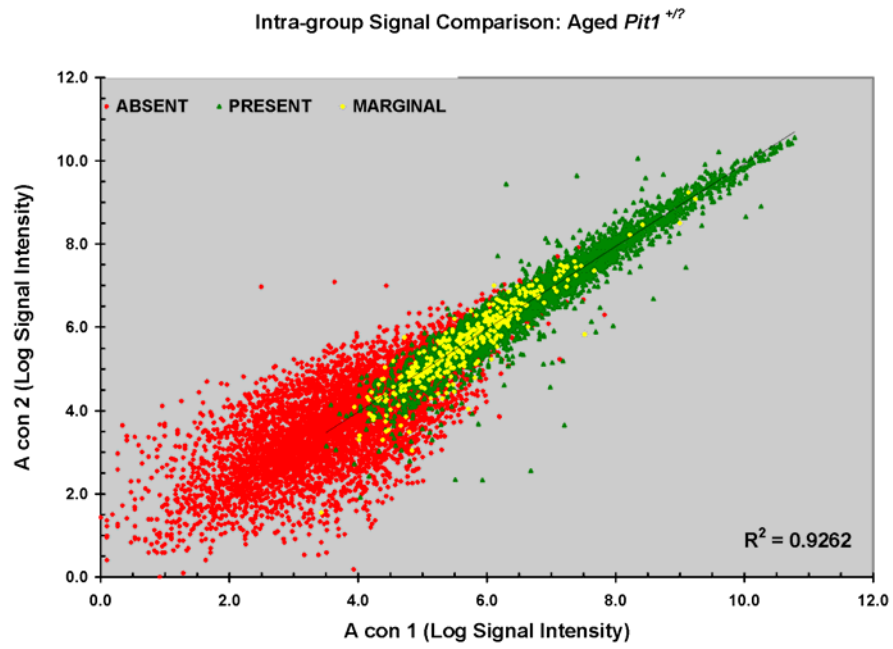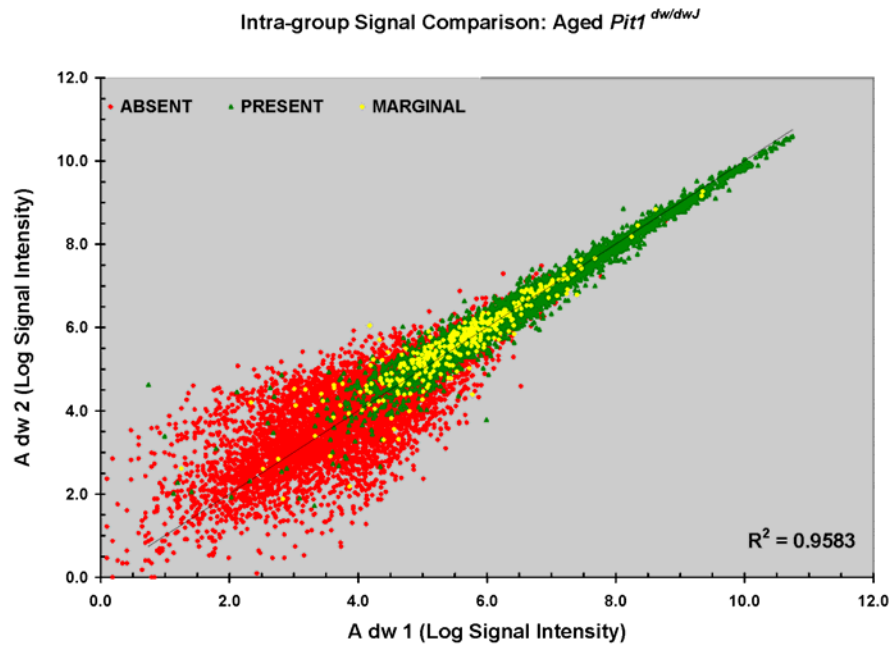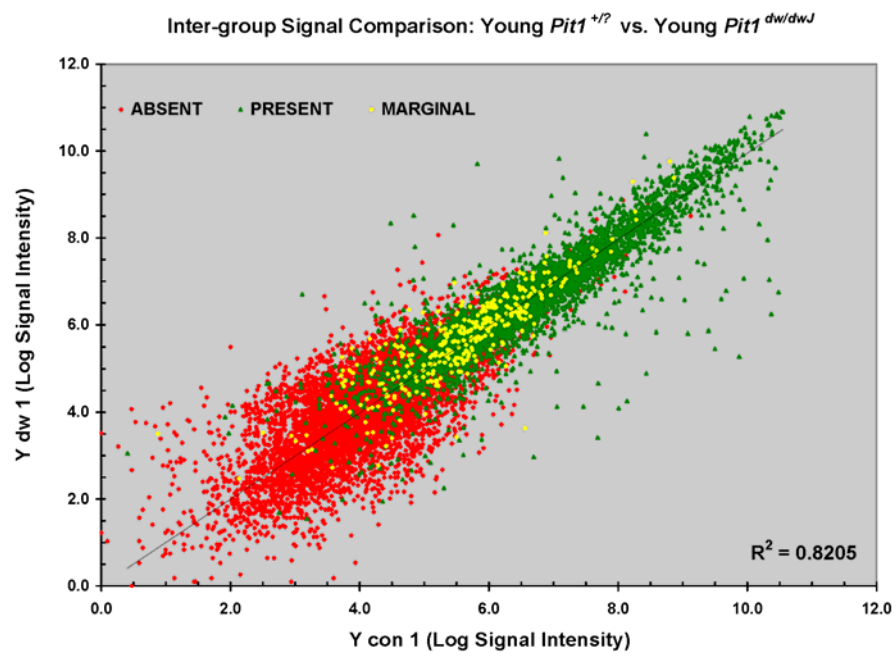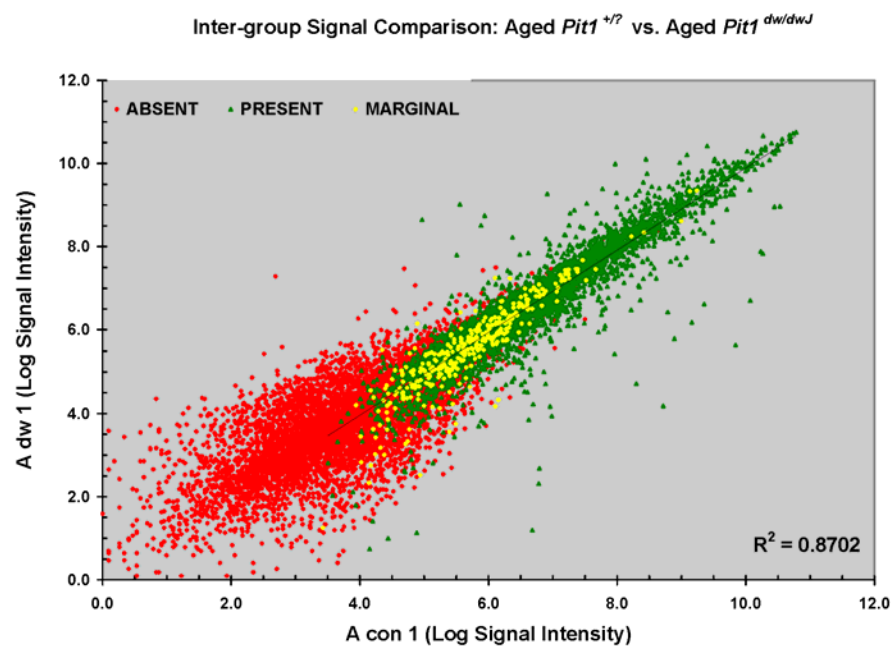
Figure 4: Age- and Phenotype-related Differences in Gene Expression

Individual probe set signal intensities were averaged per experimental group. Log-transformed mean intensity values were plotted to visualize the relative proportion of probe sets with appreciable differences in signal intensity in either 1) age-related (panels A and B), or 2) phenotype-based (panels C and D) comparisons. Supported by the Pearson's coefficients measuring the correlation between each group-wise comparison are shown. These graphical presentations of the microarray datasets indicate that greater differences in gene expression exist between young dwarf and control mice and that relatively few differences exist between young and aged mice of either phenotype. For each probe set, the "detection call" provided by MAS 5.0 is indicated by separate colors with $p \leq 0.04$, present (green); $0.04 < p \leq 0.06$, marginal (yellow), and $p > 0.06$ called as absent (red).

A.

Inter-group Mean Signal Comparison: Young $Pit1^{+/?}$ vs. Young $Pit1^{dw/dwJ}$

$R^2 = 0.8606$
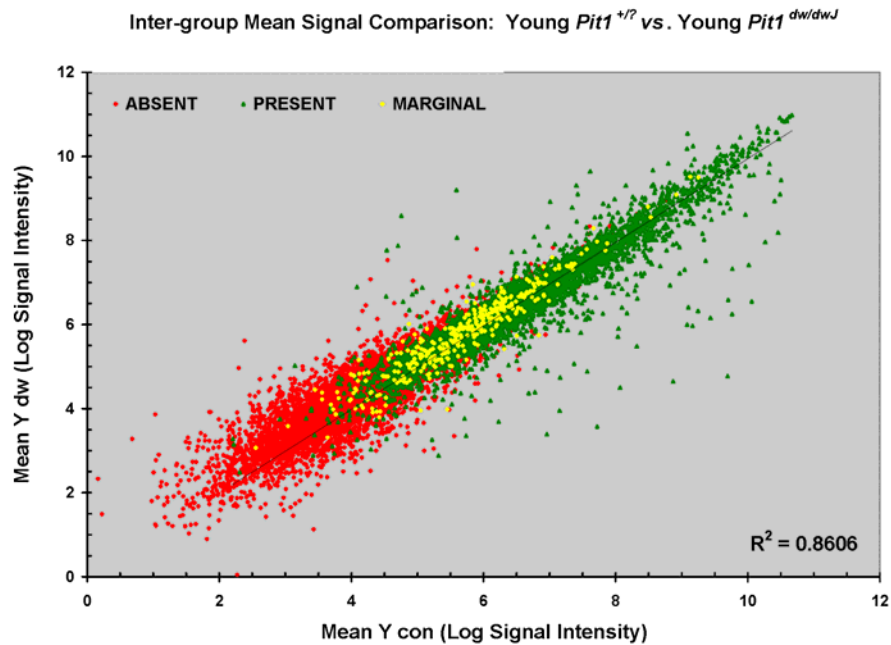
B.

Inter-group Mean Signal Comparison: Aged *Pit1* $^{+/?}$ *vs.* Aged *Pit1* $^{dw/dwJ}$
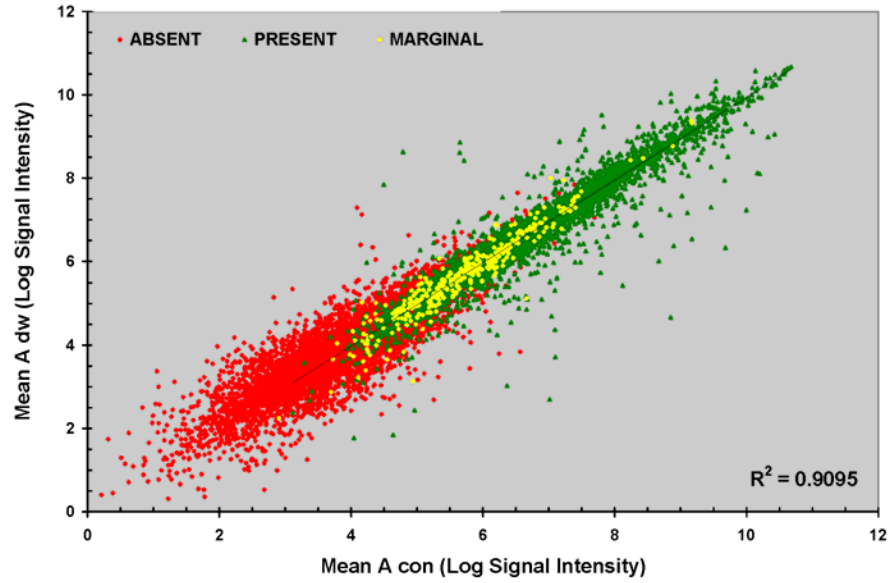
C.

Intra-group Mean Signal Comparison: Young *Pit1* $^{+/?}$ *vs.* Aged *Pit1* $^{+/?}$

41
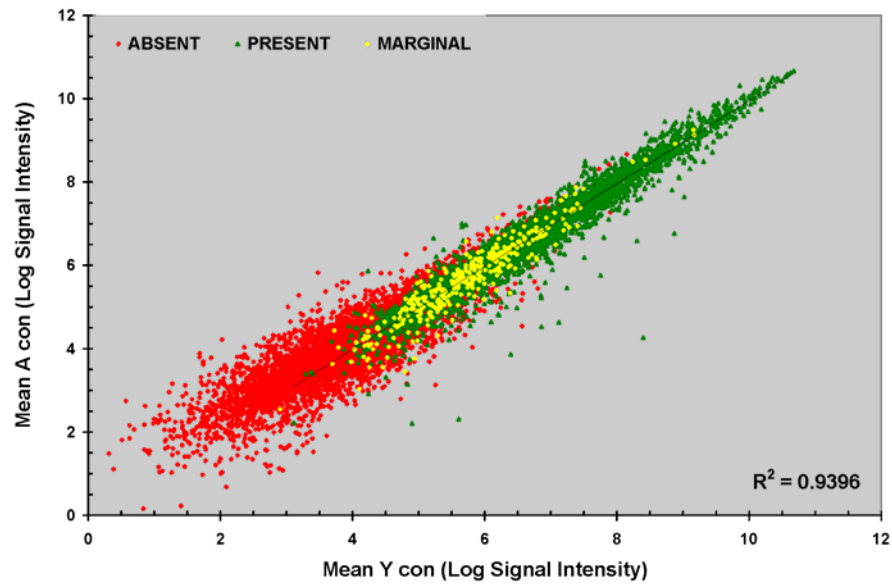
D.

Intra-group Mean Signal Comparison: Young *Pit1* $^{dw/dwJ}$ vs. Aged *Pit1* $^{dw/dwJ}$
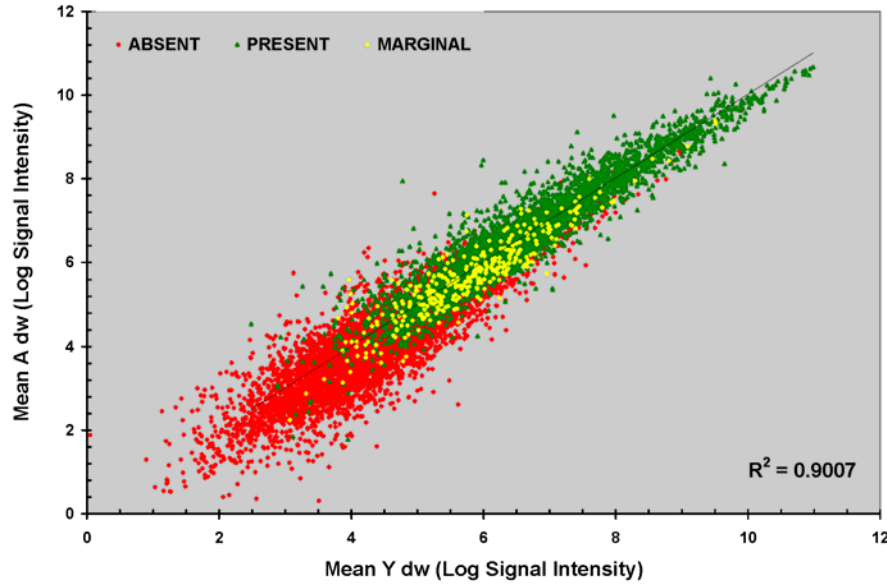
As illustrated by the scatter plots above (Figures 3 & 4), the greater variability in probe set signals of low intensity (red) reflects the decrease in signal to noise ratio for these probe sets, which are therefore generally below reliable detection limits, *i.e.*, MAS 5.0 detection *p* values <0.05. In contrast, large differences in a number of probe set signals with substantial intensities (>1000 RFU) are consistently observed between dwarf and control microarrays, suggesting true biological differences, particularly between young animals. Summarized in Table 2, the correlation (*r*) between datasets *within* all 4 experimental groups is stronger than *between* dwarf and control datasets of the same age group. The range of all intra-group mean correlations is 0.921-0.940 (SEM, ± 0.002), whereas the mean correlations of the two inter-group, age-matched comparisons is 0.904 and 0.928 (SEM, ± 0.003), indicating that the vast majority of genes are expressed at similar levels; however, substantive differences in hepatic gene expression do exist between dwarf and control mice at both ages. The stronger correlation *within* rather than

between each phenotypic group in the regression analysis implies that intensity differences in probe set signals between age-matched dwarf and control mice result from actual biological differences, *i.e.*, true transcriptional changes, rather than from systematic error or individual animal variation within a particular group.

Table 2: Mean Pearson's Correlation (*r*) of Pairwise Comparisons of Complete Microarray Datasets

Group	Mean Correlation (*r*)	SEM
Young		
Control (6)	0.9275	0.0024
Dwarf (6)	0.9211	0.0022
Dwarf vs. Control (16)	0.9043	0.0026
Aged		
Control (3)	0.9366	0.0017
Dwarf (3)	0.9403	0.0014
Dwarf vs. Control (9)	0.9280	0.0005

Discrimination of Differential Expression

To examine the relative expression status of each probe set contained on the U74Av.2 microarray, the identity and number detected across all hybridizations was determined using the Detection *p*-value generated by MAS 5.0 single chip expression analysis. An MAS 5.0 Detection *p*-value ≤ 0.05 was used as the threshold to identify transcripts reliably detected on each individual array (Figure 5). This statistical threshold is slightly less stringent than the default MAS 5.0 parameters that define probe sets with Detection *p*-values ≤ 0.04 as Present, and with *p*-values ≤ 0.06 as Marginal. Of 12, 422, an average of 4398 ± 118 (SEM) probe sets (approximately 35%) were detected in all

43

microarrays of young and aged mouse liver. For individual groups, the average number of probe sets detected in microarrays of young controls (N=4) was 4220 ± 133 and 3973 ± 202 for young dwarf mice (N=4). In microarrays of aged mice, an average of 4822 ± 87 probe sets were detected in arrays of control mice (N=3) and 4780 ± 9 for those of dwarf mice (N=3).

Shown in Figure 6, the Venn diagrams indicate that number of transcripts detected increases with aging for both dwarf and control groups, suggesting an age-related alteration in hepatic gene expression. For microarrays of young liver, 81% of the average number of probe sets detected (3435 out of 4220) were detected in all microarray hybridizations of control livers; and 77% (3076 of 3973) of the average number of probe sets detected were common to all microarrays of young $Pit1^{dw/dwJ}$ livers. Combining both phenotypes, 70% of the average number of probe sets detected in microarrays of young animals were consistently 'present' in all microarrays of young liver (2848 of 4097). Similarly, 87% of the average number of probe sets detected in aged controls were always detected in aged control livers (4213 of 4801), and at least 87% (4182 of 4797) of the average were always detected in aged Pit1dw/dwJ livers. Finally, 92% of the average number detected in aged livers was present in all microarrays of aged animals (3858 of 4198). Notably, the average number of probe sets detected increased in aged livers by more than 12% in both dwarf and control mice, indicating a general increase in the number of genes expressed in aged livers. These results imply greater variability in gene expression in young livers versus aged livers with respect to the proportion of probe sets consistently detected by microarray (70% and 92%, respectively). Of 12,422 probe sets on the array, the same 2806 were detected in all microarray hybridizations, suggesting that a specific subset of transcripts represented on the MG U74v.2 chip are constitutively expressed in murine liver, both dwarf and control.

A similar statistical threshold approach using p-values derived from the heteroscedastic t-test was invoked to analyze the inter-group comparisons with respect to phenotype (control *versus* dwarf) and age (young *versus* aged). To identify consistent transcriptional differences present in both young and aged $Pit1^{dw/dwJ}$ livers, a threshold of

greater than 2- fold change in mean signal intensity values, and a statistical significance cut-off at $p(t) \leq 0.05$ were used as combined selection criteria for age-matched dwarf *versus* control comparisons. Depicted in Figure 7, 629 probe sets demonstrated

Transcript Detection Summary
Male C3DW *Pit1$^{dw/dwJ}$* Liver Microarrays (U74Av.2)
MAS 5.0 Detection p-value ≤ 0.05
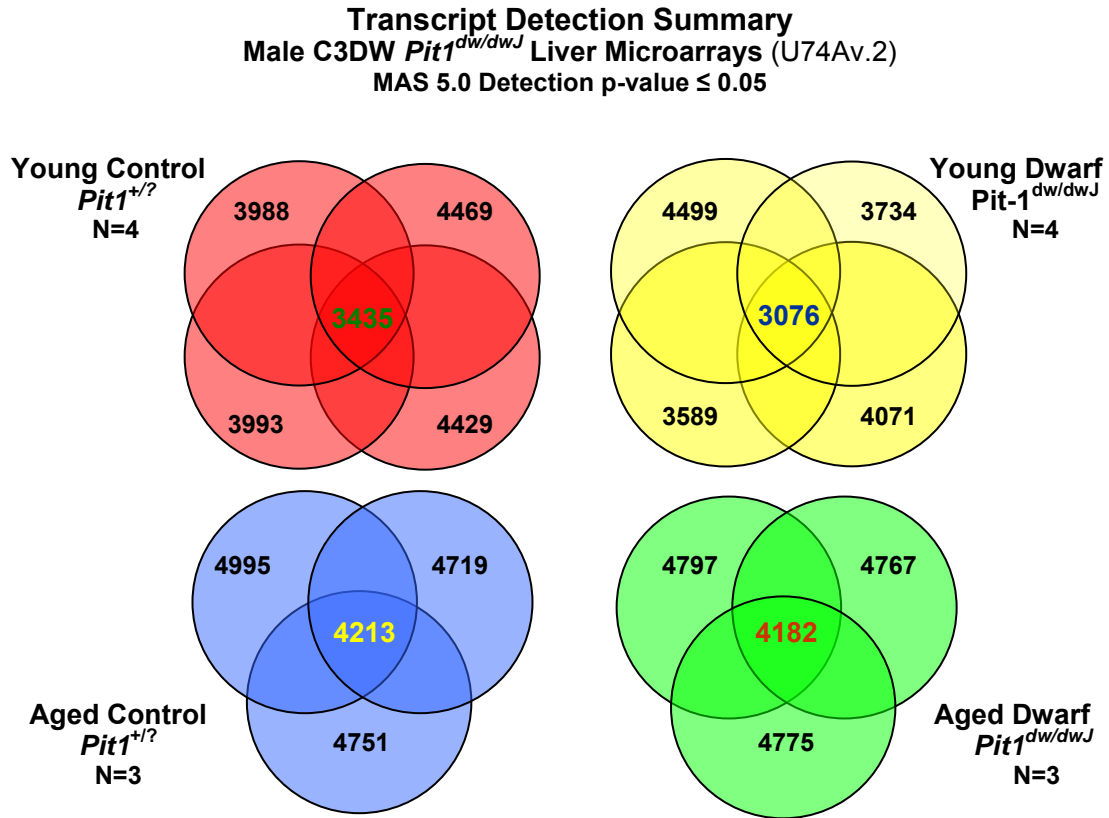
Figure 5: Probe Set Detection Summary from Male C3DW *Pit1$^{dw/dwJ}$* Liver Microarrays (U74Av.2)

The Venn diagrams above depict the number of probe sets with Affymetrix MAS 5.0 Detection *p*-values ≤ 0.05. The number of probe sets achieving this statistical threshold for each microarray is denoted in the periphery of each circle. Within the intersections, the number of probe sets detected in *all* microarrays of each experimental group is indicated.

Detection of Transcripts: Hepatic Profile
Liver Microarrays (U74Av.2)
MAS 5.0 Detection p-value ≤ 0.05

Young Control
Pit1$^{+/?}$
N=4
Detection *p*-value ≤ 0.05

3435   **2848**   **3076**

Young Dwarf
Pit1$^{dw/dwJ}$
N=4
Detection *p*-value ≤ 0.05

Young Liver
Pit1$^{dw/dwJ}$ & Pit1$^{+/?}$
N=8
Detection *p*-value ≤ 0.05

2848   **2806**   **3858**

Aged Liver
Pit1$^{dw/dwJ}$ & Pit1$^{+/?}$
N=6
Detection *p*-value ≤ 0.05

Aged Control
Pit-1$^{+/?}$
N=3
Detection *p*-value ≤ 0.05

4213   **3858**   **4182**

Aged Dwarf
Pit1$^{dw/dwJ}$
N=3
Detection *p*-value ≤ 0.05

Figure 6: Probe Set Detection Summary from Male C3DW *Pit1$^{dw/dwJ}$* Liver Microarrays (U74Av.2): Constitutive Hepatic Gene Expression Profile.

The Venn diagrams depict the number of common probe sets for each group with Affymetrix MAS 5.0 Detection *p*-values ≤ 0.05. The numbers in the intersections of the circles denote detected probe sets common to either intra- or inter-group comparisons. Depicted in the center of the figure, 2806 probe sets were consistently detected in all microarrays of mouse livers, suggesting that these genes comprise a constitutive hepatic transcriptional profile.

a statistically significant 2-fold or greater change in expression for young dwarf *versus* control comparisons; and 306 probe sets were altered significantly in microarray

46

comparisons between aged dwarf and control mice (Figure 7). Listed in the Appendix, the transcripts differentially expressed between aged control and $Pit1^{dw/dwJ}$ livers comprise a number of genes involved in the inflammatory/immune response, protein degradation, carbohydrate and lipid metabolism, and electron transport. Many of these transcriptional differences may represent age-related alterations in hepatic gene expression which are delayed in long-lived dwarf animals. Particularly, a number of chemokine and cytokine signaling mRNAs are diminished in aged dwarf liver relative to aged control suggesting an activation of stress response and immune system defenses in aged control livers.

The increased number of transcriptional differences observed between young $Pit1^{dw/dwJ}$ and control mice may indicate greater differences in gene expression in young dwarf mice, an age-related pattern that was also demonstrated in subsequent RT-PCR analyses. Of these differentially expressed probe sets, 97 were consistently altered independent of age in all dwarf microarray comparisons, with 60 probe sets decreased in expression, and 37 increased in dwarf livers. Further, 69 of these 97 probe sets were also detected (MAS detection $p \leq 0.05$) in *all* arrays of at least one group in each comparison. The genes identified by this intersection of these two age-matched comparisons are listed below. Table 3 lists transcripts significantly ($p < 0.05$) increased by >2-fold in both young and aged dwarf livers, and Table 4 lists transcripts significantly decreased by >2-fold in young and aged livers. In each table, transcripts are sorted by the mean fold change for young mice, and the associated p-value listed was calculated by the 2-tailed Student's t assuming unequal variance between the two populations. As some transcripts are represented by multiple probe sets on the U74Av.2 array, genes may thus appear more than once in the list.

Closer examination and functional classification of identified transcripts revealed specific changes in gene expression associated with energy homeostasis, particularly fatty acid metabolism and cholesterol biosynthesis. Of these differentially expressed 97 probe sets, greater than 25% represent key components of cholesterol biosynthesis, sterol metabolism, or fatty acid homeostasis, which therefore served as the subsequent focus of

this investigation of *Pit1$^{dw/dwJ}$* hepatic gene expression. Other functional classes of transcripts consistently altered in *Pit1$^{dw/dwJ}$* livers involve growth factor/IGF-1 signaling, xenobiotic/oxidative metabolism (cytochrome P450s), pheromone transport/binding (MUPs), redox balance (GSTs), immune response, and embryonic development. These transcripts thus constitute characteristic alterations in hepatic gene expression in these

Summary of Transcripts Altered >2-Fold : Dwarf *vs.* Control
Male C3DW *Pit1$^{dw/dwJ}$* Liver Microarrays (U74Av.2)
T-test *p*-value ≤ 0.05

Young Control Liver
N = 4
Detection *p*-value ≤ 0.05

3435   629   3076

Young Dwarf Liver
N = 4
Detection *p*-value ≤ 0.05

Young Comparison
Y dw *vs.* Y con
Fold Change ≥ 2X
p (t) ≤ 0.05

629   **97**   306

Aged Comparison
A dw *vs.* A con
Fold Change ≥ 2X
p (t) ≤ 0.05

Aged Control Liver
N = 3
Detection *p*-value ≤ 0.05

4213   306   4182

Aged Dwarf Liver
N = 3
Detection *p*-value ≤ 0.05

Figure 7: Male Dwarf *vs*. Control C3DW *Pit1$^{dw/dwJ}$* Liver Microarrays (U74Av.2):
Summary of Common Probe Sets Detected (*p* ≤0.05)

Presented in this diagram, the number of probe sets detected in *all* microarrays of each experimental group is shown within each circle. The number of transcripts with mean signal ratios greater than 2 or less than 0.5, and also achieving the student's *t*-test significance threshold (*p* ≤0.05) is listed within the intersections of the outer pairs of circles. The pair of circles in the center denotes the number of differentially expressed probe sets for each age-matched comparison, with the intersection indicating the number of probe sets meeting the criteria in both comparisons.

long-lived animals, and depict an age-independent transcriptional profile of altered metabolism and lipid transport in male dwarf livers which may contribute to longevity determination.

Table 3: Dwarf-specific Increases in Gene Expression

Meeting the selection thresholds of a 2-fold or greater difference in mean signal ratios and $p < 0.05$ for *both* age-matched comparisons, transcripts listed in this table are significantly up-regulated in $Pit1^{dw/dwJ}$ livers at both ages compared. Genes involved in cholesterol and lipid metabolism are indicated in bold type.

Young		Aged		
Mean Fold Change	P(*t*)	Mean Fold Change	P(*t*)	Transcript
2.03	0.03374	2.02	0.02390	RIKEN cDNA D030029J20 gene
2.18	0.00992	2.14	0.04147	B-cell translocation gene 1, anti-proliferative
2.23	0.00078	2.54	0.00209	nuclear receptor subfamily 1, group I, member 3
2.33	0.00050	11.48	0.00290	glutathione S-transferase, alpha 2 (Yc2)
2.35	0.02230	2.32	0.03335	ESTs, Highly similar to Ligatin (*M. musculus*)
2.38	0.04530	2.88	0.00462	proviral integration site 2
2.40	0.01547	5.81	0.00988	cytochrome P450, family 2, subfamily b, polypeptide 10
2.58	0.01938	2.33	0.00160	cytochrome P450, family 2, subfamily c, polypeptide 38
2.71	0.00192	3.08	0.00282	**very low density lipoprotein receptor**
2.80	0.02845	5.82	0.01457	nuclear receptor subfamily 1, group I, member 2
2.90	0.00179	2.41	0.02308	UDP-glucose pyrophosphorylase 2
3.23	0.04678	4.75	0.00791	phosphatidic acid phosphatase 2a
3.26	0.00290	3.76	0.00053	microsomal glutathione S-transferase 3
3.43	0.00154	2.41	0.00501	Cd27 binding protein (Hindu God of destruction)
3.90	0.00038	3.34	0.00441	**solute carrier family 16 (monocarboxylic acid transporters), member 7**
4.07	0.02084	7.00	0.00660	**peroxisome proliferator activated receptor gamma**
4.11	0.01485	5.81	0.01474	plasma membrane associated protein, S3-12
4.46	0.00939	23.53	0.00308	cytochrome P450, family 4, subfamily a, polypeptide 10
4.69	0.03211	8.66	0.03684	insulin-like growth factor 2
4.80	0.00044	8.90	0.02217	ESTs

Young		Aged		
Mean Fold Change	P(*t*)	Mean Fold Change	P(*t*)	Transcript
5.00	0.01430	7.26	0.00642	cytochrome P450, family 2, subfamily c, polypeptide 39
5.37	0.00100	4.60	0.02938	similar to CG1358 gene product
5.85	0.00004	4.40	0.02755	**isocitrate dehydrogenase 2 (NADP+), mitochondrial**
6.26	0.00168	2.86	0.02967	**phospholipase A2, group XII**
6.31	0.00126	27.05	0.01669	cytochrome P450, 4a14
6.63	0.01593	2.50	0.01731	defensin beta 1
7.29	0.01588	6.38	0.02068	DNA cross-link repair 1A, PSO2 homolog (*S. cerevisiae*)
7.37	0.00067	8.78	0.00051	cytochrome P450, family 2, subfamily b, polypeptide 9
8.64	0.00007	2.98	0.03214	protein related to DAN and cerberus
8.66	0.00819	3.50	0.04398	guanylate cyclase 2c
9.09	0.00485	7.77	0.01260	**adrenergic receptor, beta 3**
12.58	0.01552	32.04	0.00007	sulfotransferase, hydroxysteroid preferring 2
13.41	0.00318	33.57	0.00003	**hydroxyacid oxidase (glycolate oxidase) 3**
13.61	0.01197	7.48	0.02874	**phospholipase A2, group XII**
15.45	0.02471	8.77	0.02119	**lipoprotein lipase**
48.48	0.00089	49.87	0.01539	cytochrome P450, family 2, subfamily b, polypeptide 13
75.61	0.00017	75.15	0.00294	flavin containing monooxygenase 3

Table 4: Dwarf-specific Decreases in Gene Expression

Meeting the selection thresholds of a 2-fold or greater difference in mean signal ratios and $p < 0.05$ for both age-matched comparisons, transcripts listed in this table are significantly down-regulated in $Pit1^{dw/dwJ}$ livers. Genes involved in cholesterol and lipid metabolism are indicated in bold type.

Young		Aged		
Mean Fold Change	P(*t*)	Mean Fold Change	P(*t*)	Transcript
-208.39	0.001	**-4.57**	0.013	RIKEN cDNA 1100001G20 gene
-103.07	0.000	**-13.30**	0.002	major urinary protein 1
-78.98	0.001	**-35.07**	0.010	major urinary protein 1
-61.14	0.019	**-166.11**	0.007	**hydroxysteroid dehydrogenase-5, delta<5>-3-beta**
-45.05	0.000	**-49.47**	0.001	insulin-like growth factor binding protein, acid labile subunit
-35.11	0.002	**-50.66**	0.007	RIKEN cDNA 4632419J12 gene
-21.37	0.004	**-18.38**	0.002	major urinary protein 1
-20.52	0.001	**-21.20**	0.016	insulin-like growth factor 1
-20.38	0.000	**-2.76**	0.001	esterase 31
-19.35	0.010	**-28.37**	0.018	epidermal growth factor receptor
-18.58	0.007	**-18.82**	0.003	zeta-chain (TCR) associated protein kinase
-9.93	0.005	**-4.62**	0.010	kidney expressed gene 1
-9.76	0.004	**-6.73**	0.002	deiodinase, iodothyronine, type I
-9.37	0.000	**-3.02**	0.002	complement component 9
-9.26	0.017	**-10.22**	0.026	defensin related cryptin
-8.45	0.000	**-2.82**	0.037	protein disulfide isomerase-related protein
-7.42	0.001	**-4.65**	0.045	lymphocyte antigen 6 complex, locus A
-7.38	0.006	**-3.50**	0.025	RIKEN cDNA 2900016D05 gene
-7.34	0.018	**-3.74**	0.010	cytochrome P450, family 2, subfamily f, polypeptide 2
-7.18	0.006	**-4.53**	0.009	elastase 1, pancreatic
-6.80	0.036	**-8.11**	0.035	serine (or cysteine) proteinase inhibitor, clade A, member 3K
-5.96	0.012	**-4.15**	0.000	**squalene epoxidase**
-5.88	0.029	**-2.37**	0.022	**isopentenyl-diphosphate delta isomerase**
-5.29	0.005	**-4.64**	0.013	zeta-chain (TCR) associated protein kinase
-5.28	0.041	**-6.24**	0.038	complement receptor related protein
-5.01	0.000	**-5.04**	0.007	major urinary protein 1

Young		Aged		
Mean Fold Change	P(*t*)	Mean Fold Change	P(*t*)	Transcript
-5.00	0.001	-4.76	0.022	ubiquitin specific protease 15
-4.94	0.007	-3.21	0.000	glypican 1
-4.90	0.000	-4.91	0.003	major urinary protein 4
-4.56	0.016	-4.05	0.007	cathepsin C
-4.35	0.012	-3.87	0.014	**cytochrome P450, family 7, subfamily b, polypeptide 1**
-4.23	0.000	-4.37	0.003	major urinary protein 3
-4.07	0.010	-5.23	0.000	leukemia inhibitory factor receptor
-4.04	0.000	-2.70	0.022	camello-like 1
-3.92	0.000	-3.87	0.003	major urinary protein 5
-3.76	0.000	-4.12	0.001	insulin-like growth factor 1
-3.70	0.026	-4.20	0.010	expressed in non-metastatic cells 1, protein
-3.66	0.030	-2.21	0.008	RIKEN cDNA 2010008K16 gene
-3.61	0.036	-10.48	0.022	interferon gamma inducible protein
-3.36	0.002	-2.33	0.014	**hydroxysteroid (17-beta) dehydrogenase 2**
-3.31	0.001	-2.52	0.000	RIKEN cDNA 1300013B24 gene
-3.31	0.002	-4.91	0.000	interferon regulatory factor 6
-3.30	0.006	-5.05	0.048	deoxynucleotidyltransferase, terminal
-3.29	0.020	-3.07	0.044	ESTs
-3.28	0.011	-2.58	0.045	interferon-inducible GTPase
-3.26	0.028	-2.37	0.008	interferon-inducible GTPase
-3.23	0.012	-2.88	0.034	**serum amyloid P-component**
-3.15	0.004	-6.81	0.043	cathepsin C
-3.06	0.027	-3.81	0.011	leukemia inhibitory factor receptor
-3.01	0.009	-3.02	0.008	guanine nucleotide binding protein, alpha 14
-3.00	0.002	-2.23	0.005	RIKEN cDNA 1100001H23 gene
-2.95	0.045	-2.47	0.022	ESTs
-2.85	0.005	-2.05	0.007	**farnesyl diphosphate synthetase**
-2.70	0.005	-2.86	0.022	**ATP-binding cassette, sub-family B (MDR/TAP), member 8**
-2.68	0.000	-2.33	0.004	inter-alpha trypsin inhibitor, heavy chain 1
-2.58	0.001	-2.23	0.002	lymphocyte antigen 6 complex, locus E
-2.45	0.010	-2.78	0.027	retinol dehydrogenase 11
-2.32	0.019	-3.53	0.015	**cytochrome P450, family 7, subfamily b, polypeptide 1**

Young		Aged		
Mean Fold Change	P(*t*)	Mean Fold Change	P(*t*)	Transcript
-2.16	0.013	-3.42	0.018	**formin**
-2.05	0.015	-2.11	0.025	dipeptidylpeptidase 7

To further investigate transcriptional differences between young and aged *Pit1*^{dw/dwJ} and control livers, microarray data sets were also analyzed using the Significance Analysis of Microarrays (SAM, v.1.21), a widely accepted statistical method developed by Tusher *et al.* (Tusher et al., 2001). Although also based on *t*-test distributions, the advantage of this method is that a false discovery rate based on the inherent variation within the entire dataset is also provided. Significant differences in gene expression were identified by tuning the false discovery rate with the user-defined statistical parameter, delta. Both the 2-class and multi-class response modes of SAM were used on both raw and log-transformed data sets to analyze microarrays grouped by age and/or phenotype. Detailed in Table 5 are the top 50 probe sets found to be significantly altered in a multi-class comparison of all microarray datasets with a false discovery rate (FDR) for the 90th percentile of 1.3%. This selection strategy is similar to a 2-factor ANOVA and thus identifies both age- and *Pit1*-related differences simultaneously. For this analysis, microarray results were subdivided into the four experimental groups based on age and phenotype; the genes identified by SAM using this approach represent differences in expression between both 1) dwarf and control, and/or 2) young and aged animals. The magnitude of differences in expression is represented by the ratio of the mean signal intensities for each group, *i.e.*, young control (Y con), young dwarf (Y dw), aged control (A con) and aged dwarf (A dw). To further examine the microarray data, a heteroscedastic, 2-tailed *t*-test was performed for each probe set using the individual signals within each group to provide a measure of the statistical significance for each particular comparison made between the four experimental groups. Transcripts are sorted by the delta value provided by SAM, and the associated change *p*-

53

value calculated by the 2-tailed student's *t*-test assuming unequal variance is listed. Those transcripts identified by SAM and meeting the statistical threshold of $p < 0.05$ in comparisons of dwarf and control animals for both age groups are shown in bold type, and represent persistent transcriptional differences between *Pit1*$^{dw/dwJ}$ and control mice.

Table 5: 50 Most Significant Transcriptional Differences between Aging Pit1$^{dw/dwJ}$ and Control Livers Determined by Multi-class Response SAM (Mean False Discovery Rate <0.7%)

Differentially expressed transcripts are listed in order of significance using the delta values generated by multi-class response Significance Analysis of Microarrays (SAM), with a false discovery rate (FDR) for the 90th percentile of 1.3%. These genes identified by this approach include differences in expression between either dwarf and control, and/or between young and aged animals. The *p*-values shown for each paired comparison of phenotypic and age-related change in expression were derived from individual microarray signals using the 2-tailed *t*-test assuming unequal variances, with *p* ≤0.05 considered as significant. Transcriptional differences with significant *p*-values for *both* age-matched dwarf *vs.* control comparisons are considered *Pit1*-specific and the corresponding gene names are indicated in bold. Ratios of mean signal intensities for each comparison are expressed relative to control or young mice, *i.e.* dw/con or aged/young, and are shown in bold if greater than 2-fold.

Score (delta)	Gene Title	Y Dw *vs.* Y Con		A Dw *vs.* A Con		Y Con *vs* .A Con		Molecular Function
		Ratio	*p-Value*	Ratio	*p-Value*	Ratio	*p-Value*	
8.3	**flavin containing monooxygenase 3**	**46.23**	*0.0002*	**46.51**	*0.0029*	**3.63**	0.9096	monooxygenase activity / dimethylaniline monooxygenase (N-oxide-forming) activity / oxidoreductase activity
8.1	**major urinary protein 1**	**0.03**	*0.0001*	**15.87**	*0.0022*	**11.31**	0.4110	---
8.1	**insulin-like growth factor binding protein, acid labile subunit**	**0.03**	*0.0002*	**7.83**	*0.0011*	**7.93**	*0.0131*	cell adhesion molecule activity / insulin-like growth factor binding
6.9	**squalene epoxidase**	**0.34**	*0.0115*	**4.22**	*0.0002*	**19.62**	*0.0004*	monooxygenase activity / squalene monooxygenase activity / oxidoreductase activity

54

Score (delta)	Gene Title	Y Dw *vs.* Y Con		A Dw *vs.* A Con		Y Con *vs* .A Con		Molecular Function
		Ratio	*p-Value*	Ratio	*p-Value*	Ratio	*p-Value*	
6.0	**major urinary protein 4**	**0.10**	*0.0002*	**8.12**	*0.0030*	**7.91**	*0.0333*	transporter activity / pheromone binding
5.9	**major urinary protein 3**	**0.23**	*0.0000*	**3.83**	*0.0068*	**16.66**	0.3690	transporter activity / pheromone binding
5.5	**solute carrier family 16 (monocarboxylic acid transporters), member 7**	**2.49**	*0.0004*	**2.82**	*0.0044*	**12.25**	*0.0149*	carrier activity / symporter activity monocarboxylate porter activity
5.5	**major urinary protein 5**	**0.10**	*0.0002*	**7.72**	*0.0029*	**8.41**	0.3317	transporter activity / pheromone binding
5.3	**major urinary protein 3**	**0.25**	*0.0000*	**3.95**	*0.0027*	**10.69**	0.4346	transporter activity / pheromone binding
5.2	**protein related to DAN and cerberus**	**9.41**	*0.0001*	**2.71**	*0.0321*	**3.88**	0.4255	---
5.0	**insulin-like growth factor 1**	**0.29**	*0.0004*	**4.12**	*0.0005*	**7.92**	0.3553	hormone activity / growth factor activity
4.9	**esterase 31**	**0.09**	*0.0001*	**2.35**	*0.0013*	**7.05**	0.1624	catalytic activity / carboxylesterase activity / serine esterase activity / hydrolase activity
4.9	**camello-like 1**	**0.25**	*0.0000*	**2.57**	*0.0218*	**15.02**	0.0664	N-acetyltransferase activity / transferase activity
4.8	**complement component 9**	**0.16**	*0.0003*	**2.90**	*0.0019*	**7.28**	*0.0353*	---
4.7	**EST**	**0.03**	*0.0008*	**28.63**	*0.0100*	**6.29**	0.5220	---
4.7	annexin A8	0.51	0.1119	**7.48**	*0.0019*	**2.17**	*0.0314*	calcium ion binding / calcium-dependent phospholipid binding
4.5	**sulfotransferase, hydroxysteroid preferring 2**	**16.64**	*0.0155*	**28.49**	*0.0001*	**2.61**	0.7418	alcohol sulfotransferase activity / sulfotransferase activity / transferase activity
4.4	secreted phosphoprotein 1	0.64	0.0914	**5.12**	*0.0002*	**10.77**	*0.0001*	cytokine activity / cell adhesion molecule activity
4.4	**Mus musculus transcribed sequences**	1.89	*0.0001*	1.53	*0.0031*	**7.16**	*0.0237*	---
4.3	**hydroxyacid oxidase (glycolate oxidase) 3**	**6.25**	*0.0032*	**24.41**	*0.0000*	0.65	0.1898	oxidoreductase activity / (S)-2-hydroxy-acid oxidase activity
4.2	**insulin-like growth factor 1**	**0.07**	*0.0010*	**14.34**	*0.0158*	**4.20**	*0.0279*	hormone activity / growth factor activity

Score (delta)	Gene Title	Y Dw vs. Y Con		A Dw vs. A Con		Y Con vs .A Con		Molecular Function
		Ratio	p-Value	Ratio	p-Value	Ratio	p-Value	
4.2	lactamase, beta 2	0.40	0.0002	1.05	0.5437	6.24	0.0005	---
4.1	**gap junction membrane channel protein beta 2**	0.38	0.0001	1.76	0.0085	13.50	0.0793	gap-junction forming channel activity / protein binding / connexon channel activity
4.1	**mannose binding lectin, serum (C)**	0.60	0.0038	1.49	0.0093	55.53	0.0003	sugar binding / mannose binding
4.1	**inter-alpha trypsin inhibitor, heavy chain 1**	0.39	0.0004	2.19	0.0037	28.40	0.0314	serine-type endopeptidase inhibitor activity / copper ion binding
3.9	**cytochrome P450, 2b13, phenobarbitol inducible, type c**	23.72	0.0009	19.37	0.0154	4.92	0.1632	---
3.9	**microsomal glutathione S-transferase 3**	2.60	0.0029	3.53	0.0005	5.14	0.2072	transferase activity
3.9	**RIKEN cDNA 1100001G20 gene**	0.01	0.0013	5.60	0.0135	5.79	0.8561	---
3.9	**paxillin**	1.47	0.0005	1.14	0.0449	12.31	0.6541	protein binding / receptor signaling complex / scaffold activity
3.9	**serine (or cysteine) proteinase inhibitor, clade A (alpha-1 antiproteinase, antitrypsin), member 12**	0.02	0.0024	14.66	0.0074	7.25	0.0623	endopeptidase inhibitor activity / serine-type endopeptidase inhibitor activity
3.9	vanin 3	1.14	0.1383	2.14	0.0015	14.40	0.3940	hydrolase activity / hydrolase activity, acting on carbon-nitrogen (but not peptide) bonds
3.8	**interferon regulatory factor 6**	0.30	0.0019	5.22	0.0003	5.78	0.4898	DNA binding / transcription factor activity
3.8	**autophagy 5-like (S. cerevisiae)**	0.56	0.0007	1.34	0.0013	17.42	0.0000	---
3.8	eukaryotic translation initiation factor 2, subunit 3, structural gene Y-linked	0.90	0.5538	1.15	0.0238	8.05	0.0021	translation initiation factor activity / GTP binding / protein-synthesizing GTPase activity

Score (delta)	Gene Title	Y Dw *vs.* Y Con		A Dw *vs.* A Con		Y Con *vs.* A Con		Molecular Function
		Ratio	*p-Value*	Ratio	*p-Value*	Ratio	*p-Value*	
3.7	Mus musculus, clone IMAGE:4037400, mRNA	0.48	*0.0001*	1.03	0.7225	21.88	0.1003	lactoylglutathione lyase activity
3.7	T-cell immunoglobulin and mucin domain containing 2	0.40	*0.0001*	1.28	0.1140	8.35	*0.0010*	---
3.7	guanine nucleotide binding protein, alpha inhibiting 2	1.34	*0.0032*	1.03	0.6541	6.46	*0.0071*	heterotrimeric G-protein GTPase activity / signal transducer activity / GTP binding
3.7	**EST**	0.05	*0.0036*	13.94	*0.0021*	4.02	0.5860	---
3.6	**glutathione S-transferase, mu 3**	1.75	*0.0017*	3.24	*0.0106*	16.95	0.7840	glutathione transferase activity / transferase activity
3.6	**cytochrome P450, family 4, subfamily a, polypeptide 14**	6.80	*0.0013*	24.71	*0.0167*	0.83	*0.0148*	monooxygenase activity / oxidoreductase activity / alkane 1-monooxygenase activity
3.5	retinoic acid induced 12	2.63	*0.0007*	1.26	0.3090	4.65	*0.0362*	---
3.4	**dehydrocholesterol reductase**	0.70	*0.0459*	1.57	*0.0350*	25.51	*0.0139*	oxidoreductase activity / 7-dehydrocholesterol reductase activity
3.4	**cat eye syndrome chromosome region, candidate 5 homolog (human)**	0.63	*0.0413*	1.57	*0.0158*	22.32	*0.0063*	---
3.4	ATP-binding cassette, sub-family D (ALD), member 3	0.38	*0.0006*	1.17	0.1514	4.35	*0.0019*	nucleotide binding / ATP-binding cassette (ABC) transporter activity / ATP binding
3.4	**sialyltransferase 6 (N-acetyllacosaminide alpha 2,3-sialyltransferase)**	0.43	*0.0132*	1.75	*0.0408*	12.26	*0.0126*	N-acetyllactosaminide alpha-2,3-sialyltransferase activity / transferase activity, transferring glycosyl groups
3.4	**farnesyl diphosphate synthetase**	0.47	*0.0179*	1.56	*0.0118*	9.17	*0.0013*	transferase activity
3.3	ectonucleoside triphosphate diphosphohydrolase 2	1.09	0.6156	2.05	*0.0162*	60.56	*0.0139*	magnesium ion binding / apyrase activity / hydrolase activity
3.3	stathmin 1	1.66	0.2266	1.92	*0.0006*	4.84	*0.0039*	---

Score (delta)	Gene Title	Y Dw *vs.* Y Con		A Dw *vs.* A Con		Y Con *vs .*A Con		Molecular Function
		Ratio	p-Value	Ratio	p-Value	Ratio	p-Value	
3.3	**lysosomal-associated protein transmembrane 5**	1.44	*0.0001*	1.34	*0.0144*	28.73	*0.0056*	---
3.3	RIKEN cDNA 5033425B17 gene	0.34	*0.0003*	1.41	0.0691	20.82	0.2352	---

To exclude the effect of aging in our analysis of differential gene expression, 2-class SAM comparisons were also made between age-matched dwarf and control datasets to characterize further dwarf-specific patterns of gene expression (see supplementary data provided in Boylston *et al.*, 2004 and available online at *Aging Cell*). Since the statistical significance analysis was performed using individual probe sets rather than unique transcripts, genes may therefore appear more than once in the list.

In addition to the approach outlined above, additional selection strategies were also utilized to analyze the microarray data sets. In particular, the identification of age-related changes in control animals was of great interest, as these would provide insight into the normal aging process of the liver. To reveal age-related patterns of gene expression in either dwarf or control livers, separate 2-class SAM comparisons were performed between young and aged animals of each phenotype. Since it could not be assumed that patterns of age-related gene expression in aging dwarf mice parallel those of 'normal' aging, phenotype-matched comparisons of young and aged animals were made to separate potentially different aging-associated patterns of gene expression in dwarf and control livers. Intriguingly, compared to the analysis of $Pit1^{dw/dwJ}$-related differences in gene expression, far fewer aging-related genes were identified by the SAM analysis of controls (Table 6). Further, the false discovery rate for these genes was substantially greater than for those associated with dwarf-related changes in gene expression. However, among these, several cholesterologenic enzymes including squalene epoxidase and farnesyl diphosphate synthetase were identified by SAM, and are in agreement with the RT-PCR findings. Surprisingly, 7-dehydrocholesterol reductase,

which was not shown to be differentially expressed in *Pit1*^{dw/dwJ} livers, was included in this relatively short list of 'normal' aging genes, indicating that cholesterol biosynthesis is affected by aging in these mice. In addition to age-related changes in cholesterol biosynthetic enzymes, the expression of demethyl-CoQ, the mouse homolog of the nematode *clk-1* gene was unexpectedly shown to be significantly increased in aged control livers, an important discovery which directly relates to a number of longevity studies in *C. elegans* (Jonassen et al., 2003; Larsen and Clarke, 2002; Miyadera et al., 2001).

Table 6: Significant Aging-related Transcriptional Differences in Control Pit1$^{+/?}$ Livers Determined by SAM 2-class Response (Mean False Discovery Rate < 8%)

Differentially expressed transcripts are listed in order of significance using the delta values generated by multi-class response Significance Analysis of Microarrays (SAM). The *p*-values shown for aging control comparison were derived from individual microarray signals using the 2-tailed *t*-test assuming unequal variances, with $p \leq 0.05$ considered as significant. Transcriptional differences with significant *p*-values are indicated in bold italics. Ratios of mean signal intensities for each comparison are expressed relative to young control mice, *i.e.* aged/young, and are shown in bold if greater than 2-fold.

Score (delta)	q-Value (%)	Gene Title	Signal Ratio	p-Value	Gene Ontology Biological Process
18.3	5.64	mannose binding lectin, serum (C)	1.48	*0.0003*	complement activation, classical pathway / heterophilic cell adhesion
17.1	5.64	retinol binding protein 1, cellular	**5.96**	*0.0004*	retinoid metabolism / transport /
16.9	5.64	**squalene epoxidase**	**5.56**	*0.0004*	electron transport / aromatic compound metabolism / metabolism

Score (delta)	q-Value (%)	Gene Title	Signal Ratio	p-Value	Gene Ontology Biological Process
16.4	5.64	matrix metalloproteinase 14 (membrane-inserted)	1.43	*0.0000*	proteolysis and peptidolysis / collagen catabolism
13.9	5.64	forkhead box A3	**2.27**	*0.0000*	cell glucose homeostasis / regulation of transcription, DNA-dependent / cellular response to starvation
12.0	5.64	dihydroorotate dehydrogenase	**2.07**	*0.0020*	'de novo' pyrimidine base biosynthesis / pyrimidine nucleotide biosynthesis
11.9	5.64	chaperonin subunit 5 (epsilon)	1.66	*0.0001*	protein folding
11.8	5.64	adaptor protein complex AP-2, mu1	1.15	*0.0034*	intracellular protein transport / vesicle-mediated transport
10.4	5.64	secreted phosphoprotein 1	**3.11**	*0.0001*	ossification / cell adhesion
10.4	5.64	mitochondrial ribosomal protein S12	1.44	*0.0003*	protein biosynthesis
10.1	5.64	enhancer of polycomb homolog 1 (*Drosophila*)	1.18	*0.0100*	---
10.0	5.64	intracisternal A particles	1.88	*0.0093*	---
9.9	7.52	lysosomal-associated protein 5	1.80	*0.0056*	---
9.7	7.52	**demethyl-Q 7 (Coq7)**	1.76	*0.0071*	ubiquinone biosynthesis
9.6	7.52	ectonucleoside triphosphate diphosphohydrolase 2	**3.48**	*0.0139*	G-protein coupled receptor protein signaling pathway / purine ribonucleoside diphosphate catabolism/ platelet activation
9.3	7.52	cat eye syndrome chromosome region, candidate 5	**2.23**	*0.0063*	Metabolism

Score (delta)	q-Value (%)	Gene Title	Signal Ratio	p-Value	Gene Ontology Biological Process
9.1	7.52	inosine 5'-phosphate dehydrogenase 2	1.48	*0.0088*	purine nucleotide biosynthesis / GMP biosynthesis / lymphocyte proliferation
9.0	7.52	RIKEN cDNA 1110002B05 gene	1.51	*0.0070*	---
9.0	7.52	unc-13 homolog A (*C. elegans*)	**5.49**	*0.0038*	intracellular signaling cascade / synaptic transmission / synaptic vesicle maturation
8.9	7.52	Era (G-protein)-like 1 (*E. coli*)	**2.71**	*0.0002*	---
8.5	7.52	**7-dehydrocholesterol reductase**	**3.08**	*0.0139*	cholesterol biosynthesis / sterol biosynthesis
-10.6	7.52	RIKEN cDNA 1110049F12 gene	0.61	*0.0003*	---
-11.0	7.52	cell death-inducing DNA fragmentation factor, alpha subunit-like	0.61	*0.0060*	apoptosis / induction of apoptosis
-13.9	5.64	expressed sequence C78977	0.66	*0.0000*	---
-16.3	5.64	autophagy 5-like (*S. cerevisiae*)	0.59	*0.0000*	autophagic vacuole formation / autophagy

Following the statistical analysis of the microarray data sets, biochemical, cellular, and functional classification of probe sets identified was accomplished using the Gene Ontology (GO) annotations obtained via the NetAffx™ bioinformatics center. To visualize groups of genes which follow age-related or dwarf-specific patterns of expression, cluster analysis of all probe set signal intensities was performed using the

updated Hierarchical Clustering Explorer 3.0 (HCE) which is publicly available at www.cs.umd.edu/hcil/hce (Seo et al., 2004; D'andrade, 1978; Johnson, 1967). While cluster analysis does not provide any measure of statistical significance, it does allow the identification of genes with similar patterns of expression, and can thus reveal co-regulation by similar biological pathways and or transcription factors, such as the SREBPs. As one of the largest differences in hepatic gene expression between dwarf and control mice, the major urinary proteins cluster tightly together and form a clearly identifiable clade on the dendrogram with greater than 98% similarity (Figure 8). Surprisingly, the weighted hierarchical clustering algorithm was also able to group the arrays correctly by genotype and age, based simply on the global pattern of expression of all probe sets on each array. Thus, the pattern of gene expression in dwarf livers is sufficiently distinct to be distinguished by hierarchical clustering, and dwarf-specific patterns of gene expression are clearly visible on the dendrogram. Finally, Figure 9 demonstrates that several cholesterologenic and sterol metabolic genes cluster together with a minimum similarity of 90%, strongly suggesting co-regulation by a common factor such as the SREBP transcription factors.

Of the differentially expressed probe sets identified by both statistical approaches described above, many $Pit1^{dw/dwJ}$ –related differences represent key components of cholesterol biosynthesis, sterol metabolism, or fatty acid homeostasis, and therefore served as the subsequent focus of this study of $Pit1^{dw/dwJ}$ hepatic gene expression. Other functional classes of transcripts consistently altered in $Pit1^{dw/dwJ}$ livers involve growth factor/IGF-1 signaling, xenobiotic/oxidative metabolism (cytochrome P450s), pheromone transport/binding (MUPs), redox balance (GSTs), and immune response. These transcripts constitute definitive alterations in hepatic gene expression of these long-lived animals, and define an age-independent transcriptional profile of male dwarf livers that may contribute to longevity determination.

Figure 8: Weighted Hierarchical Clustering Using the MAS 5.0 Detection *p*-Value

Using log-transformed signals for all U74Av.2 probe sets, complete datasets (N=14) were clustered by the average group linkage algorithm with detection *p*-values as weights. At a minimum similarity of 98%, a distinct cluster is formed which contains transcripts decreased in *Pit1*$^{dw/dwJ}$ livers including the major urinary proteins (MUPs) indicated by arrows. Many of these probe sets were identified by both SAM analysis and the selection strategy described above.

transcription factor Dp 1
heat shock factor binding protein 1
RIKEN cDNA 2310057H16 gene
RIKEN cDNA 1110059P08 gene
major urinary protein 3
major urinary protein 1
major urinary protein 5
epidermal growth factor receptor
zeta-chain (TCR) associated protein kinase
hydroxysteroid dehydrogenase-5, delta<5>-3-beta
insulin-like growth factor 1
insulin-like growth factor 1
major urinary protein 4
epidermal growth factor receptor
major urinary protein 1
major urinary protein 1
major urinary protein 1
epidermal growth factor receptor
elastase 1, pancreatic
retinol dehydrogenase 11
RIKEN cDNA 4632419J12 gene
cysteine sulfinic acid decarboxylase
complement component 9
insulin-like growth factor binding protein, acid labile subunit
gap junction membrane channel protein beta 2
cytochrome P450, family 2, subfamily f, polypeptide 2
kidney expressed gene 1
RIKEN cDNA 1100001H23 gene
RIKEN cDNA 1300013B24 gene
cofilin 2, muscle
camello-like 1
UDP-glucuronosyltransferase 2 family, member 5
leukemia inhibitory factor receptor
leukemia inhibitory factor receptor
interferon regulatory factor 6
serine (or cysteine) proteinase inhibitor, clade A, member 3C
ubiquitin specific protease 15
cysteine-rich protein 3
dopachrome tautomerase
ESTs
deiodinase, iodothyronine, type I
cytochrome P450, family 7, subfamily b, polypeptide 1
cytochrome P450, family 7, subfamily b, polypeptide 1
hydroxysteroid (17-beta) dehydrogenase 2
RIKEN cDNA 9130009C22 gene
SEC61, alpha subunit (S. cerevisiae)
mannan-binding lectin serine protease 1
complement component 4 binding protein
serum amyloid P-component
lymphocyte antigen 6 complex, locus E
cathepsin C
H1 histone family, member 0
guanine nucleotide binding protein (G protein), gamma 10
serine (or cysteine) proteinase inhibitor, clade A, member 3K
guanine nucleotide binding protein, alpha 14
mannose binding lectin, liver (A)
complement component 4 (within H-2S)
RIKEN cDNA 1300002F13 gene
ESTs
lymphotoxin B receptor
RIKEN cDNA 1300017J02 gene
coagulation factor XII (Hageman factor)
inter-alpha trypsin inhibitor, heavy chain 1
phospholipid transfer protein
epidermal growth factor receptor pathway substrate 15
cytochrome P450, family 2, subfamily c, polypeptide 70
RIKEN cDNA 3930401E15 gene
RIKEN cDNA 6330407G04 gene
ESTs
cDNA sequence BC019977
immediate early response 5
catechol-O-methyltransferase
deoxynucleotidyltransferase, terminal
deoxynucleotidyltransferase, terminal
inhibitor of DNA binding 2
RIKEN cDNA 1810073M23 gene
serum amyloid A 2
serum amyloid A 2

A DWDWU #8
A DWDWU #4
A DWDWU #3
A CON #24
A CON #2
A CON #1
Y CON #99
Y DWDWU #97
Y DWDWU (#95)
Y DWDWU #93
Y DWDWU #83
Y CON #88
Y CON #86
Y CON #84
Y CON #82

64

Figure 9: Weighted Hierarchical Clustering Using the MAS 5.0 Detection *p*-Value: *Pit1^{dw/dwJ}* Related Patterns of Gene Expression

Cluster analysis using the complete linkage algorithm identifies a single cluster with greater than 90% similarity which contains a large number of cholesterol biosynthetic genes (indicated by arrows). Additional sterol metabolism genes are members of this cluster suggesting co-regulation of many of these by SREBPs. Below this cluster can be seen a large group of age-related genes which increase in both dwarf and control livers.
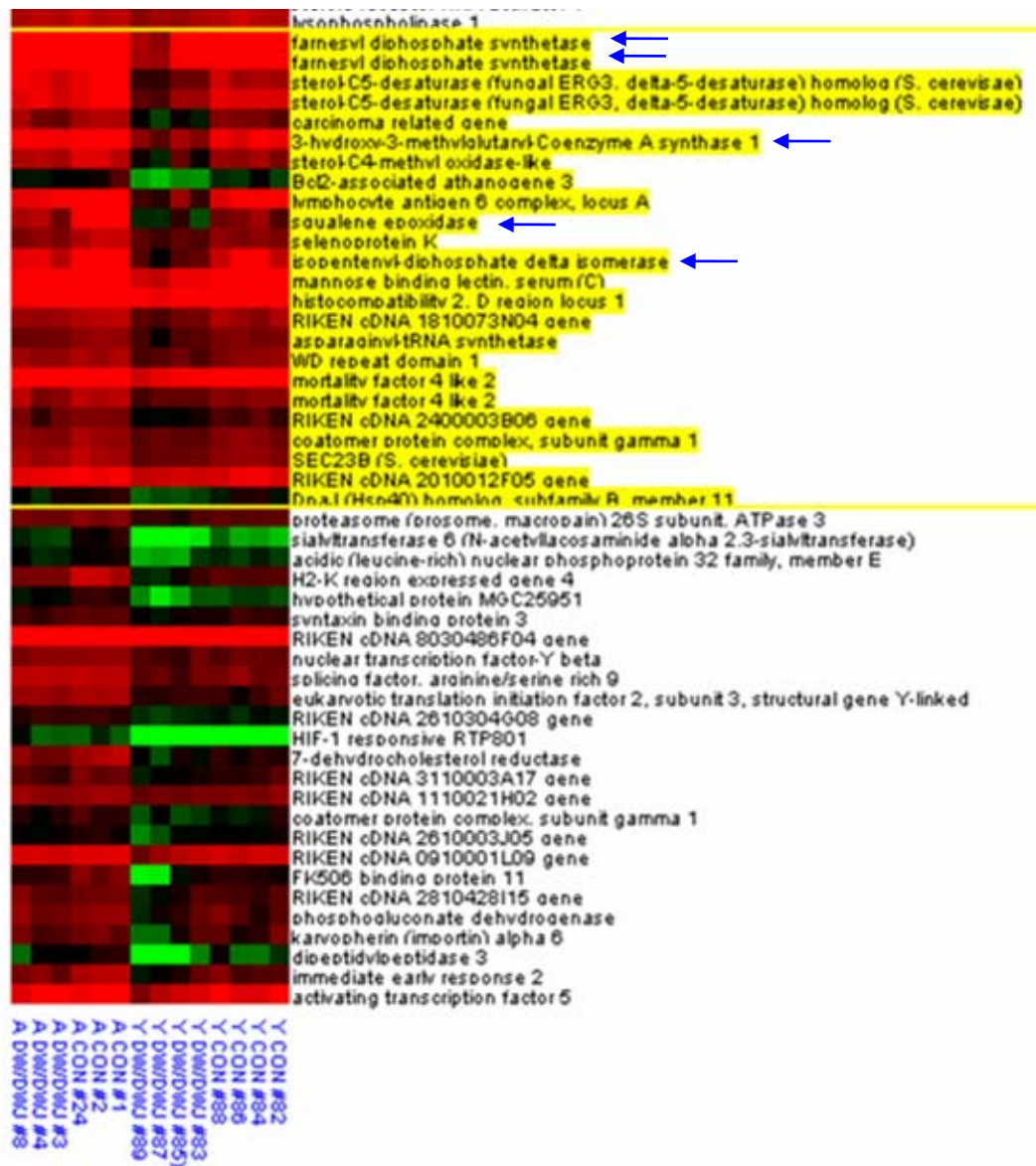
Real-time RT-PCR of Hepatic RNA

Since the effect of either the combined pituitary hormone deficiencies, or the aging process itself on the expression of commonly used housekeeping genes was initially unknown, three separate genes were used as invariant controls for normalization of input cDNA quantities. Shown in Figure 10, the non-corrected, mean C_t values for each group demonstrate some variation in these genes, as anticipated. However, the generation of composite normalization factors for each sample thus minimizes the error of correcting raw C_t values to a single 'invariant' control that shows statistically significant variation due to inherent biology, i.e., dwarfism and/or aging. For each transcript analyzed by real-time RT-PCR, amplification efficiencies were determined to ensure proper normalization and accurate calibration of relative differences in gene expression. Melting curves were generated to confirm the formation of a single product in each PCR reaction.
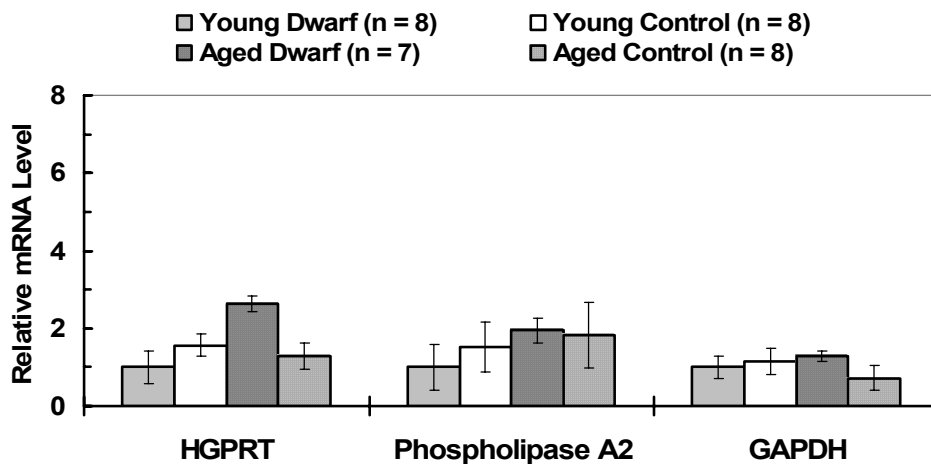
Figure 10: Relative Expression of Housekeeping Genes Used as Invariant Controls for Normalization

The relative mRNA abundance of each internal control transcript was quantified by real-time PCR amplification of cDNA libraries prepared from livers of 32 individual animals as described in 'Materials and Methods'. Depicted relative to the young control group, the mean C_t values and corresponding standard error shown for each experimental group are derived from the raw, non-corrected data, and were used to generate composite normalization factors for subsequent analysis.

66

Decreased Abundance of Cholesterologenic Transcripts in *Pit1^{dw/dwJ}* mice.

Comparative microarray analysis of male hepatic gene expression in young and aged Pit1^{dw/dwj} and control mice revealed persistent changes in key transcripts involved in cholesterol and oxysterol metabolism, *e.g.*, farnesyl diphosphate synthase, isopentenyl pyrophosphate isomerase, squalene epoxidase, CYP7b1, and two hydroxysteroid dehydrogenases (Tables 3, 4, and 5). Taken collectively, these transcriptional changes suggest that biosynthetic pathways essential for cholesterol and steroid homeostasis may be significantly altered in *Pit1^{dw/dwJ}* livers, particularly in young dwarf animals. Interestingly, squalene epoxidase exhibits one of the most significant differences in hepatic gene expression between young and aged control mice, indicating that increased squalene epoxidase expression is characteristic of the normal aging process. To investigate these differences further and to examine both male and female animals, selected cholesterologenic and lipogenic transcripts identified by microarray were analyzed by real-time RT-PCR. The relative expression of these transcripts as determined from individual cDNA libraries demonstrates that key enzymes throughout the cholesterol biosynthetic pathway are collectively diminished in dwarf livers of both ages and genders. Shown in Figure 11 below are the fluorescence-based thermal cycling traces for the amplification of squalene epoxidase from cDNA libraries constructed from individual dwarf and control livers. Measuring the accumulation of double-stranded PCR products by means of an intercalating fluorophore, SYBR® Green, these thermal cycling profiles demonstrate the marked decrease in squalene epoxidase (*Sqle*) expression in *Pit1^{dw/dwJ}* mice of both genders and ages relative to littermate controls. Additionally, the traces illustrate that there is a substantial increase in *Sqle* expression with age, particularly in both male and female dwarf animals. The bar graph (Figure 11B) of the non-normalized, group-wise mean C_t values clearly depicts both the dwarf-specific decrease and age-related increase in *Sqle* expression (C_t values are indirectly proportional to starting template abundance). The tight distribution of C_t values within each age- and phenotype-matched group is clearly indicated by the small standard errors shown. Finally, the graph also demonstrates gender-related differences in *Sqle* expression.

Figure 11: Thermal Cycling Profiles and Mean C$_t$ Values for Squalene Epoxidase

A.

B.
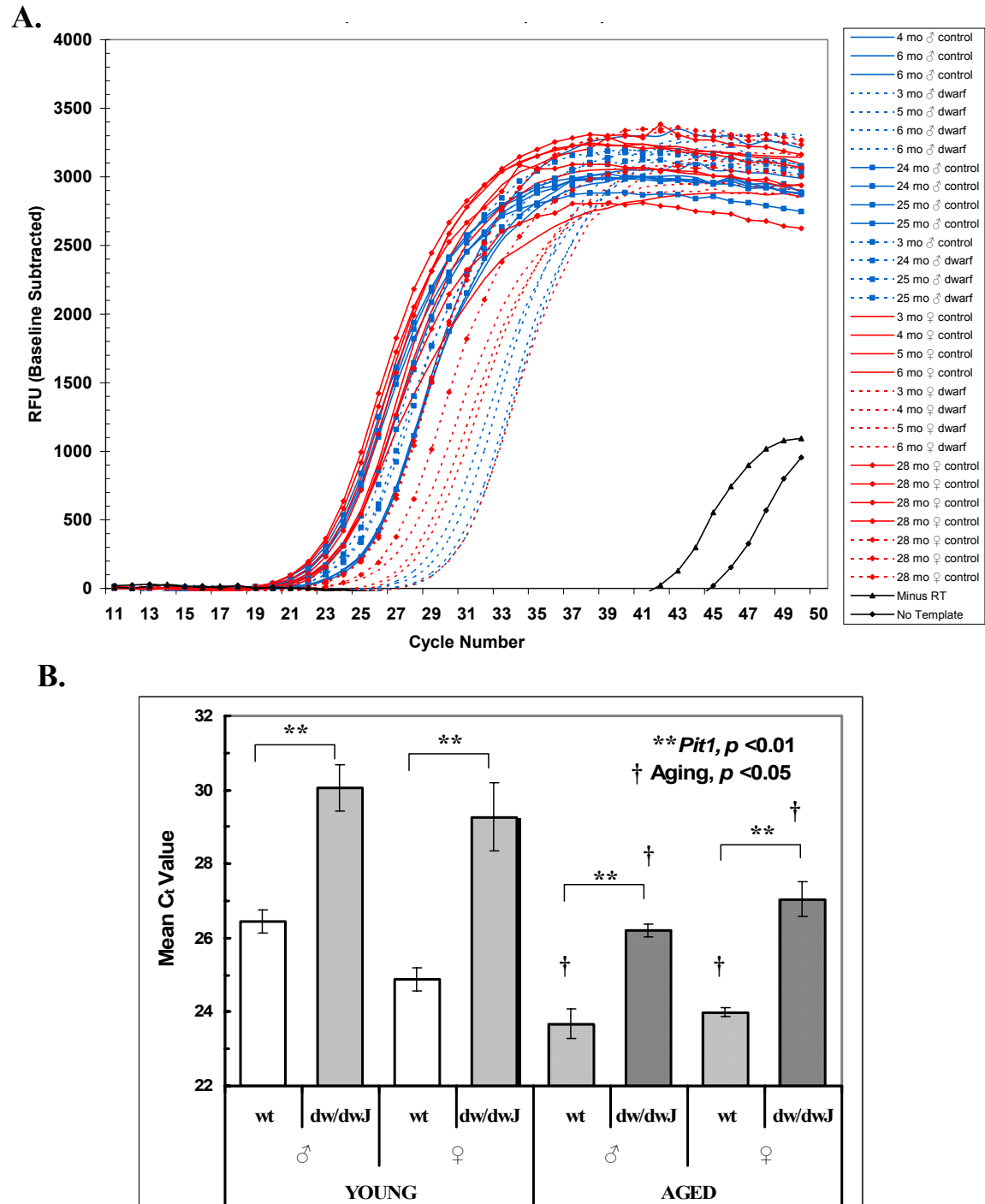
Figures 12 and 13 summarize the collective decreases in cholesterologenic transcripts including HMG-CoA synthase-1, mevalonate decarboxylase, isopentenyl isomerase, farnesyl diphosphate synthase, squalene epoxidase, and lanosterol demethylase (CYP51). The microarray hybridization experiments indicated no significant change in HMG-CoA synthase-2 (HMGCS2) expression in male dwarf livers relative to either young (-1.2 fold, $p = 0.07$) and aged (1.2-fold, $p = 0.15$) control mice, and real-time RT-PCR analysis of HMGCS2 expression further demonstrated no statistical difference between $Pit1^{dw/dwJ}$ animals of either age-group or gender. The normalized C_t values and statistical analysis of grouped comparisons have been previously published in *Aging Cell*, and can be accessed online as supplementary information (Boylston et al., 2004). Interestingly, HMGCS2 is a mitochondrial isoform critical for hepatic ketogenesis during carbohydrate depletion and enhanced fatty acid oxidation, but this isoform is not directly involved in cholesterol biosynthesis. In contrast, HMGCS1 is a cytosolic isoform that appropriates acetyl-CoA for cholesterol biosynthesis occurring in both the ER and peroxisomes. Both real-time RT-PCR and microarray analyses indicate that dwarf-related differences in the mRNA expression of these cholesterol biosynthetic enzymes are generally larger in young animals than in aged dwarf and age-matched controls for many of these cholesterol biosynthetic transcripts. Consequently, some of these transcripts did not achieve the level of statistical significance used by SAM to generate the list of 50 differentially expressed genes shown in Table 1; nevertheless, all of these genes met the statistical threshold of $p \leq 0.05$) in microarray comparisons of young dwarf *vs.* control animals. This fact demonstrates that real biological changes can be left undetected by microarray analysis when using statistical methods or thresholds which are too stringent, i.e., a small false discovery rate simultaneously imparts are large false negative, or Type II error, rate. For this reason, several levels of stringency should be utilized in microarray experiments in order to mine the datasets more thoroughly for potentially meaningful biological phenomena, which can be confirmed by additional methods.

With aging, statistically significant changes in the expression of several cholesterologenic genes were also found to occur in both control and dwarf animals. Figure 13 presents the real-time RT-PCR results for grouped comparisons of young and aged mice, and depicts age-related effects on the hepatic gene expression of a number of biosynthetic enzymes and transcription factors regulating cholesterol metabolism. These data indicate a general age-related increase in transcripts encoding several cholesterol biosynthetic enzymes in both dwarf and control livers. Microarray analysis of young and aged male control mice revealed significant age-associated increases in squalene epoxidase, farnesyl diphosphate synthase, and 7-dehydrocholesterol reductase expression, two of which were also demonstrated by RT-PCR. Further, several statistically significant, age-related transcriptional differences also show gender-specific patterns of expression in both phenotypes. Specifically, transcripts encoding HMG-CoA reductase, farnesyl diphosphate synthase, and squalene epoxidase are elevated in aged male livers of both dwarf and control animals, but the measured increase in aged females is not statistically significant. However, the inherent variability of gene expression in aged tissues makes achieving statistical significance difficult using relatively small sample sizes, and the aged female dwarf group was comprised of unfortunately three rather than four animals.

Recent studies have established that sterol regulatory element binding proteins (SREBPs) play a key role in the regulation of cholesterol biosynthesis (Horton et al., 2003; Horton et al., 2002; Shimomura et al., 1999; Horton et al., 1998). In particular, SREBP-2 preferentially activates the coordinated expression of cholesterologenic genes, whereas SREBP-1 regulates the expression of lipogenic genes (Horton et al., 2002). To explore the strong possibility that diminished SREBP expression could be responsible for the coordinated repression of cholesterol biosynthetic transcripts, the relative mRNA abundance of both SREBP-1 and SREBP-2 was determined by real-time RT-PCR, as only SREBP-1 was contained on the microarray. A small but statistically significant age-related increase in SREBP-2 expression was observed only in control mice (Figure 13).

70

Consequently, age-matched dwarf mice have comparatively lower levels of SREBP-2
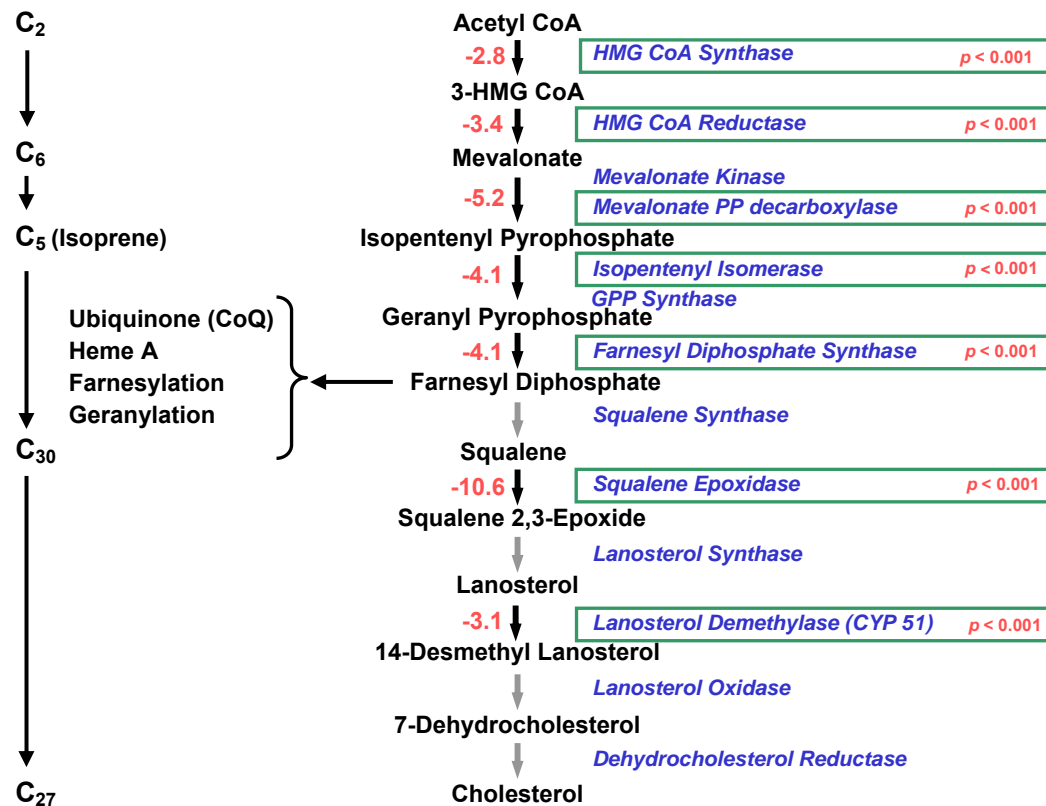mRNA relative to aged controls; however, the difference actually results from a modest

	Acetyl CoA		
C_2	-2.8 ↓	HMG CoA Synthase	$p < 0.001$
	3-HMG CoA		
	-3.4 ↓	HMG CoA Reductase	$p < 0.001$
C_6	Mevalonate		
		Mevalonate Kinase	
	-5.2 ↓	Mevalonate PP decarboxylase	$p < 0.001$
C_5 (Isoprene)	Isopentenyl Pyrophosphate		
	-4.1 ↓	Isopentenyl Isomerase	$p < 0.001$
		GPP Synthase	
	Geranyl Pyrophosphate		
Ubiquinone (CoQ)	-4.1 ↓	Farnesyl Diphosphate Synthase	$p < 0.001$
Heme A	Farnesyl Diphosphate		
Farnesylation	↓	Squalene Synthase	
Geranylation	Squalene		
C_{30}	-10.6 ↓	Squalene Epoxidase	$p < 0.001$
	Squalene 2,3-Epoxide		
	↓	Lanosterol Synthase	
	Lanosterol		
	-3.1 ↓	Lanosterol Demethylase (CYP 51)	$p < 0.001$
	14-Desmethyl Lanosterol		
	↓	Lanosterol Oxidase	
	7-Dehydrocholesterol		
	↓	Dehydrocholesterol Reductase	
C_{27}	Cholesterol		

**Figure 12: Collective Decrease in Cholesterol Biosynthetic Transcripts in *Pit1*[dw/dwJ]
Livers.**

The biosynthetic pathway for *de novo* cholesterol production is depicted with
enzymes catalyzing each step and the number of carbons contained in each intermediate
shown on the left. Fold changes and *p*-values listed in this figure were calculated from
combined real-time RT-PCR analyses of *all* dwarf *vs*. control animals (N=15, N=16,
respectively). Several important bioactive molecules and cellular processes derived from
pre-squalene intermediates are also listed.
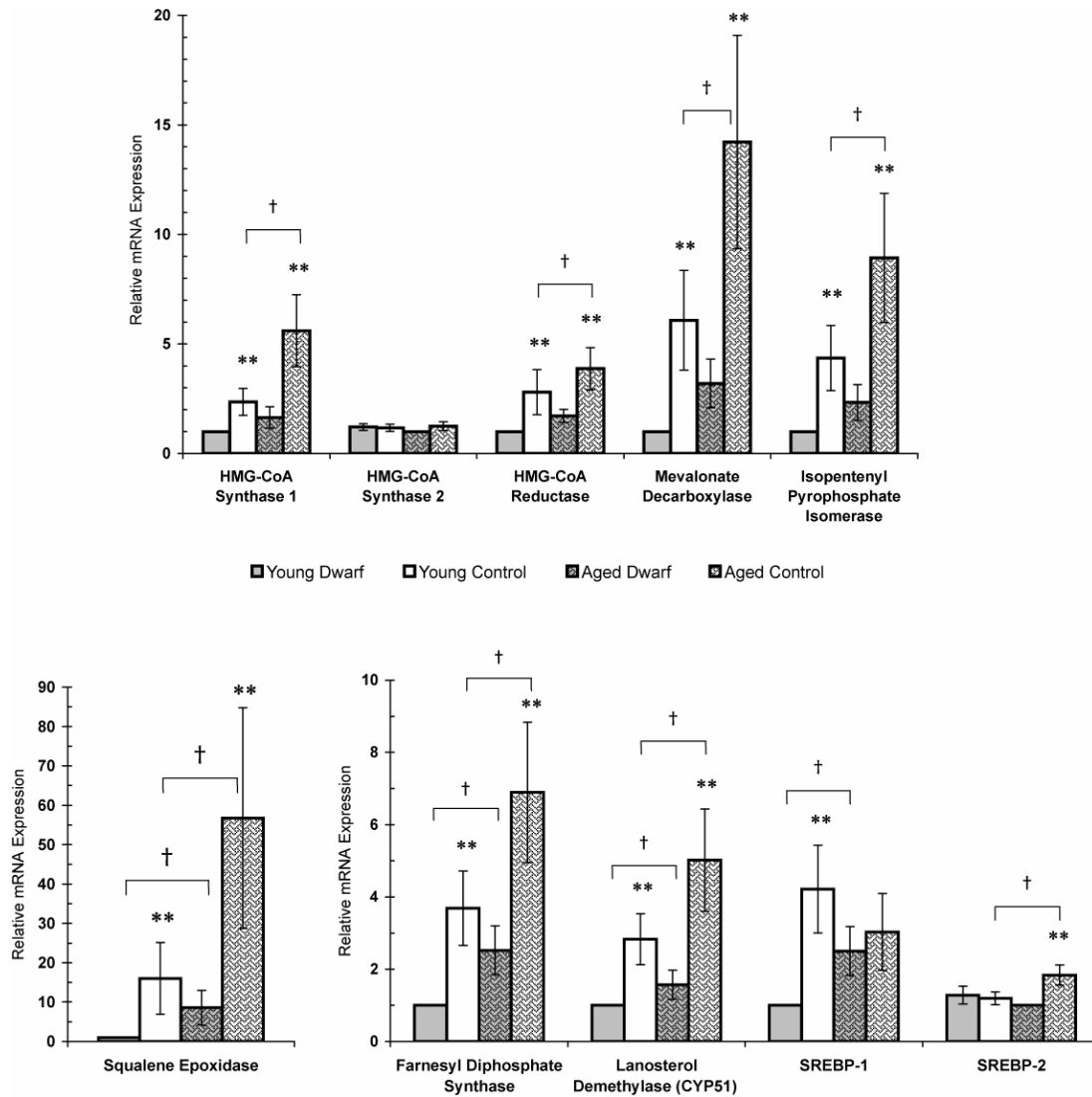
Figure 13: Diminished Expression of Cholesterol Biosynthetic Genes in *Pit1$^{dw/dwJ}$* Liver.

The relative mRNA abundance for cholesterologenic transcripts was quantified by real-time PCR. Differences in normalized mean C_t values between groups were converted to relative expression levels by the formula $2^{\Delta Ct}$ with the propagated standard errors indicated. Depicted relative to the young dwarf, the abundance of each cholesterologenic transcript is graphically presented. (N=32) * p <0.05 and ** p <0.01, dwarf *vs.* control; † p <0.05, young *vs.* aged.

72

age-associated increase in expression of SREBP-2 in aged control mice. In contrast, the abundance of SREBP-1 mRNA was significantly reduced in young dwarf animals, but with aging the level of SREBP-1 expression in the dwarf increased to that of the age-matched controls (Figure 13). Thus, the collective decrease in cholesterol and fatty acid synthesis in the young dwarf livers may be mediated at the transcriptional level through reduced SREBP-1 expression, and possibly through insulin-regulated, post-transcriptional processing of SREBP-2 (Matsuda et al., 2001).

Lipid and fatty acid metabolism in *Pit1$^{dw/dwJ}$* mice

These microarray and real-time RT-PCR analyses indicate that the combined hormonal deficiencies, *i.e.*, GH, TSH, prolactin, and IGF-1/insulin, result in profound changes in the hepatic expression of genes involved in fatty acid metabolism and transport. Supported by a large number of previous studies, many of these transcriptional changes may directly result from the GH deficiency of these mice, as administration or lack of this hormone is well known to cause abnormalities in lipoprotein and lipid profiles (Bramnert et al., 2003; Tollet-Egnell et al., 2003; Colao et al., 2002; Gardmo et al., 2002; Frick et al., 2002; Flores-Morales et al., 2001; Frick et al., 2001; Heffernan et al., 2001; Tollet-Egnell et al., 2001; Fain and Bahouth, 2000; Beentjes et al., 2000; Christ et al., 1999; Kopchick et al., 1999; Oscarsson et al., 1999; Russell-Jones et al., 1994; Asayama et al., 1984). However, other transcriptional differences identified in these mice cannot be fully explained by the growth hormone deficiency alone. Presented in Figure 14, significant transcriptional changes in hepatic lipid homeostasis and fatty acid metabolism appear characteristic of *Pit1$^{dw/dwJ}$* mouse livers.

The persistent increase in peroxisome proliferator-activated receptor gamma (PPARγ) expression in both young and aged *Pit1$^{dw/dwJ}$* liver is of particular importance to energy metabolism, insulin sensitivity, mitochondrial biogenesis, and perhaps longevity. Notably, microarray hybridizations of three PPAR isoforms on the U74Av.2 gene chip indicated that only PPARγ was found to be significantly up-regulated in male dwarf livers at both ages. By real-time RT-PCR analysis, a similar 3.8-fold increase ($p < 0.001$)

in PPARγ mRNA was demonstrated for male and female dwarf livers at both ages, relative to littermate controls. As shown in Figure 14, the increase in PPARγ expression relative to age-matched controls was approximately 4.0- and 3.4-fold ($p < 0.001$) in young and aged *Pit1*$^{dw/dwJ}$ livers, respectively. The increased expression of PPARγ in dwarf livers may directly alter energy homeostasis by affecting the transcriptional regulation of hepatic triglyceride content, glucose metabolism, and the modulation of insulin sensitivity (Matsusue et al., 2003; Oberkofler et al., 2002).

The combined increase (8.6-fold, $p < 0.001$) in β$_3$ adrenergic receptor (β$_3$-AR) mRNA in male and female dwarf livers (Figure 14) may also indicate altered energy metabolism. Specifically, β$_3$-AR expression is increased 10.8-fold ($p<0.001$) in the young male dwarf and young females exhibit a 6.9-fold increase ($p < 0.001$) in mRNA levels of this receptor relative to control animals. Intriguingly, male dwarfs demonstrate an age-related 3.1-fold decrease ($p < 0.01$) in β$_3$-AR expression, thereby reducing the magnitude of the difference in β$_3$-AR expression between aged dwarf and control mice; nevertheless, β$_3$-AR mRNA is still significantly elevated in the aged dwarf livers relative to their littermate controls (2.4-fold, $p = 0.005$). Central to energy homeostasis and metabolic control, adrenergic signaling antagonizes insulin action, inhibiting glucose uptake, fatty acid biosynthesis, and fat storage; further, this transcriptional change in β$_3$-AR may also affect the catabolism of glycogen and fatty acids as well as the mobilization of intracellular triglyceride stores in *Pit1*$^{dw/dwJ}$ mice.

Also influencing fatty acid metabolism, the very low-density lipoprotein receptor (VLDLR) and lipoprotein lipase are strikingly up-regulated in both male and female dwarf mice, and are key components of lipid transport and uptake (Figure 14). In particular, the VLDLR exhibits an 11.4-fold up-regulation in the young dwarf mice (p <0.001), and a 7.0-fold ($p < 0.001$) increase in aged dwarf mice compared to age-matched controls. However, there is an apparent gender-specific difference in VLDLR expression levels. Young male *Pit1*$^{dw/dwJ}$ mice exhibit a greater difference in the
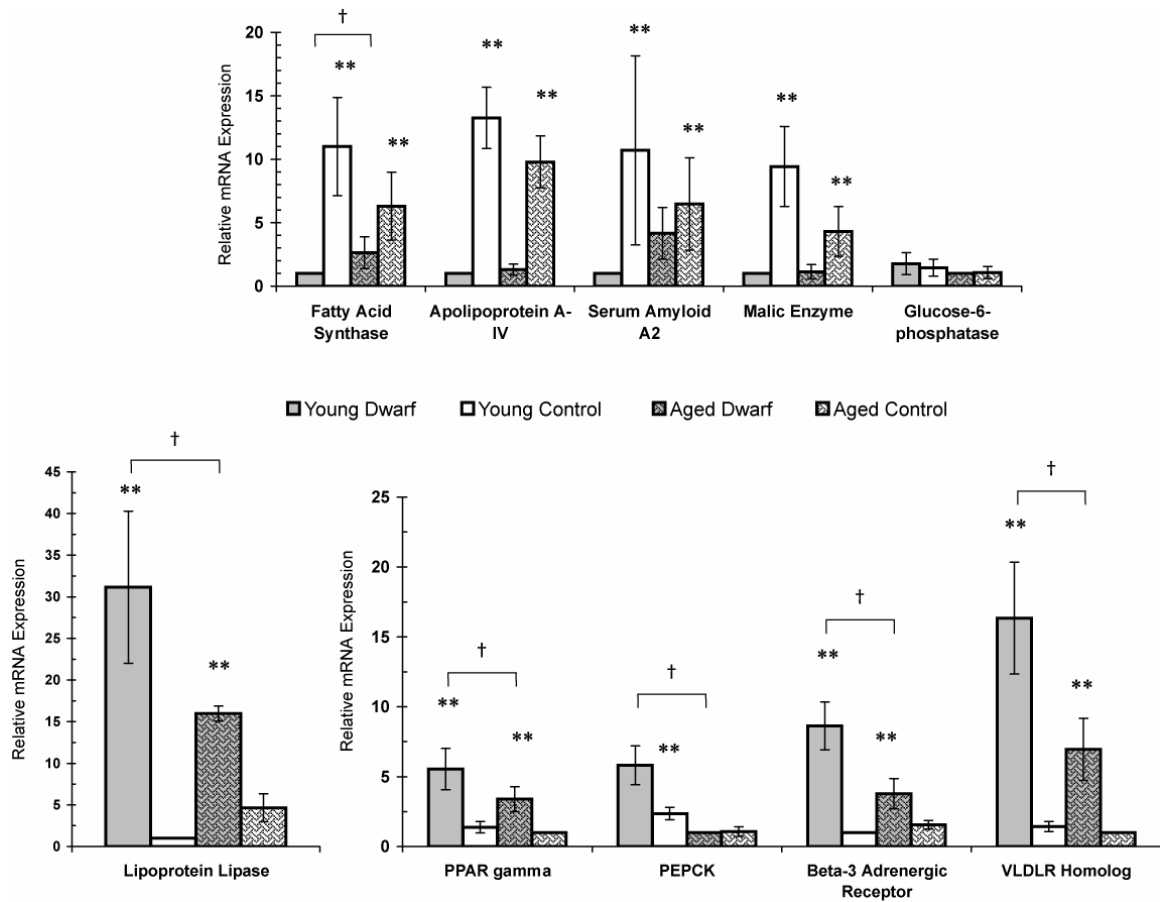
Figure 14: Relative Abundance of Lipogenic and Gluconeogenic Transcripts in Young and Aged *Pit1^{dw/dwJ}* Livers.

The relative mRNA abundance for lipogenic and gluconeogenic transcripts was quantified by real-time PCR. Differences in normalized mean C_t values between groups were converted to relative expression levels by the formula $2^{\Delta Ct}$ with the propagated standard errors shown. The abundance of each transcript is graphically represented relative to the young dwarf in the upper panel, and relative to the young control in the lower panel. (N=32) * $p < 0.05$ and ** $p < 0.01$, dwarf *vs.* control; † $p < 0.05$, young *vs.* aged.

abundance of VLDLR mRNA than do young female dwarfs relative to young control mice (16.4-fold *vs.* 8.0-fold); further, this gender effect persists in the aged dwarf livers with males demonstrating a greater difference in expression relative to gender- and age-matched controls (see supplementary data for Boylston *et al.*, 2004). Similarly, lipoprotein lipase expression was increased greater than 10-fold ($p<0.001$) in all dwarf mouse livers; however, the largest increase was observed in young female dwarf mice (44.4-fold), which is twice that of the young male dwarf mice (21.9 fold) compared to littermate controls. Interestingly, the data do not indicate any significant gender-related differences in lipoprotein lipase mRNA expression for aged dwarf mice relative to littermate controls. Lipoprotein lipase catalyzes the removal of triglycerides from circulating lipoproteins, and its relative expression level in a particular tissue is the rate-limiting factor for fatty acid uptake (Preiss-Landl et al., 2002). Newly synthesized fatty acids in the liver are transported via very low density lipoproteins (VLDL) to adipocytes for storage and to heart and muscle for energy production (Lee et al., 2003a). Since lipoproteins are the primary transporters of lipids and cholesterol in the blood, and are composed of triglycerides (TG), cholesterol esters (CE), phospholipids, and constituent apolipoproteins, these observations indicate substantial changes in lipid and fatty acid transport and uptake in $Pit1^{dw/dwJ}$ mice.

Relative quantification by real-time RT-PCR also demonstrates a significant decrease in the expression of genes central to lipogenesis, *i.e.,* fatty acid synthase (FAS) and malic enzyme. The data show that the down-regulation in fatty acid synthase expression in young $Pit1^{dw/dwJ}$ livers is 11.0-fold ($p < 0.001$), and the difference is nearly the same for both male (9.4-fold) and female (12.9-fold) young dwarf mice. However, the observed difference in FAS expression between aged dwarf and control mice (2.3-fold) is no longer statistically significant ($p = 0.066$). An age-associated pattern of expression was also observed for malic enzyme mRNA. Young $Pit1^{dw/dwJ}$ livers exhibit a 9.4-fold decrease in malic enzyme expression ($p < 0.001$), but the difference between aged dwarf and control is only 3.8 fold ($p = 0.013$). This large dwarf-related difference in malic enzyme and fatty acid synthase (FAS) expression in young mice does not persist

in aged dwarf mice, demonstrating a more profound shift in energy metabolism in young dwarf mice. Perhaps established in young animals, this apparent metabolic shift toward enhanced fatty acid utilization and decreased lipogenesis reflects a coordinated program of gene expression which may participate in longevity extension.

Comparative microarray results revealed a specific down-regulation of apolipoprotein A-IV (Apo A-IV) expression by 4.7-fold in the young male dwarf and by 5.6-fold in the aged male (Figure 15). The difference in hepatic Apo A-IV expression was statistically significant only for comparisons of young mice ($p << 0.05$), and did not reach the statistical threshold in the aged comparison ($p = 0.6$). Apo F expression was significantly different only between young dwarf and control livers. Intriguingly, the effect of the *Pit1* mutation on hepatic apolipoprotein expression appears to be quite selective. Of the probe sets on the array representing apolipoproteins, only the expression of Apo A-IV was consistently and significantly affected by the *Pit1* mutation.

Apolipoproteins comprise a family of secreted proteins whose functions involve the transport of triglycerides and cholesterol to tissues for either energy storage or immediate oxidation. Interestingly, recent evidence links human longevity to increased lipoprotein particle size and cholesterol ester transfer protein (CETP) abundance which define an aging phenotype which is associated with a lower prevalence of hypertension and cardiovascular disease (Barzilai et al., 2003). The summary of real-time RT-PCR analyses depicted in Figure 14 indicates that Apo A-IV mRNA levels are decreased by 13.3-fold (p < 0.001) in young dwarf mice and by 7.5-fold (p < 0.001) in aged dwarf mice. The down-regulation in dwarf expression of Apo A-IV is approximately twice as great in young females compared to the young males. The relative decrease in mRNA level persists in aged female dwarf mice (12.2-fold), whereas in aged males the decrease is not as large as in the young male dwarf mice (compare 9.6-fold vs. 5.3-fold in young vs. aged male dwarf mice). Interestingly, Apo A-IV expression is also altered significantly in the livers of GH-deficient mice, caloric restriction, and aging liver (Olsson et al., 2003; Miller et al., 2002; Tollet-Egnell et al., 2001). These RT-PCR data indicate that the selective decrease in hepatic Apo A-IV expression is characteristic of

long-lived Snell dwarf livers and further demonstrate that the GH-deficiency of these mice is likely responsible for the diminished expression of this apolipoprotein.

In light of the substantial transcriptional alterations potentially affecting lipid and fatty acid metabolism, we also examined key regulators of carbohydrate metabolism in dwarf livers, in particular gluconeogenesis and glycogenolysis. As key regulatory mechanisms for these pathways, two rate limiting enzymes, phosphoenolpyruvate carboxykinase (PEPCK) and glucose-6-phosphatase (G6Pase) were subjected to real-time RT-PCR analysis. Our microarray analysis demonstrated no statistical difference in the expression of many glycolytic and gluconeogenic transcripts between male dwarf and control animals for both age group comparisons. Shown in Figure 14, real-time RT-PCR of male and female mice also demonstrated no statistical difference in G6Pase expression, and few statistically significant changes in G6Pase expression were observed in aged livers relative to young animals. In contrast, PEPCK mRNA was significantly increased in young male and female dwarf livers by 2.4-fold ($p < 0.05$) and 2.6-fold ($p < 0.05$) respectively, suggesting an enhanced gluconeogenic capacity in young dwarf animals. Similarly, hepatic activation of gluconeogenesis also occurs during fasting and low circulating insulin levels. With aging, PEPCK expression was significantly decreased in both dwarf and control mice, but dwarf animals demonstrated a greater decline in expression (5.8-fold *vs*. 2.2-fold, respectively). As suggested by the diminished PEPCK but similar G6Pase expression levels, young dwarf livers may thus have a greater gluconeogenic activity with normal hepatic glucose export compared to control mice.

To determine whether these differences in cholesterologenic and lipogenic gene expression had an actual effect on circulating triglycerides and cholesterol, plasma lipid profiles were performed for both male and female *Pit1*$^{dw/dwJ}$ mice. Shown in Figure 16, significant differences in young dwarf livers were found in total cholesterol and triglycerides for both male and female animals and are in agreement with the altered transcriptional profiles. However, decreased plasma cholesterol and triglycerides does

not persist in aged dwarf animals, a finding also in agreement with the decrease in the

magnitude of gene expression differences between aged dwarf and control livers.
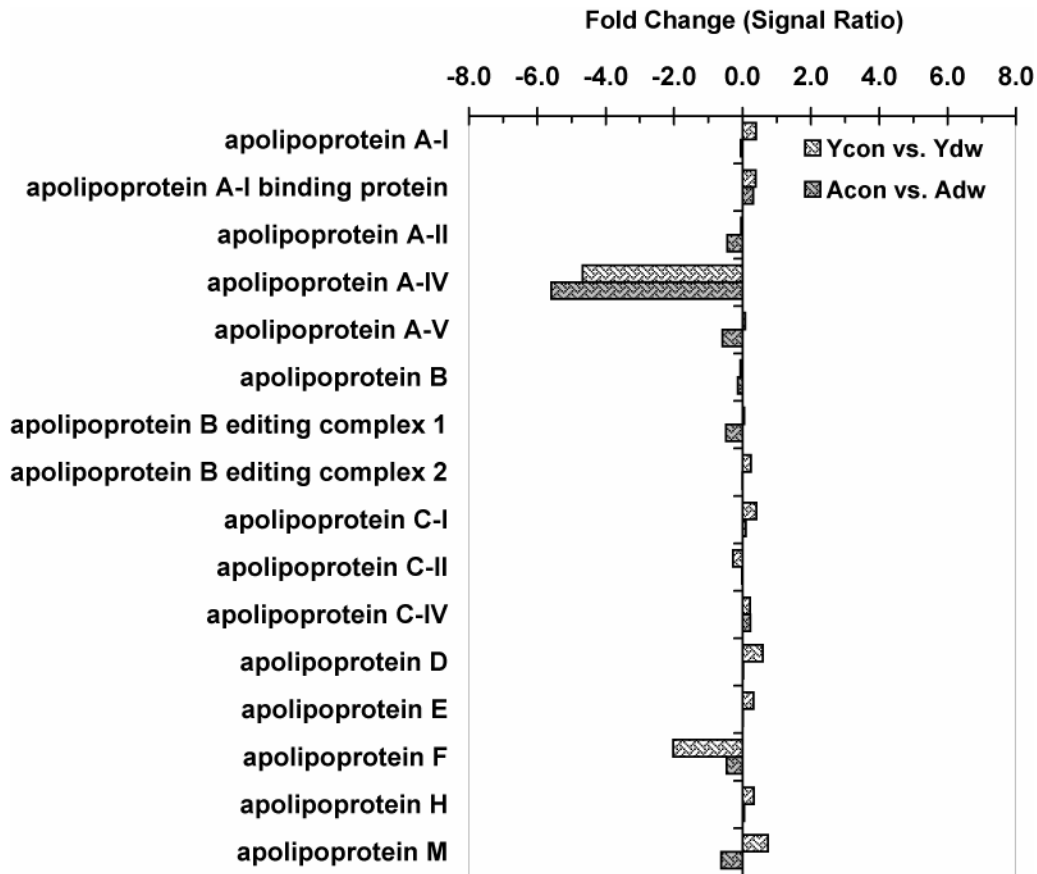
Figure 15: Microarray Analysis of Apolipoprotein Expression in *Pit1^{dw/dwJ}* Livers.

All apolipoproteins and editing complexes contained on the array were examined for age-matched differences in expression between dwarf and control mice. As shown, only Apo A-IV expression was consistently altered in dwarf livers at both ages compared. Relative fold changes were calculated from the ratios of mean signal intensities as described in Materials and Methods.

Notably, pancreatic lipase activity, which is distinct from lipoprotein lipase

activity, was significantly diminished in both male and female dwarf plasma at both ages,

which is counter to the observed increase in hepatic lipoprotein lipase expression.

Figure 16: Plasma Lipid Profiles

81
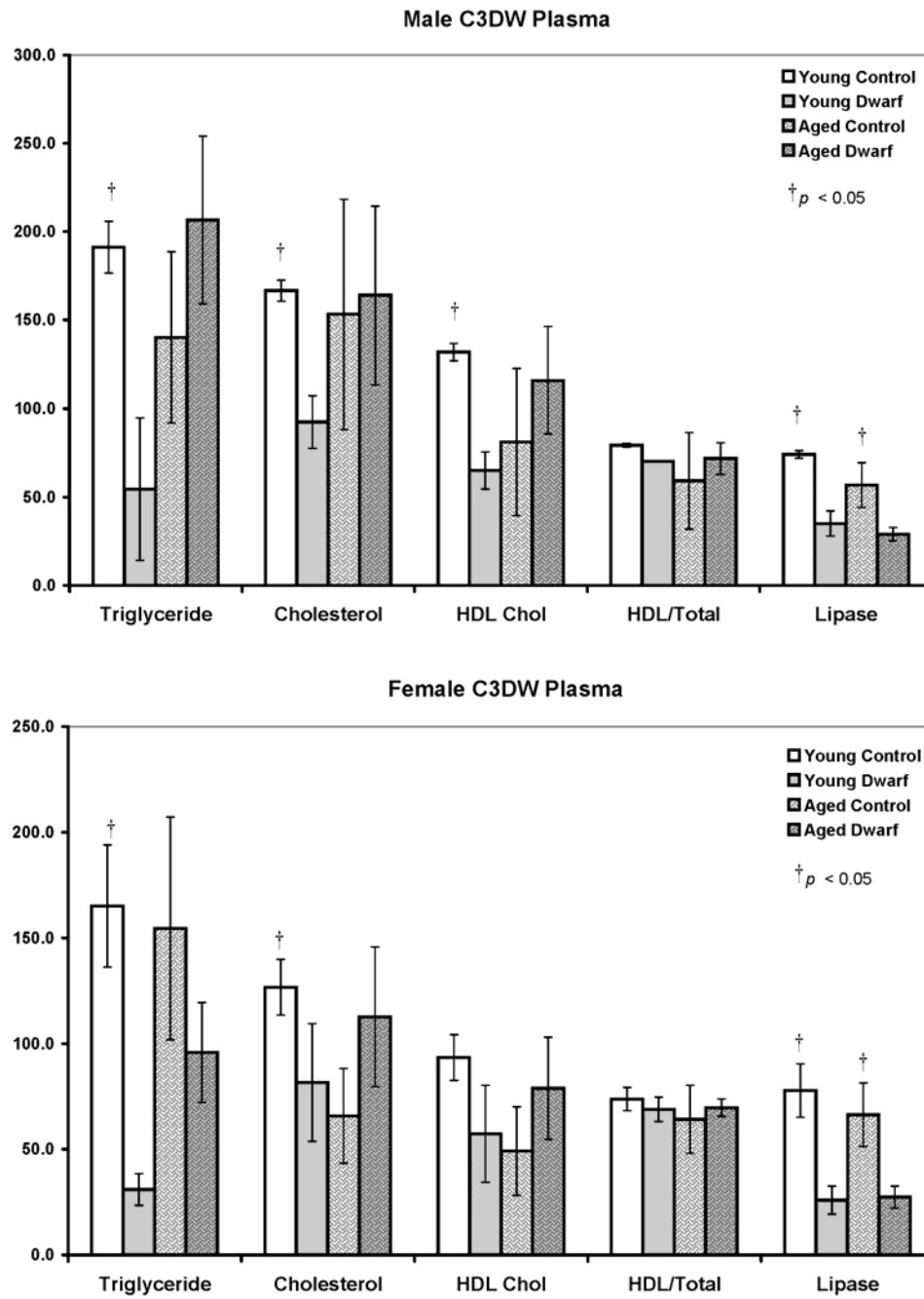
DISCUSSION

These studies have identified striking changes in the hepatic expression of genes regulating cholesterol biosynthesis, lipid transport, and fatty acid metabolism in $Pit1^{dw/dwJ}$ mice. Increased lifespan in Snell and Ames dwarf mice and other GH-deficient mice is believed to result from decreased IGF-1 production and lower plasma insulin; yet, the pro-longevity effects of combined GH/insulin/IGF-1 deficiency on hepatic carbohydrate and fatty acid metabolism are largely unknown. In the current study, the transcriptional profile of both young and aged $Pit1^{dw/dwJ}$ livers is characterized by significant decreases in the expression of genes regulating lipid and cholesterol biosynthesis and metabolism, and of key gluconeogenic enzymes. This global shift in hepatic metabolism related to combined GH, insulin/IGF-1 and TSH deficiencies may be a critical factor in the increased longevity of $Pit1^{dw/dwJ}$ dwarf mice, and may parallel alterations in hepatic gene expression induced by caloric restriction.

GH, IGF-1/insulin and TSH play crucial roles in the regulation of hepatic fatty acid oxidation, lipogenesis, gluconeogenesis, and glycogenolysis, and are important factors in longevity determination. The regulation of hepatic gene expression by insulin and TSH is mediated by at least two families of transcription factors, the SREBPs and the forkheads (Foufelle and Ferre, 2002). In the mammalian liver, three SREBPs have been directly linked to the transcriptional activation of over 30 genes regulating cholesterol and fatty acid metabolism (Horton et al., 2002); SREBP-1a is a potent activator of cholesterol, fatty acid, and triglyceride biosynthesis, and its isoform SREBP-1c is a weaker, yet more selective activator of fatty acid and triglyceride biosynthesis. Recently, SREBP-1c has been linked to the transcriptional activation of glycolytic and lipogenic genes by insulin (Chen et al., 2004; Zhang et al., 2003; Tobin et al., 2002). Of the three hepatic isoforms, SREBP-2 preferentially targets cholesterologenic transcripts (Horton et al., 2002). Our microarray and real-time RT-PCR studies reveal a concerted decrease in the expression of many SREBP-regulated genes in $Pit1^{dw/dwJ}$ livers at both ages investigated, and decreased SREBP-1 mRNA abundance in young dwarf animals. Consequently, SREBPs are strong candidate genes responsible for the observed

activation and repression of cholesterol and fatty acid metabolic genes in $Pit1^{dw/dwJ}$ livers. This collective down-regulation is similar to the inhibitory effect of fasting on the expression and proteolytic activation of SREBPs in the liver, and may therefore parallel those of caloric restriction. Of particular relevance to lifespan extension by CR is that the mRNA levels of PPARγ, SREBP-1 and SREBP-2, farnesyl diphosphate synthase (FDPS), HMG-CoA synthase, and LDLR are down regulated by fasting (24 hr), and return to normal levels within 12 hours after re-feeding (Engelking et al., 2004; Laffitte et al., 2003; Liang et al., 2002). FAS mRNA was also diminished by 24 hour fasting, but re-feeding induced supra-normal expression of the enzyme. Given their response to fasting conditions and their direct activation by insulin stimulation, the status of the SREBPs may thus play an integral role in the extended life spans of $Pit1^{dw/dwJ}$ and CR mice.

In this report, we demonstrate that mRNAs encoding cholesterol and fatty acid biosynthetic enzymes are coordinately down-regulated in dwarf livers, while key transcripts for lipid mobilization and oxidation are increased in both young and aged $Pit1^{dw/dwJ}$ dwarf livers. These results imply that essential precursors of isoprenoid biosynthesis may be decreased in dwarf livers perhaps resulting in CoQ and Heme A deficiencies. Supported by recent longevity studies in *C. elegans*, these data substantiate the possibility that altered mitochondrial and/or peroxisomal oxidative metabolism may play a key role in the extended life span of $Pit1^{dw/dwJ}$ mice.

Our results suggest that the coordinated down regulation of cholesterol biosynthesis pathway may affect important metabolic and intracellular processes that are derived from this pathway. In particular, farnesyl diphosphate serves as the common biosynthetic precursor for the isoprenoid tail of ubiquinone/coenzyme Q (CoQ) and heme A, as well as for lipophilic modifications to proteins by farnesylation and geranylation. Further, the discovery that Coq7 expression is significantly increased in aged control liver further implicates CoQ in the mammalian aging process.

It is plausible that decreased cholesterol biosynthesis may also diminish functional CoQ levels and thus affect mitochondrial electron transport and the

83

concomitant release of reactive oxygen species (ROS). This investigation of hepatic gene expression has revealed that a substantial number of cholesterologenic transcripts are coordinately decreased in $Pit1^{dw/dwJ}$ livers, implying that essential precursors of isoprenoid biosynthesis used in the formation of the polyprenyl tail of ubiquinone may be decreased in dwarf livers. Consistent with recent longevity studies in *C .elegans,* these data indicate that altered CoQ production in $Pit1^{dw/dwJ}$ livers may likewise increase lifespan by diminishing oxidative stress in rodents as demonstrated in nematode models, further supporting the hypothesis that oxidative stress and mitochondrial generation of ROS play a key role in longevity determination (Jonassen et al., 2003; Larsen and Clarke, 2002; Golden et al., 2002; Sohal et al., 2002; Jonassen et al., 2001; Larsen, 1993).

In the last several years, genetic evidence and dietary studies have firmly established the importance of CoQ in regulating life span in *C. elegans*. The *clk-1* gene encodes a terminal enzyme in CoQ biosynthesis and has long been known to extend nematode life-span (Johnson et al., 2000), although the mechanism has only recently been elucidated. Removal of CoQ from the diet of wild-type nematodes increases adult lifespan by approximately 60%, and also further extends the longevity of several long-lived *daf* mutants (Larsen and Clarke, 2002). Recently, long-lived *clk-1* mutants have been demonstrated to be defective in CoQ_9 biosynthesis, and consequently accumulate an intermediate of CoQ synthesis, demethoxyubiquinone (DMQ_9), which alters mitochondrial electron transport and may even be a more efficient scavenger of free radicals in the mitochondrion (Tatar and Rand, 2002; Jonassen et al., 2002; Jonassen et al., 2001). Dietary studies in *C. elegans* substantiate the importance of CoQ in longevity determination, and indicate that CoQ may modulate longevity by affecting mitochondrial respiration and function (Larsen and Clarke, 2002; Stenmark et al., 2001). Biochemical studies have also demonstrated alterations in mitochondrial respiratory function and reproductive fitness by varying the length of the polyprenyl tail of Co Q, thereby affecting its solubility in mitochondrial membranes (Jonassen et al., 2003; Hihi et al., 2003; Miyadera et al., 2001).

Recent evidence in murine models links the regulation of CoQ biosynthesis to retinoid X receptor alpha (RXRα) signaling (Bentinger et al., 2003). As heterodimers with liver X receptors (LXRs), retinoid X receptors regulate hepatic cholesterol and fatty acid metabolism through activation of SREBP expression (Maxwell et al., 2003). Notably, the expression of LXRs is not altered by fasting, but their activity is regulated by oxysterols, an oxygenated product of cholesterol metabolism (Chen et al., 2004; Adams et al., 2004; Laffitte et al., 2003; Lu et al., 2001). Further, these mammalian nuclear hormone receptors belong to the same class of steroid receptors as the *C. elegans* nuclear steroid hormone receptor, *daf-12*, shown to modulate the *daf-2/daf-16* longevity-promoting pathway. (Shostak et al., 2004; Ludewig et al., 2004; Dowell et al., 2003; Murakami et al., 2000; Snow and Larsen, 2000)

Pertinent to longevity studies of the conserved insulin-like *daf-2/daf-16* pathway, recent evidence demonstrates that PPARγ interacts with the forkhead transcription factor, FKHR (Foxo1), indicating a convergence of PPAR and FKHR signaling in mammalian systems (Dowell et al., 2003). The FKHR protein is a mammalian ortholog of *daf-16*, and plays a central role in the transcriptional activation of insulin-regulated genes. In more complex mammalian systems, PPARγ may thus be one functional equivalent of *daf-12*, whose putative steroid ligand influences nematode longevity by modulating *daf-16* signaling. Two PPAR isoforms, α and γ, are predominantly expressed in the liver, and PPARα is known to stimulate hepatic β-oxidation and ketogenesis during fasting (Ip et al., 2003). In contrast, PPARγ plays a central role in glucose and cholesterol homeostasis by regulating genes controlling carbohydrate utilization and influencing insulin sensitivity, as well as those regulating cholesterol efflux and transport (Akiyama et al., 2002; Picard and Auwerx, 2002). Consequently, peroxisome proliferator-activated receptors are implicated in a number of metabolic diseases including diabetes, obesity, and hyperlipidemia, and are the primary targets of anti-diabetic agents (Lee et al., 2003a). Heterodimerizing with RXRs, PPARs and LXRs interact to induce the expression of SREBPs thereby orchestrating a complete program of metabolic gene expression (Yoshikawa et al., 2003; Yamauchi et al., 2001). In rats, PPARs regulate the expression

of genes induced by thyroid hormone stimulation including malic enzyme, mitochondrial glycerol-3-phosphate dehydrogenase, glucose-6-phosphate dehydrogenase, and SPOT14 (Viguerie and Langin, 2003). Hence, the TSH-deficiency in dwarf mice may be responsible for the observed decrease in malic enzyme as well as other key lipogenic transcripts via attenuated transcriptional activation of PPAR-regulated genes. PPARγ is also known to influence mitochondrial function, and one isoform, PPARγ2 has recently been demonstrated to be localized within the mitochondrial matrix (Casas et al., 2000). Thus, the up-regulation of PPARγ in dwarf mice may influence mitochondrial function and the availability of substrates for energy metabolism. In addition to the role of GH, these gene expression studies therefore strongly suggest that the TSH- deficiency of *Pit1$^{dw/dwJ}$* mice most likely contributes substantially to the altered metabolic profile of these mice, and may also play an important role in longevity determination through changes in hepatic energy metabolism (Shin and Osborne, 2003; Viguerie and Langin, 2003; Zhang et al., 2003; Tobin et al., 2002; Staels et al., 1990).

Also relating to oxidative metabolism and mitochondrial function, PPARγ specifically interacts with the peroxisome proliferator-activated receptor gamma coactivator-1 alpha (PGC-1α) to activate genes involved in cellular energy metabolism, adaptive thermogenesis, mitochondrial biogenesis, hepatic gluconeogenesis, and beta-oxidation of fatty acids (Lin et al., 2003; Rhee et al., 2003; Bramnert et al., 2003). Responsive to insulin, the expression of PGC-1α is increased in both type-1 and type-2 diabetes, and is thought to contribute to elevated hepatic glucose production in diabetic states (Mootha et al., 2003). Via the activation of gluconeogenesis and fatty acid oxidation, PGC-1α has also been demonstrated to mediate the hepatic response to fasting (Rhee et al., 2003). Consequently, PGC-1α and PPARγ may also mediate many transcriptional changes in metabolic genes induced by caloric restriction. The constitutive increase in PPARγ expression in dwarf livers therefore has strong implications for altered oxidative metabolism in dwarf animals, and is particularly relevant to the molecular mechanism of life-span extension by caloric restriction (Casas

86

et al., 2000). As demonstrated by these studies, increased hepatic PPARγ expression is characteristic of dwarf livers of both genders and ages and may thus be involved in longevity determination by potently affecting hepatic utilization and provision of critical metabolic substrates in these long-lived mice.

These results indicating altered energy homeostasis are also consistent with recent systematic RNAi screening studies in nematodes that identified genes responsible for mitochondrial metabolic and oxidative functions as having critical roles in determining life span. Specifically, RNAi suppression of phosphoglycerate mutase, a highly conserved glycolytic enzyme, significantly extends life span in *C. elegans* (Lee et al., 2003b). Correspondingly, these microarray studies of young male dwarf mice also demonstrate that phosphoglycerate mutase is down-regulated by 3-fold ($p < 0.001$) relative to littermate controls, suggesting that alteration of glycolytic and oxidative metabolism may be critical for life-span control in both nematodes and mice (Dillin et al., 2002; Van Voorhies, 2002a; Van Voorhies, 2002b).

These transcriptional profiling studies of young and aged $Pit1^{dw/dwJ}$ livers depict a pattern of gene expression indicative of altered utilization of energy substrates which is characterized by a coordinated down-regulation of cholesterol and lipid biosynthesis, and by changes in expression of central regulators of fatty acid mobilization and oxidation. These substantial and striking changes in the hepatic expression of energy metabolism genes may modify mitochondrial and peroxisomal oxidative functions, and may thus affect life span through diminishing the production of free radicals inherently generated by normal intracellular oxidative metabolism. Possibly mediated through liver X receptors (LXRs), SREBPs and PPARγ, $Pit1^{dw/dwJ}$ livers exhibit a distinct program of metabolic gene expression that may enhance fatty acid utilization and gluconeogenic capacity. Further, these *Pit1*-related differences in the hepatic abundance of transcripts regulating cholesterol biosynthesis, fatty acid oxidation, lipid transport and uptake, and glucose production are predominantly age and gender independent. Affecting whole body energy metabolism, this stable shift in hepatic cholesterologenic and lipogenic gene expression may not only parallel metabolic changes induced by caloric restriction in

mice, but may also play an integral role in determining lifespan by influencing mitochondrial and peroxisomal function in these long-lived mice.

ACKNOWLEDGEMENTS

CHAPTER IV

SUMMARY AND CONCLUSIONS

Recent advances in molecular gerontology have provided important clues about the fundamental biology of the aging process including the role of oxidative stress and the genetic basis of longevity. Progressive accumulation of oxidative damage to macromolecules is thought to underlie the aging-associated decline in physiologic function characteristic of the senescent phenotype. Mitochondria are a major intracellular source of reactive oxygen species (ROS); however, other organelles are also endogenous sources of oxyradicals and oxidants that can damage macromolecules. This investigation examines the relationship between aging and oxidative damage to ER resident proteins, which exist in a strongly oxidizing environment necessary for disulfide bond formation. In these studies, young and aged mouse liver homogenates were separated by differential centrifugation into enriched sub-cellular fractions, and the ER/mitochondrial proteins were resolved by 2-dimensional gel electrophoresis, and then assayed for oxidative damage as measured by protein carbonylation. MALDI/TOF analysis and N-terminal sequencing of these immunoreactive proteins identified BiP/Grp78, protein disulfide isomerase (PDI), and calreticulin as exhibiting a selective age-associated increase in carbonyl content. This increase in oxidative damage to critical ER proteins in aged liver strongly indicates an impairment in protein folding, disulfide cross-linking, and glycosylation which may significantly contribute to the functional decline observed in aging liver.

Providing evidence for the genetic basis of aging, several murine models demonstrate that longevity can be increased by mutations affecting endocrine signaling, particularly via the GH/IGF-1 axis. In this investigation of long-lived GH/IGF-1-deficient mice, characteristic patterns of hepatic gene expression in $Pit1^{dw/dwJ}$ dwarf mice which may directly relate to longevity determination were revealed. Comparative microarray analysis of young and aged male livers was performed to identify specific

genes differentially expressed in *Pit1^{dw/dwJ}* mice. Further examination of both male and female livers by real-time RT-PCR demonstrated striking transcriptional differences in *Pit1^{dw/dwJ}* mice which include genes regulating cholesterol biosynthesis, fatty acid utilization, and lipoprotein metabolism. By affecting whole body energy homeostasis, this stable shift in hepatic gene expression may contribute to longevity determination by influencing particular metabolic and oxidative functions compartmentalized within the mitochondrion and peroxisome. Further, these stable alterations in metabolic gene expression may also parallel transcriptional changes induced by caloric restriction thereby indicating a common genetic mechanism for life-span extension.

The studies described herein were designed to investigate the molecular basis of aging and longevity extension in mammals utilizing recently developed technologies and approaches that have sufficient power to effectively probe these highly complex processes. Using well-established strains and lines of laboratory mice to investigate the complex and multi-factorial process of aging, these proteomic and genomic studies have provided further support for the central role of oxidative damage to macromolecules as a causative factor in the 'normal' aging process, and have provided strong evidence for the influence of metabolism on life-span extension. With respect to 'normal' aging, the finding that specific chaperone proteins of the ER are oxidatively modified in aged liver imparts new evidence for the basis of the accumulation of misfolded proteins, and provides a potential mechanism for the functional decline in aged liver. These studies have also provided important clues regarding the basic molecular endocrinology of hepatic gene expression by identifying transcriptional changes associated with GH and TSH deficiencies. Further, these microarray studies parallel with recent research into the transcriptional regulation of cholesterol biosynthesis by the SREBPs (Chen et al., 2004; Horton et al., 2003), and shed new light on the role of GH in lipid and steroid metabolism. Most intriguingly, the microarray analysis of long-lived *Pit1* dwarf mice strongly implies a central role for peroxisomal beta-oxidation of fatty acids, which, in terms of ATP production, is not as efficient as mitochondrial fatty acid oxidation, may however provide a means of reducing the level of oxidative stress generated by the

release of free radicals from the electron transport chain. Recent evidence in *C. elegans* supports the involvement of alternative metabolic pathways in the extension of lifespan which utilize a modified glyoxylate cycle occurring in the peroxisome (Holt and Riddle, 2003; Rea and Johnson, 2003). Similarly, the process of metabolic imprinting is also implied by the extension of lifespan following short-term caloric restriction which shifts energy metabolism from carbohydrate utilization to fatty acid oxidation (Higami et al., 2004; Miller et al., 2002; Cao et al., 2001). Metabolic imprinting in *Pit1^{dw/dwJ}* mice may also perhaps be implied by the increased magnitude of hepatic transcriptional differences observed in young mice which may thereby establish life-long preferences for specific bioenergetic substrates and metabolic pathways. In conclusion, the investigation of long-lived mice presented herein strongly suggests that the underlying genetic mechanism of longevity extension in mammals may operate through shifting energy metabolism to the use of alternate bioenergetic substrates which may have the concomitant advantage of reducing the damaging intracellular production of ROS by mitochondria, ER, and peroxisomes.

APPENDIX

Significant Transcriptional Differences between Aged *Pit1$^{dw/dwJ}$* and Control Livers

Differentially expressed transcripts (306) between aged control and dwarf livers are listed in order of significance using the *p*-value calculated from the 2-tailed *t*-test assuming unequal variances, with $p \leq 0.05$ considered as significant. Ratios of mean signal intensities are expressed relative to aged dwarf mice, *i.e.* A dw/A con, and all represent differences greater than 2-fold. Transcriptional differences also confirmed for both male and female animals by RT-PCR are indicated in bold type.

Signal Ratio	*p-value*	Gene Title	Probe Set ID	Gene Ontology Biological Process
24.40	0.00003	hydroxyacid oxidase (glycolate oxidase) 3	103649_at	6118 electron transport / 6605 protein targeting
28.48	0.00007	sulfotransferase, hydroxysteroid preferring 2	104484_at	8202 steroid metabolism
0.26	0.00014	glypican 1	104614_at	---
0.19	0.00015	secreted phosphoprotein 1	97519_at	1503 ossification / 7155 cell adhesion
0.28	0.00016	leukemia inhibitory factor receptor	104658_at	---
0.49	0.00017	complement component 1, r subcomponent	95415_f_at	6508 proteolysis and peptidolysis
0.35	0.00021	epidermal growth factor receptor pathway substrate 15	104367_at	---
0.23	0.00025	**squalene epoxidase**	94322_at	6118 electron transport / 6725 aromatic compound metabolism
3.23	0.00025	muscle glycogen phosphorylase	160754_at	5975 carbohydrate metabolism / 5977 glycogen metabolism
0.19	0.00027	interferon regulatory factor 6	92440_at	6355 regulation of transcription, DNA-dependent
0.48	0.00034	cysteine sulfinic acid decarboxylase	99184_at	6520 amino acid metabolism
2.84	0.00036	aldehyde dehydrogenase family 3, subfamily A2	161401_f_at	8152 metabolism
5.55	0.00051	cytochrome P450, family 2, subfamily b, polypeptide 9	101862_at	6118 electron transport
0.24	0.00052	insulin-like growth factor 1	95545_at	6916 anti-apoptosis / 7399 neurogenesis
3.52	0.00053	microsomal glutathione S-transferase 3	96258_at	---
4.16	0.00068	myxovirus (influenza virus) resistance 1	98417_at	6952 defense response / 6955 immune response
0.24	0.00105	SERTA domain containing 1	160834_at	6355 regulation of transcription, DNA-dependent
2.82	0.00107	3-hydroxyacyl Coenzyme A dehydrogenase	97316_at	6631 fatty acid metabolism / 6635 fatty acid beta-oxidation
3.71	0.00109	zinc finger protein 179	100383_at	---
0.12	0.00111	insulin-like growth factor binding protein, acid labile subunit	97987_at	7155 cell adhesion

Signal Ratio	p-value	Gene Title	Probe Set ID	Gene Ontology Biological Process
0.50	0.00116	amyloid beta (A4) precursor protein-binding protein	102710_at	7218 neuropeptide signaling pathway
0.34	0.00124	calpain 10	97331_at	6508 proteolysis and peptidolysis
2.46	0.00129	EST	161106_r_at	---
0.42	0.00132	esterase 31	99941_at	---
2.86	0.00145	aldehyde dehydrogenase family 3, subfamily A2	99559_at	8152 metabolism
2.13	0.00151	vanin 3	104181_at	6807 nitrogen metabolism
2.39	0.00160	cytochrome P450, family 2, subfamily c, polypeptide 39	102084_f_at	6118 electron transport
2.20	0.00175	cytochrome P450, family 3, subfamily a, polypeptide 11	101638_s_at	6118 electron transport
2.00	0.00177	semaphorin 5B / thrombospondin	97791_at	7275 development / 7399 neurogenesis
0.50	0.00179	lymphocyte antigen 6 complex, locus E	101487_f_at	6952 defense response
0.34	0.00188	complement component 9	104424_at	6956 complement activation
2.26	0.00190	phosphodiesterase 1A, calmodulin-dependent	160861_s_at	7165 signal transduction
3.07	0.00193	tumor necrosis factor receptor superfamily, member 18	104662_at	---
3.50	0.00193	NAD(P)H dehydrogenase, quinone 1	94351_r_at	6118 electron transport
7.47	0.00193	annexin A8	97529_at	7596 blood coagulation
2.62	0.00198	RIKEN cDNA 2810402A17 gene	94759_at	---
2.68	0.00209	nuclear receptor subfamily 1, group I, member 3	104507_g_at	6355 regulation of transcription, DNA-dependent
4.13	0.00211	lectin, galactose binding, soluble 1	99669_at	7157 heterophilic cell adhesion / 45445 myoblast differentiation
0.07	0.00215	major urinary protein 1	102096_f_at	6810 transport / 16068 type I hypersensitivity
0.06	0.00216	major urinary protein 1	101566_f_at	6810 transport / 16068 type I hypersensitivity
0.08	0.00234	deiodinase, iodothyronine, type I	95552_at	---
2.90	0.00235	ATPase, Na+/K+ transporting, beta 2 polypeptide	93664_at	6813 potassium ion transport / 6814 sodium ion transport / 7155 cell adhesion
2.15	0.00245	RIKEN cDNA 4931406C07 gene	96089_at	---
7.40	0.00247	gap junction membrane channel protein beta 6	94391_at	7154 cell communication / 7267 cell-cell signaling
3.44	0.00259	bystin-like	96644_at	7155 cell adhesion
0.44	0.00260	forkhead box D4	101648_at	6355 regulation of transcription, DNA-dependent
0.25	0.00265	major urinary protein 3	101909_f_at	6810 transport
3.34	0.00282	**very low density lipoprotein receptor**	96534_at	6869 lipid transport / 8203 cholesterol metabolism
0.12	0.00288	major urinary protein 1	101635_f_at	6810 transport / 16068 type I hypersensitivity
5.08	0.00290	glutathione S-transferase, alpha 2 (Yc2)	101872_at	---
46.51	0.00294	flavin containing	104421_at	6118 electron transport

Signal Ratio	*p-value*	Gene Title	Probe Set ID	Gene Ontology Biological Process
		monooxygenase 3		
0.12	*0.00297*	major urinary protein 4	101682_f_at	6810 transport
0.22	*0.00299*	cysteinyl-tRNA synthetase	104048_at	6412 protein biosynthesis / 6423 cysteinyl-tRNA aminoacylation
0.06	*0.00307*	zeta-chain (TCR) associated protein kinase	93662_s_at	6468 protein amino acid phosphorylation / 7242 intracellular signaling cascade
14.97	*0.00308*	cytochrome P450, family 4, subfamily a, polypeptide 10	92600_f_at	---
0.15	*0.00310*	transmembrane protein 1 (Tmeff1)	160472_r_at	---
2.49	*0.00322*	cyclin-dependent kinase 2	94411_at	910 cytokinesis / 7049 cell cycle / 7067 mitosis
0.32	*0.00328*	unc-13 homolog A (C. elegans)	92498_at	7242 intracellular signaling cascade/ 7268 synaptic transmission
4.44	*0.00348*	ribosomal protein L31	96339_at	---
2.11	*0.00351*	fucosyltransferase 1	99381_at	5975 carbohydrate metabolism
0.30	*0.00353*	olfactory receptor 1507	96981_at	---
0.46	*0.00354*	properdin factor, complement	101468_at	6957 complement activation, alternative pathway
0.46	*0.00368*	B-cell translocation gene 3	96146_at	45930 negative regulation of mitotic cell cycle
0.45	*0.00370*	inter-alpha trypsin inhibitor, heavy chain 1	98014_at	---
0.49	*0.00376*	interferon, gamma-inducible protein 16	98465_f_at	6355 regulation of transcription, DNA-dependent / 6955 immune response
2.30	*0.00429*	CUG triplet repeat,RNA binding protein 2	97255_at	6376 mRNA splice site selection
4.30	*0.00436*	RIKEN cDNA B230113M03 gene	161396_f_at	6464 protein modification / 6512 ubiquitin cycle
2.82	*0.00441*	solute carrier family 16 (monocarboxylic acid transporters), member 7	95060_at	6810 transport / 15711 organic anion transport
0.45	*0.00452*	RIKEN cDNA 1100001H23 gene	98033_at	---
0.47	*0.00459*	eyes absent 4 homolog (Drosophila)	92453_at	6355 regulation of transcription, DNA-dependent / 7275 development
2.30	*0.00462*	proviral integration site 2	101926_at	6468 protein amino acid phosphorylation / 8637 apoptotic mitochondrial changes
0.42	*0.00507*	carbamoyl-phosphate synthetase 2	96827_at	6207 'de novo' pyrimidine base biosynthesis
0.40	*0.00525*	ankyrin repeat domain 17	102118_at	7492 endoderm development
0.23	*0.00534*	gamma-aminobutyric acid (GABA-A) receptor, subunit gamma 2	93163_at	6810 transport / 6811 ion transport / 7214 GABA signaling pathway
2.60	*0.00564*	expressed sequence C76533	94686_at	---
2.33	*0.00576*	inositol polyphosphate-5-phosphatase D	161678_at	7165 signal transduction 8340 determination of adult life span
0.39	*0.00592*	tetratricopeptide repeat domain 1	96921_at	---
0.41	*0.00628*	allograft inflammatory factor 1	102330_at	---
4.27	*0.00642*	cytochrome P450, family 2, subfamily c, polypeptide 39	98295_at	6118 electron transport
0.29	*0.00647*	ethanolamine kinase 1	103495_at	---

Signal Ratio	p-value	Gene Title	Probe Set ID	Gene Ontology Biological Process
0.45	0.00649	cytochrome P450, family 2, subfamily c, polypeptide 70	95043_at	---
0.37	0.00652	WW domain binding protein 2	161991_at	---
3.23	0.00653	cytosolic acyl-CoA thioesterase 1	103581_at	1676 long-chain fatty acid metabolism / 6629 lipid metabolism
4.22	0.00660	**peroxisome proliferator activated receptor gamma**	97926_s_at	6355 regulation of transcription, DNA-dependent / 45444 adipocyte differentiation
0.01	0.00664	hydroxysteroid dehydrogenase-4, delta<5>-3-beta	94795_at	6694 steroid biosynthesis / 6700 C21-steroid hormone biosynthesis
2.74	0.00669	microsomal glutathione S-transferase 2	104742_at	---
0.42	0.00679	neuregulin 3	99834_at	7243 protein kinase cascade / 9790 embryonic development
0.26	0.00681	major urinary protein 3	101910_f_at	6810 transport
0.50	0.00683	ribosomal protein L13a	92834_at	6412 protein biosynthesis
0.47	0.00697	nuclear factor, erythroid derived 2	98010_at	6355 regulation of transcription, DNA-dependent
0.22	0.00706	cathepsin C	101019_at	6508 proteolysis and peptidolysis
0.49	0.00710	**farnesyl diphosphate synthetase**	99098_at	---
2.07	0.00722	cytochrome P450, family 3, subfamily a, polypeptide 25	104024_at	6118 electron transport
3.12	0.00726	nuclear receptor subfamily 1, group I, member 3	102171_r_at	6355 regulation of transcription, DNA-dependent
0.46	0.00731	proteasome (prosome, macropain) subunit, beta type 10	101486_at	6511 ubiquitin-dependent protein catabolism
0.06	0.00736	serine (or cysteine) proteinase inhibitor, member 12	160951_at	---
2.30	0.00757	expressed sequence AI593864	103776_at	---
0.15	0.00791	guanine nucleotide binding protein, alpha 14	95364_at	7186 G-protein coupled receptor protein signaling pathway
2.37	0.00791	phosphatidic acid phosphatase 2a	98508_s_at	6470 protein amino acid dephosphorylation / 6651 diacylglycerol biosynthesis
3.59	0.00806	connective tissue growth factor	93294_at	1503 ossification / 1525 angiogenesis / 1558 regulation of cell growth
0.41	0.00822	expressed sequence AW111922	96764_at	19221 cytokine and chemokine mediated signaling pathway
3.00	0.00822	expressed sequence AA960558	161027_f_at	---
2.36	0.00826	protein tyrosine phosphatase, receptor type, B	92289_at	6470 protein amino acid dephosphorylation
2.07	0.00892	myoglobin	100615_at	6810 transport / 7517 muscle development 15671 oxygen transport
2.94	0.00900	protein tyrosine phosphatase, receptor type Z, polypeptide 1	92378_at	6470 protein amino acid dephosphorylation
0.31	0.00915	fragile X mental retardation gene 2, autosomal homolog	99516_at	9405 pathogenesis
0.33	0.00930	elastase 1, pancreatic	93783_at	---
0.33	0.00931	interferon gamma induced GTPase	160933_at	---
2.73	0.00982	protease, serine, 8 (prostasin)	100909_at	6508 proteolysis and peptidolysis

Signal Ratio	*p-value*	Gene Title	Probe Set ID	Gene Ontology Biological Process
0.26	0.00984	kidney expressed gene 1	96938_at	---
4.63	0.00988	cytochrome P450, family 2, subfamily b, polypeptide 20	102701_at	6118 electron transport
0.03	0.00998	major urinary protein 1	161815_f_at	6810 transport / 16068 type I hypersensitivity
0.46	0.01006	RIKEN cDNA 2610510H01 gene	95514_at	---
0.23	0.01016	cytochrome P450, family 2, subfamily f, polypeptide 2	100069_at	6118 electron transport
0.41	0.01038	expressed sequence AI481100	98410_at	---
3.23	0.01065	glutathione S-transferase, mu 3	97681_f_at	8152 metabolism
0.34	0.01074	EST	103489_at	---
3.27	0.01075	oxysterol binding protein-like 5	103311_at	6810 transport / 6869 lipid transport / 8202 steroid metabolism
2.29	0.01128	fibulin 2	100928_at	---
0.33	0.01132	interferon activated gene 205	94224_s_at	6955 immune response
0.33	0.01133	leukemia inhibitory factor receptor	104659_g_at	---
2.78	0.01187	homeo box, msh-like 3	92912_at	6355 regulation of transcription, DNA-dependent / 7275 development
2.24	0.01260	**adrenergic receptor, beta 3**	92536_at	7186 G-protein coupled receptor protein signaling pathway
0.28	0.01266	zeta-chain (TCR) associated protein kinase	93661_at	6468 protein amino acid phosphorylation 7242 intracellular signaling cascade
2.02	0.01266	RIKEN cDNA 4931406C07 gene	96090_g_at	---
2.25	0.01303	sarcosine dehydrogenase	96763_at	---
0.37	0.01304	interleukin 18 binding protein	92689_at	---
0.36	0.01318	proline 4-hydroxylase, alpha 1 polypeptide	104139_at	18401 peptidyl-proline hydroxylation / 19538 protein metabolism
0.17	0.01350	RIKEN cDNA 1100001G20 gene	101912_at	---
3.98	0.01354	RIKEN cDNA 0710001P09 gene	93561_at	---
0.27	0.01356	cytochrome P450, family 7, subfamily b, polypeptide 1	92898_at	6118 electron transport / 8203 cholesterol metabolism
0.34	0.01369	hydroxysteroid (17-beta) dehydrogenase 2	101891_at	6694 steroid biosynthesis / 8152 metabolism
2.16	0.01396	ketohexokinase	104323_at	5975 carbohydrate metabolism
0.40	0.01421	WD repeat and SOCS box-containing 1	98946_at	7242 intracellular signaling cascade
0.31	0.01422	cathepsin C	161251_f_at	6508 proteolysis and peptidolysis
0.44	0.01426	inhibitor of DNA binding 2	93013_at	7275 development
0.32	0.01461	cytochrome P450, family 7, subfamily b, polypeptide 1	161345_f_at	6118 electron transport / 8203 cholesterol metabolism
2.07	0.01470	odd Oz/ten-m homolog 3 (Drosophila)	92500_at	---
9.40	0.01474	plasma membrane associated protein, S3-12	102763_at	---
2.85	0.01507	parotid secretory protein	100080_at	---
2.09	0.01534	ribosomal protein S6 kinase,	98007_at	6468 protein amino acid phosphorylation /

Signal Ratio	*p-value*	Gene Title	Probe Set ID	Gene Ontology Biological Process
		polypeptide 2		7046 ribosome biogenesis
0.49	*0.01539*	protein tyrosine phosphatase, receptor type, C	101048_at	6470 protein amino acid dephosphorylation / 6968 cellular defense response
19.36	*0.01539*	cytochrome P450, family 2, subfamily b, polypeptide 13	102820_at	---
0.06	*0.01577*	insulin-like growth factor 1	95546_g_at	48009 insulin-like growth factor receptor signaling pathway
0.42	*0.01594*	cDNA sequence BC037135	103391_at	---
0.10	*0.01599*	vesicle-associated membrane protein, associated protein A	161516_r_at	---
0.48	*0.01617*	ectonucleoside triphosphate diphosphohydrolase 2	97986_at	7186 G-protein coupled receptor protein signaling pathway
0.50	*0.01619*	nuclear receptor subfamily 6, group A, member 1	92696_at	122 negative regulation of transcription from Pol II promoter
2.87	*0.01642*	Fanconi anemia, complementation group C	161709_at	6281 DNA repair / 6289 nucleotide-excision repair /
24.70	*0.01669*	cytochrome P450, family 4, subfamily a, polypeptide 14	101103_at	6118 electron transport
0.49	*0.01681*	signal recognition particle 19	160343_at	6605 protein targeting / 6613 cotranslational membrane targeting
2.34	*0.01730*	sphingosine phosphate lyase 1	96126_at	6520 amino acid metabolism / 6629 lipid metabolism / 6915 apoptosis
0.28	*0.01734*	chemokine (C-C motif) receptor 5	102718_at	6935 chemotaxis / 6952 defense response
2.85	*0.01743*	hexosaminidase A	162488_at	5975 carbohydrate metabolism
0.46	*0.01743*	cytochrome P450, family 4, subfamily f, polypeptide 13	162058_f_at	6118 electron transport
0.47	*0.01752*	macrophage expressed gene 1	99071_at	---
0.22	*0.01772*	neuropilin	95016_at	1525 angiogenesis / 7155 cell adhesion / 7399 neurogenesis
0.01	*0.01796*	epidermal growth factor receptor	101841_at	74 regulation of cell cycle 902 cellular morphogenesis
0.16	*0.01800*	suppressor of cytokine signaling 3	92232_at	1558 regulation of cell growth / 7165 signal transduction
0.37	*0.01810*	major histocompatibility complex, class I-related	101433_at	6955 immune response
0.30	*0.01847*	formin	92953_at	7275 development / 9401 PEP-dependent sugar phosphotransferase system
3.75	*0.01849*	glutathione S-transferase, alpha 4	96085_at	---
0.21	*0.01932*	signal sequence receptor, alpha	94511_at	---
2.77	*0.01953*	secretin	92755_f_at	---
0.36	*0.01960*	proteasome subunit, beta type 8 (Lmp 7)	102791_at	6511 ubiquitin-dependent protein catabolism / 6955 immune response
0.38	*0.01967*	pyruvate dehydrogenase kinase, isoenzyme 3	92810_at	---
3.19	*0.02039*	carnitine acetyltransferase	103646_at	6631 fatty acid metabolism / 6810 transport
3.96	*0.02040*	calcium channel, voltage-dependent, L type, alpha 1S subunit	101128_at	6811 ion transport / 6812 cation transport / 6816 calcium ion transport
0.44	*0.02059*	hairy and enhancer of split 6 (*Drosophila*)	97334_at	6357 regulation of transcription / 7399 neurogenesis / 30154 cell differentiation

Signal Ratio	*p-value*	Gene Title	Probe Set ID	Gene Ontology Biological Process
4.52	0.02064	CD36 antigen	93332_at	6810 transport / 7155 cell adhesion
3.14	0.02068	DNA cross-link repair 1A, PSO2 homolog (*S. cerevisiae*)	104230_at	6289 nucleotide-excision repair
3.29	0.02119	**lipoprotein lipase**	160083_at	6629 lipid metabolism / 16042 lipid catabolism
0.48	0.02145	interferon regulatory factor 7	104669_at	6355 regulation of transcription, DNA-dependent
0.45	0.02153	tyrosine kinase, non-receptor, 2	102850_at	6468 protein amino acid phosphorylation
0.47	0.02154	ubiquitin specific protease 15	161870_at	6511 ubiquitin-dependent protein catabolism / 6512 ubiquitin cycle
0.32	0.02160	immunoglobulin heavy chain (J558 family)	97575_f_at	---
0.38	0.02177	camello-like 1	92835_at	7162 negative regulation of cell adhesion
0.46	0.02186	interleukin 13 receptor, alpha 1	103723_at	7166 cell surface receptor linked signal transduction
9.50	0.02217	cytochrome P450, family 4, subfamily a, polypeptide 10	98353_at	---
2.72	0.02221	dedicator of cytokinesis 7	103356_at	---
0.24	0.02229	interferon gamma inducible protein	104750_at	6952 defense response
0.38	0.02233	**isopentenyl-diphosphate delta isomerase**	96269_at	6694 steroid biosynthesis / 6695 cholesterol biosynthesis / 8299 isoprenoid biosynthesis
2.07	0.02248	checkpoint suppressor 1	104665_g_at	77 DNA damage response / 85 G2 phase of mitotic cell cycle
0.26	0.02254	makorin, ring finger protein, 3	102740_at	---
0.35	0.02280	SM-11044 binding protein	96275_f_at	6810 transport
0.47	0.02300	RIKEN cDNA 4432406C08 gene	103203_f_at	---
3.08	0.02301	aquaporin 4	102703_s_at	6810 transport / 6833 water transport
2.20	0.02308	UDP-glucose pyrophosphorylase 2	94481_at	6355 regulation of transcription, DNA-dependent / 8152 metabolism
0.25	0.02309	involucrin	92739_at	30216 keratinocyte differentiation
0.06	0.02323	chemokine (C-C motif) receptor 5	161968_f_at	6935 chemotaxis / 6952 defense response
2.00	0.02328	transgene insert site 737	162392_r_at	7368 determination of left/right symmetry / 9952 anterior/posterior pattern formation
0.43	0.02340	6-phosphofructo-2-kinase/fructose-2,6-biphosphatase 3	160641_at	6003 fructose 2,6-bisphosphate metabolism / 8152 metabolism
0.43	0.02371	CD86 antigen	102831_s_at	6952 defense response
2.86	0.02406	cytochrome P450, family 3, subfamily a, polypeptide 11	101639_r_at	6118 electron transport
0.27	0.02438	signal recognition particle receptor, B subunit	101114_at	---
0.29	0.02502	RIKEN cDNA 2810417H13 gene	93952_r_at	---
3.24	0.02546	microfibrillar-associated protein 4	96826_at	7155 cell adhesion
4.26	0.02548	solute carrier family 19 (sodium/hydrogen exchanger)	94419_at	6810 transport
2.00	0.02553	transcription factor AP-2, alpha	92923_g_at	6355 regulation of transcription, DNA-

Signal Ratio	p-value	Gene Title	Probe Set ID	Gene Ontology Biological Process
				dependent
0.29	0.02629	defensin related cryptdin 17	92812_f_at	6805 xenobiotic metabolism / 6952 defense response
0.39	0.02643	secretin	162163_at	---
0.32	0.02657	RNA polymerase 1-3	161852_i_at	6350 transcription
0.36	0.02687	retinol dehydrogenase 11	99592_f_at	8152 metabolism
2.34	0.02687	histocompatibility 2, class II antigen E alpha	102904_at	6952 defense response / 6955 immune response
0.42	0.02706	EST	161718_at	---
0.47	0.02709	RIKEN cDNA 2310061O04 gene	161060_i_at	---
0.43	0.02734	vacuolar protein sorting 52 (yeast)	96118_at	---
2.03	0.02743	leucine rich repeat protein 1, neuronal	161959_f_at	---
3.42	0.02755	isocitrate dehydrogenase 2 (NADP+), mitochondrial	95693_at	6092 carbohydrate metabolism / 6097 glyoxylate cycle / 6099 tricarboxylic acid cycle
3.25	0.02759	RIKEN cDNA 6330580J24 gene	161766_i_at	---
2.30	0.02762	RIKEN cDNA 1500001M20 gene	160723_at	---
0.25	0.02778	caspase 12	92488_at	6508 proteolysis and peptidolysis / 6915 apoptosis
2.51	0.02778	phosphatidylinositol glycan, class N	92296_at	---
4.59	0.02800	tumor necrosis factor receptor superfamily, member 19	160670_at	---
0.47	0.02800	mutS homolog 5 (*E. coli*)	103719_at	6298 mismatch repair / 7126 meiosis / 7131 meiotic recombination
2.77	0.02873	frizzled homolog 4 (*Drosophila*)	95771_i_at	7166 cell surface receptor linked signal transduction / 16055 Wnt signaling pathway
2.23	0.02874	phospholipase A2, group XIIA	104342_i_at	16042 lipid catabolism
2.55	0.02875	choline phosphotransferase 1	93994_at	---
2.10	0.02891	corin	103289_at	6508 proteolysis and peptidolysis / 7275 development
3.09	0.02938	cDNA sequence BC011209	160622_at	6810 transport
2.14	0.02958	non-neuronal SNAP25-like protein homolog 1 (*C. elegans*)	93251_at	---
3.04	0.02967	phospholipase A2, group XIIA	104343_f_at	16042 lipid catabolism
7.07	0.03001	sulfotransferase family 3A, member 1	99854_at	---
2.08	0.03005	Igkappa gene for immunoglobulin kappa chain	101348_at	---
0.50	0.03094	myosin, light polypeptide 4	160487_at	7010 cytoskeleton organization and biogenesis / 7517 muscle development
2.01	0.03112	non-ubiquitously expressed CaM kinase	93910_at	6468 protein amino acid phosphorylation
0.42	0.03150	leukocyte specific transcript 1	103571_at	902 cellular morphogenesis / 6955 immune response
0.12	0.03153	seminal vesicle antigen	97757_at	---

Signal Ratio	p-value	Gene Title	Probe Set ID	Gene Ontology Biological Process
5.50	0.03195	glutathione S-transferase, mu 3	97682_r_at	8152 metabolism
2.71	0.03214	protein related to DAN and cerberus	103975_at	---
0.40	0.03234	murine leukemia virus modified polytropic provirus DNA	93860_i_at	---
0.45	0.03251	sorting nexin 17	161257_r_at	6898 receptor mediated endocytosis
0.43	0.03254	homeo box A4	97746_f_at	6355 regulation of transcription, DNA-dependent
2.00	0.03275	flavin containing monooxygenase 5	160088_at	6118 electron transport
2.22	0.03291	glycine decarboxylase	95603_at	---
2.69	0.03335	ligatin	102127_at	6413 translational initiation
0.43	0.03345	EST	162017_at	---
2.66	0.03376	small proline-rich protein 2H	94121_at	---
0.30	0.03380	serum amyloid P-component	104072_at	7157 heterophilic cell adhesion
0.47	0.03401	CD5 antigen	93637_at	6952 defense response
0.22	0.03416	fatty acid binding protein 5, epidermal	160544_at	6810 transport
0.50	0.03459	RIKEN cDNA 1500004O14 gene	104303_i_at	6355 regulation of transcription, DNA-dependent
0.22	0.03482	B-cell linker	100771_at	6952 defense response / 7242 intracellular signaling cascade
2.64	0.03505	Transcribed sequences	96599_at	---
0.16	0.03538	serine (or cysteine) proteinase inhibitor, clade A, member 3K	92583_at	---
2.83	0.03552	protein tyrosine phosphatase, non-receptor type substrate 1	161742_r_at	6910 phagocytosis, recognition / 6911 phagocytosis, engulfment
2.39	0.03587	diablo homolog (*Drosophila*)	100117_at	6915 apoptosis
0.50	0.03632	nuclear interacting partner of Alk	95750_at	6916 anti-apoptosis
0.46	0.03743	surfeit gene 6	96663_at	---
2.08	0.03746	guanine nucleotide binding protein, alpha 12	97227_at	7165 signal transduction / 7186 G-protein coupled receptor protein signaling pathway
0.42	0.03753	complement receptor related protein	161648_at	30449 regulation of complement activation
0.45	0.03783	brain glycogen phosphorylase	97489_at	5975 carbohydrate metabolism / 5977 glycogen metabolism
0.29	0.03792	RIKEN cDNA 1110008H02 gene	161635_f_at	---
0.35	0.03819	proteasome subunit, beta type 9 (Lmp 2)	93085_at	6511 ubiquitin-dependent protein catabolism / 6955 immune response
2.25	0.03825	H2.0-like homeo box gene	102657_at	6355 regulation of transcription, DNA-dependent
0.45	0.03844	arginine vasopressin receptor 1A	161189_r_at	7186 G-protein coupled receptor protein signaling pathway
4.11	0.03869	crystallin, gamma B	161780_f_at	7423 sensory organ development
2.79	0.03935	Transcribed sequences	101598_at	---
4.16	0.03947	galactosidase, beta 1	161754_f_at	5975 carbohydrate metabolism
0.50	0.03980	EST	96484_at	---
2.18	0.04018	tropomyosin 4	95543_at	---

Signal Ratio	*p-value*	Gene Title	Probe Set ID	Gene Ontology Biological Process
0.16	*0.04021*	suppressor of cytokine signaling 2	99475_at	1558 regulation of cell growth / 7165 signal transduction
0.43	*0.04039*	kallikrein 6	100061_f_at	6508 proteolysis and peptidolysis
2.59	*0.04039*	RIKEN cDNA C030034J04 gene	99364_at	---
2.43	*0.04103*	EST	161375_at	---
0.42	*0.04109*	hemoglobin Y, beta-like embryonic chain	103535_at	6810 transport / 15671 oxygen transport
2.94	*0.04127*	procollagen, type IV, alpha 5	93220_at	7155 cell adhesion
0.42	*0.04150*	protease (prosome, macropain) 26S subunit, ATPase 5	161921_f_at	6366 regulation of transcription from Pol II promoter
0.49	*0.04213*	maternal embryonic leucine zipper kinase	100416_at	6468 protein amino acid phosphorylation
2.29	*0.04238*	retinol dehydrogenase 6	102013_at	8152 metabolism
2.57	*0.04300*	DNA segment, Chr 8, ERATO Doi 67, expressed	95863_at	---
0.43	*0.04301*	angiopoietin-like 2	103556_at	---
0.35	*0.04322*	cathepsin C	101020_at	6508 proteolysis and peptidolysis
2.95	*0.04338*	sal-like 3 (Drosophila)	98852_at	6355 regulation of transcription, DNA-dependent
2.08	*0.04352*	P450 (cytochrome) oxidoreductase	161668_f_at	6118 electron transport
0.42	*0.04389*	retinol dehydrogenase 11	99591_i_at	8152 metabolism
0.33	*0.04398*	expressed sequence AW112010	100944_at	---
2.05	*0.04398*	guanylate cyclase 2c	103942_at	6182 cGMP biosynthesis / 9636 response to toxin
0.46	*0.04406*	hemolytic complement	103458_at	6954 inflammatory response / 6956 complement activation
0.37	*0.04453*	expressed sequence AW111922	103963_f_at	19221 cytokine and chemokine mediated signaling pathway
2.03	*0.04463*	ectonucleoside triphosphate diphosphohydrolase 5	92561_at	---
0.23	*0.04467*	lymphocyte antigen 6 complex, locus A	93078_at	---
0.41	*0.04530*	RIKEN cDNA D130059B05 gene	162048_r_at	---
2.10	*0.04534*	fibroblast growth factor 4	98826_at	74 regulation of cell cycle / 7165 signal transduction
2.66	*0.04545*	RIKEN cDNA 4833441D16 gene	94662_at	---
0.44	*0.04565*	sal-like 4 (Drosophila)	96169_at	---
2.25	*0.04584*	olfactory receptor 140	96986_at	7186 G-protein coupled receptor protein signaling pathway
0.29	*0.04607*	ecotropic viral integration site 2a	98025_at	8151 cell growth and/or maintenance
0.47	*0.04615*	proton-coupled divalent metal ion transporters, member 1	96562_at	6810 transport / 6826 iron ion transport
0.16	*0.04631*	pleckstrin homology-like domain, family A, member 1	160829_at	45210 FasL biosynthesis
2.58	*0.04651*	regulator of G-protein signalling 10	103384_at	7165 signal transduction

Signal Ratio	p-value	Gene Title	Probe Set ID	Gene Ontology Biological Process
3.06	0.04739	RIKEN cDNA 1600023A02 gene	96643_at	---
0.42	0.04773	EST	162000_r_at	---
2.14	0.04788	cholinergic receptor, nicotinic, alpha polypeptide 7	101131_at	6810 transport / 6811 ion transport / 7268 synaptic transmission
3.24	0.04790	zinc finger protein 90	92934_at	6355 regulation of transcription, DNA-dependent
0.47	0.04800	EST	101219_at	---
2.16	0.04835	integrin alpha M	98828_at	7155 cell adhesion / 7160 cell-matrix adhesion
0.26	0.04841	deoxynucleotidyltransferase, terminal	161409_f_at	6259 DNA metabolism / 6260 DNA replication / 6304 DNA modification
2.56	0.04855	trypsin 4	101043_f_at	---
2.50	0.04871	sarcospan	102378_at	74 regulation of cell cycle / 8151 cell growth and/or maintenance
2.50	0.04893	RIKEN cDNA 1300011C24 gene	161289_at	---
0.49	0.04914	acyl-CoA synthetase long-chain family member 4	102381_at	6631 fatty acid metabolism
2.18	0.04919	polo-like kinase 1 (Drosophila)	93099_f_at	6468 protein amino acid phosphorylation / 7049 cell cycle
0.45	0.04973	RIKEN cDNA 1110029F20 gene	160376_at	---

REFERENCES CITED

Adams, C. M., Reitz, J., De Brabander, J. K., Feramisco, J. D., Li, L., Brown, M. S., and Goldstein, J. L. (2004). Cholesterol and 25-hydroxycholesterol inhibit activation of SREBPs by different mechanisms, both involving SCAP and insigs. *J Biol. Chem.*

Affymetrix (2002a). Affymetrix Microarray Suite Users Guide Version 5.0. (Santa Clara, CA: Affymetrix).

Affymetrix (2002b). GeneChip Expression Analysis: Data Analysis Fundamentals. (Santa Clara, CA: Affymetrix).

Aigaki, T., Seong, K., and Matsuo, T. (2002). Longevity determination genes in Drosophila melanogaster. *Mech. Ageing Dev.* **123:** 1531-1541.

Akiyama, T. E., Sakai, S., Lambert, G., Nicol, C. J., Matsusue, K., Pimprale, S., Lee, Y. H., Ricote, M., Glass, C. K., Brewer, H. B., Jr., and Gonzalez, F. J. (2002). Conditional disruption of the peroxisome proliferator-activated receptor gamma gene in mice results in lowered expression of ABCA1, ABCG1, and apoE in macrophages and reduced cholesterol efflux. *Mol. Cell Biol* **22:** 2607-2619.

Ames, B. N., Shigenaga, M. K., and Hagen, T. M. (1993). Oxidants, antioxidants, and the degenerative diseases of aging. *Proc. Natl. Acad. Sci. U. S. A* **90:** 7915-7922.

An, M. R., Hsieh, C. C., Reisner, P. D., Rabek, J. P., Scott, S. G., Kuninger, D. T., and Papaconstantinou, J. (1996). Evidence for posttranscriptional regulation of C/EBPalpha and C/EBPbeta isoform expression during the lipopolysaccharide-mediated acute-phase response. *Mol. Cell Biol.* **16:** 2295-2306.

Anisimov, S. V. and Boheler, K. R. (2003). Aging-associated changes in cardiac gene expression: large scale transcriptome analysis. *Adv. Gerontol* **11:** 67-75.

Asa, S. L., Coschigano, K. T., Bellush, L., Kopchick, J. J., and Ezzat, S. (2000). Evidence for growth hormone (GH) autoregulation in pituitary somatotrophs in GH antagonist-transgenic mice and GH receptor-deficient mice. *Am J Pathol.* **156:** 1009-1015.

Asayama, K., Amemiya, S., Kusano, S., and Kato, K. (1984). Growth-hormone-induced changes in postheparin plasma lipoprotein lipase and hepatic triglyceride lipase activities. *Metabolism* **33:** 129-131.

Barger, J. L., Walford, R. L., and Weindruch, R. (2003). The retardation of aging by caloric restriction: its significance in the transgenic era. *Exp. Gerontol.* **38:** 1343-1351.

Barja, G. (1999). Mitochondrial oxygen radical generation and leak: sites of production in states 4 and 3, organ specificity, and relation to aging and longevity. *J. Bioenerg. Biomembr.* **31:** 347-366.

Barja, G. (2002). Rate of generation of oxidative stress-related damage and animal longevity. *Free Radic. Biol. Med.* **33:** 1167-1172.

Barja, G. (2004). Aging in vertebrates, and the effect of caloric restriction: a mitochondrial free radical production-DNA damage mechanism? *Biol. Rev. Camb. Philos. Soc.* **79:** 235-251.

Barsyte, D., Lovejoy, D. A., and Lithgow, G. J. (2001). Longevity and heavy metal resistance in daf-2 and age-1 long-lived mutants of Caenorhabditis elegans. *FASEB J.* **15:** 627-634.

Bartke, A., Wright, J. C., Mattison, J. A., Ingram, D. K., Miller, R. A., and Roth, G. S. (2001). Extending the lifespan of long-lived mice. *Nature* **414:** 412.

Barzilai, N., Atzmon, G., Schechter, C., Schaefer, E. J., Cupples, A. L., Lipton, R., Cheng, S., and Shuldiner, A. R. (2003). Unique lipoprotein phenotype and genotype associated with exceptional longevity. *JAMA* **290:** 2030-2040.

Beal, M. F. (2002). Oxidatively modified proteins in aging and disease. *Free Radic. Biol. Med.* **32:** 797-803.

Beentjes, J. A., van Tol, A., Sluiter, W. J., and Dullaart, R. P. (2000). Low plasma lecithin:cholesterol acyltransferase and lipid transfer protein activities in growth hormone deficient and acromegalic men: role in altered high density lipoproteins. *Atherosclerosis* **153:** 491-498.

Bentinger, M., Turunen, M., Zhang, X. X., Wan, Y. J., and Dallner, G. (2003). Involvement of retinoid X receptor alpha in coenzyme Q metabolism. *J Mol. Biol* **326:** 795-803.

Berlett, B. S. and Stadtman, E. R. (1997). Protein oxidation in aging, disease, and oxidative stress. *J. Biol. Chem.* **272:** 20313-20316.

Bluher, M., Kahn, B. B., and Kahn, C. R. (2003). Extended Longevity in Mice Lacking the Insulin Receptor in Adipose Tissue. *Science* **299:** 572-574.

Boylston, W. H., Gerstner, A., DeFord, J. H., Madsen, M., Flurkey, K., Harrison, D. E., and Papaconstantinou, J. (2004). Altered cholesterologenic and lipogenic transcriptional profile in livers of aging Snell dwarf (Pit1) mice. *Aging Cell* **3:** 283-296.

Bramnert, M., Segerlantz, M., Laurila, E., Daugaard, J. R., Manhem, P., and Groop, L. (2003). Growth hormone replacement therapy induces insulin resistance by activating the glucose-fatty acid cycle. *J Clin. Endocrinol Metab* **88:** 1455-1463.

Cadenas,E. and Packer,L. (1999). Understanding the Process of Aging. In Mitochondrial generation of reactive oxygen species and oxidative damage during aging: roles of coenzyme Q and tocopherol, R.S.Sohal, A.Lass, L.-J.Yan, and L.-K.Kwong, eds. (New York: Marcel Dekker), pp. 119-142.

Cao, S. X., Dhahbi, J. M., Mote, P. L., and Spindler, S. R. (2001). Genomic profiling of short- and long-term caloric restriction effects in the liver of aging mice. *Proc. Natl. Acad. Sci U. S. A* **98:** 10630-10635.

Casas, F., Domenjoud, L., Rochard, P., Hatier, R., Rodier, A., Daury, L., Bianchi, A., Kremarik-Bouillaud, P., Becuwe, P., Keller, J., Schohn, H., Wrutniak-Cabello, C., Cabello, G., and Dauca, M. (2000). A 45 kDa protein related to PPARgamma2, induced by peroxisome proliferators, is located in the mitochondrial matrix. *FEBS Lett.* **478:** 4-8.

Chen, G., Liang, G., Ou, J., Goldstein, J. L., and Brown, M. S. (2004). Central role for liver X receptor in insulin-mediated activation of Srebp-1c transcription and stimulation of fatty acid synthesis in liver. *Proc. Natl. Acad. Sci. U. S. A* **101:** 11245-11250.

Christ, E. R., Cummings, M. H., Albany, E., Umpleby, A. M., Lumb, P. J., Wierzbicki, A. S., Naoumova, R. P., Boroujerdi, M. A., Sonksen, P. H., and Russell-Jones, D. L. (1999). Effects of growth hormone (GH) replacement therapy on very low density lipoprotein apolipoprotein B100 kinetics in patients with adult GH deficiency: a stable isotope study. *J Clin. Endocrinol Metab* **84:** 307-316.

Clancy, D. J., Gems, D., Harshman, L. G., Oldham, S., Stocker, H., Hafen, E., Leevers, S. J., and Partridge, L. (2001). Extension of life-span by loss of CHICO, a Drosophila insulin receptor substrate protein. *Science* **292:** 104-106.

Clancy, D. J., Gems, D., Hafen, E., Leevers, S. J., and Partridge, L. (2002). Dietary Restriction in Long-Lived Dwarf Flies. *Science* **296:** 319.

Colao, A., Di Somma, C., Salerno, M., Spinelli, L., Orio, F., and Lombardi, G. (2002). The cardiovascular risk of GH-deficient adolescents. *J Clin. Endocrinol Metab* **87:** 3650-3655.

Coschigano, K. T., Clemmons, D., Bellush, L. L., and Kopchick, J. J. (2000). Assessment of growth parameters and life span of GHR/BP gene-disrupted mice. *Endocrinology* **141:** 2608-2613.

Coschigano, K. T., Holland, A. N., Riders, M. E., List, E. O., Flyvbjerg, A., and Kopchick, J. J. (2003). Deletion, but not antagonism, of the mouse growth hormone receptor results in severely decreased body weights, insulin, and insulin-like growth factor I levels and increased life span. *Endocrinology* **144:** 3799-3810.

106

Cottrell, D. A., Blakely, E. L., Borthwick, G. M., Johnson, M. A., Taylor, G. A., Brierley, E. J., Ince, P. G., and Turnbull, D. M. (2000). Role of mitochondrial DNA mutations in disease and aging. *Ann. N. Y. Acad. Sci.* **908:** 199-207.

D'andrade, R. (1978). U-Statistic Hierchical Clustering. *Psychometrika* **4:** 58-67.

Dhahbi, J. M., Kim, H. J., Mote, P. L., Beaver, R. J., and Spindler, S. R. (2004). Temporal linkage between the phenotypic and genomic responses to caloric restriction. *Proc. Natl. Acad. Sci. U. S. A* **101:** 5524-5529.

Dhahbi, J. M., Mote, P. L., Tillman, J. B., Walford, R. L., and Spindler, S. R. (1997). Dietary energy tissue-specifically regulates endoplasmic reticulum chaperone gene expression in the liver of mice. *J. Nutr.* **127:** 1758-1764.

Dillin, A., Hsu, A. L., Arantes-Oliveira, N., Lehrer-Graiwer, J., Hsin, H., Fraser, A. G., Kamath, R. S., Ahringer, J., and Kenyon, C. (2002). Rates of behavior and aging specified by mitochondrial function during development. *Science* **298:** 2398-2401.

Dominici, F. P., Hauck, S., Argentino, D. P., Bartke, A., and Turyn, D. (2002). Increased insulin sensitivity and upregulation of insulin receptor, insulin receptor substrate (IRS)-1 and IRS-2 in liver of Ames dwarf mice. *J Endocrinol* **173:** 81-94.

Dowell, P., Otto, T. C., Adi, S., and Lane, M. D. (2003). Convergence of Peroxisome Proliferator-activated Receptor {gamma} and Foxo1 Signaling Pathways. *J Biol Chem.* **278:** 45485-45491.

Dozmorov, I., Bartke, A., and Miller, R. A. (2001). Array-Based Expression Analysis of Mouse Liver Genes: Effect of Age and of the Longevity Mutant Prop1df. *J Gerontol A Biol Sci Med Sci* **56:** B72-B80.

Dozmorov, I., Galecki, A., Chang, Y., Krzesicki, R., Vergara, M., and Miller, R. A. (2002). Gene Expression Profile of Long-Lived Snell Dwarf Mice. *J Gerontol A Biol Sci Med Sci* **57:** B99-108.

107

Drew, B. and Leeuwenburgh, C. (2002). Aging and the role of reactive nitrogen species. *Ann. N. Y. Acad. Sci.* **959:** 66-81.

Engelking, L. J., Kuriyama, H., Hammer, R. E., Horton, J. D., Brown, M. S., Goldstein, J. L., and Liang, G. (2004). Overexpression of Insig-1 in the livers of transgenic mice inhibits SREBP processing and reduces insulin-stimulated lipogenesis. *J Clin. Invest* **113:** 1168-1175.

Esposito, L. A., Melov, S., Panov, A., Cottrell, B. A., and Wallace, D. C. (1999). Mitochondrial disease in mouse results in increased oxidative stress. *Proc. Natl. Acad. Sci. U. S. A* **96:** 4820-4825.

Fain, J. N. and Bahouth, S. W. (2000). Regulation of lipolysis and leptin biosynthesis in rodent adipose tissue by growth hormone. *Metabolism* **49:** 239-244.

Fewell, S. W., Travers, K. J., Weissman, J. S., and Brodsky, J. L. (2001). The action of molecular chaperones in the early secretory pathway. *Annu. Rev. Genet.* **35:** 149-191.

Finkel, T. and Holbrook, N. J. (2000). Oxidants, oxidative stress and the biology of ageing. *Nature* **408:** 239-247.

Flores-Morales, A., Stahlberg, N., Tollet-Egnell, P., Lundeberg, J., Malek, R. L., Quackenbush, J., Lee, N. H., and Norstedt, G. (2001). Microarray analysis of the in vivo effects of hypophysectomy and growth hormone treatment on gene expression in the rat. *Endocrinology* **142:** 3163-3176.

Flurkey, K., Papaconstantinou, J., Miller, R. A., and Harrison, D. E. (2001). Lifespan extension and delayed immune and collagen aging in mutant mice with defects in growth hormone production. *Proc. Natl. Acad. Sci U. S. A* **98:** 6736-6741.

Foufelle, F. and Ferre, P. (2002). New perspectives in the regulation of hepatic glycolytic and lipogenic genes by insulin and glucose: a role for the transcription factor sterol regulatory element binding protein-1c. *Biochem. J* **366:** 377-391.

Frick, F., Bohlooly, Y., Linden, D., Olsson, B., Tornell, J., Eden, S., and Oscarsson, J. (2001). Long-term growth hormone excess induces marked alterations in lipoprotein metabolism in mice. *Am J Physiol Endocrinol Metab* **281:** E1230.

Frick, F., Linden, D., Ameen, C., Eden, S., Mode, A., and Oscarsson, J. (2002). Interaction between growth hormone and insulin in the regulation of lipoprotein metabolism in the rat. *Am J Physiol Endocrinol Metab* **283:** E1023.

Friguet, B., Bulteau, A. L., Chondrogianni, N., Conconi, M., and Petropoulos, I. (2000). Protein degradation by the proteasome and its implications in aging. *Ann. N. Y. Acad. Sci.* **908:** 143-154.

Furuyama, T., Yamashita, H., Kitayama, K., Higami, Y., Shimokawa, I., and Mori, N. (2002). Effects of aging and caloric restriction on the gene expression of Foxo1, 3, and 4 (FKHR, FKHRL1, and AFX) in the rat skeletal muscles. *Microsc. Res. Tech.* **59:** 331-334.

Gardmo, C., Swerdlow, H., and Mode, A. (2002). Growth hormone regulation of rat liver gene expression assessed by SSH and microarray. *Mol. Cell Endocrinol* **190:** 125-133.

Gems, D. and McElwee, J. J. (2003). Ageing: Microarraying mortality. *Nature* **424:** 259-261.

Gems, D., Pletcher, S., and Partridge, L. (2002). Interpreting interactions between treatments that slow aging. *Aging Cell* **1:** 1-9.

Gething,M. (2004). Guidebook to Molecular Chaperones and Protein-Folding Catalysis. In Mammalian BiP, M.Gething and M.Sambrook, eds. (Oxford: Oxford University Press), pp. 59-65.

Golden, T. R., Hinerfeld, D. A., and Melov, S. (2002). Oxidative stress and aging: beyond correlation. *Aging Cell* **1:** 117-123.

Golden, T. R. and Melov, S. (2001). Mitochondrial DNA mutations, oxidative stress, and aging. *Mech. Ageing Dev.* **122:** 1577-1589.

109

Guarente, L. and Kenyon, C. (2000). Genetic pathways that regulate ageing in model organisms. *Nature* **408:** 255-262.

Hamilton, M. L., Van Remmen, H., Drake, J. A., Yang, H., Guo, Z. M., Kewitt, K., Walter, C. A., and Richardson, A. (2001). Does oxidative damage to DNA increase with age? *PNAS* **98:** 10469-10474.

Harman, D. (1956). Aging: a theory based on free radical and radiation chemistry. *J Gerontol.* **2:** 298-300.

Hasty, P., Campisi, J., Hoeijmakers, J., van Steeg, H., and Vijg, J. (2003). Aging and genome maintenance: lessons from the mouse? *Science* **299:** 1355-1359.

Hauck, S. J., Aaron, J. M., Wright, C., Kopchick, J. J., and Bartke, A. (2002). Antioxidant enzymes, free-radical damage, and response to paraquat in liver and kidney of long-living growth hormone receptor/binding protein gene-disrupted mice. *Horm. Metab Res.* **34:** 481-486.

Heffernan, M., Summers, R. J., Thorburn, A., Ogru, E., Gianello, R., Jiang, W. J., and Ng, F. M. (2001). The effects of human GH and its lipolytic fragment (AOD9604) on lipid metabolism following chronic treatment in obese mice and beta(3)-AR knock-out mice. *Endocrinology* **142:** 5182-5189.

Hekimi, S. and Guarente, L. (2003). Genetics and the specificity of the aging process. *Science* **299:** 1351-1354.

Higami, Y., Pugh, T. D., Page, G. P., Allison, D. B., Prolla, T. A., and Weindruch, R. (2004). Adipose tissue energy metabolism: altered gene expression profile of mice subjected to long-term caloric restriction. *FASEB J.* **18:** 415-417.

Hihi, A. K., Kebir, H., and Hekimi, S. (2003). Sensitivity of Caenorhabditis elegans clk-1 mutants to ubiquinone side-chain length reveals multiple ubiquinone-dependent processes. *J. Biol. Chem.* **278:** 41013-41018.

Holt, S. J. and Riddle, D. L. (2003). SAGE surveys C. elegans carbohydrate metabolism: evidence for an anaerobic shift in the long-lived dauer larva. *Mech. Ageing Dev.* **124:** 779-800.

Holzenberger, M., Dupont, J., Ducos, B., Leneuve, P., Geloen, A., Even, P. C., Cervera, P., and Le Bouc, Y. (2003). IGF-1 receptor regulates lifespan and resistance to oxidative stress in mice. *Nature* **421:** 182-187.

Horton, J. D., Goldstein, J. L., and Brown, M. S. (2002). SREBPs: activators of the complete program of cholesterol and fatty acid synthesis in the liver. *J Clin. Invest* **109:** 1125-1131.

Horton, J. D., Shah, N. A., Warrington, J. A., Anderson, N. N., Park, S. W., Brown, M. S., and Goldstein, J. L. (2003). Combined analysis of oligonucleotide microarray data from transgenic and knockout mice identifies direct SREBP target genes. *Proc. Natl. Acad. Sci U. S. A* **100:** 12027-12032.

Horton, J. D., Shimomura, I., Brown, M. S., Hammer, R. E., Goldstein, J. L., and Shimano, H. (1998). Activation of cholesterol synthesis in preference to fatty acid synthesis in liver and adipose tissue of transgenic mice overproducing sterol regulatory element-binding protein-2. *J Clin. Invest* **101:** 2331-2339.

Hsieh, C. C., Xiong, W., Xie, Q., Rabek, J. P., Scott, S. G., An, M. R., Reisner, P. D., Kuninger, D. T., and Papaconstantinou, J. (1998). Effects of age on the posttranscriptional regulation of CCAAT/enhancer binding protein alpha and CCAAT/enhancer binding protein beta isoform synthesis in control and LPS-treated livers. *Mol. Biol. Cell* **9:** 1479-1494.

Hwangbo, D. S., Gersham, B., Tu, M. P., Palmer, M., and Tatar, M. (2004). Drosophila dFOXO controls lifespan and regulates insulin signalling in brain and fat body. *Nature* **429:** 562-566.

Ip, E., Farrell, G. C., Robertson, G., Hall, P., Kirsch, R., and Leclercq, I. (2003). Central role of PPARalpha-dependent hepatic lipid turnover in dietary steatohepatitis in mice. *Hepatology* **38:** 123-132.

Jaenisch, R. and Bird, A. (2003). Epigenetic regulation of gene expression: how the genome integrates intrinsic and environmental signals. *Nat. Genet.* **33 Suppl:** 245-254.

Jazwinski, S. M. (2002). Growing old: metabolic control and yeast aging. *Annu. Rev. Microbiol.* **56:** 769-792.

Johnson, F. B., Sinclair, D. A., and Guarente, L. (1999). Molecular biology of aging. *Cell* **96:** 291-302.

Johnson, S. C. (1967). Hierarchical Clustering Schemes. *Psychometrika* **2:** 241-254.

Johnson, T. E., Cypser, J., de Castro, E., de Castro, S., Henderson, S., Murakami, S., Rikke, B., Tedesco, P., and Link, C. (2000). Gerontogenes mediate health and longevity in nematodes through increasing resistance to environmental toxins and stressors. *Exp. Gerontol.* **35:** 687-694.

Jonassen, T., Davis, D. E., Larsen, P. L., and Clarke, C. F. (2003). Reproductive fitness and quinone content of C. elegans clk-1 mutants fed coenzyme Q isoforms of varying length. *J Biol Chem.*

Jonassen, T., Larsen, P. L., and Clarke, C. F. (2001). A dietary source of coenzyme Q is essential for growth of long-lived Caenorhabditis elegans clk-1 mutants. *Proc. Natl. Acad. Sci U. S. A* **98:** 421-426.

Jonassen, T., Marbois, B. N., Faull, K. F., Clarke, C. F., and Larsen, P. L. (2002). Development and fertility in Caenorhabditis elegans clk-1 mutants depend upon transport of dietary coenzyme Q8 to mitochondria. *J Biol Chem.* **277:** 45020-45027.

Kayo, T., Allison, D. B., Weindruch, R., and Prolla, T. A. (2001). Influences of aging and caloric restriction on the transcriptional profile of skeletal muscle from rhesus monkeys. *Proc. Natl. Acad. Sci U. S. A* **98:** 5093-5098.

Kenyon, C. (2001). A conserved regulatory system for aging. *Cell* **105:** 165-168.

112

Kirkwood, T. B. (1977). Evolution of aging. *Nature* **270:** 301-304.

Kirkwood, T. B. (2000). Molecular gerontology. Bridging the simple and the complex. *Ann. N. Y. Acad. Sci.* **908:** 14-20.

Kirkwood, T. B. (2002). Molecular gerontology. *J Inherit. Metab Dis.* **25:** 189-196.

Kirkwood, T. B. and Austad, S. N. (2000). Why do we age? *Nature* **408:** 233-238.

Knauf, F., Rogina, B., Jiang, Z., Aronson, P. S., and Helfand, S. L. (2002). Functional characterization and immunolocalization of the transporter encoded by the life-extending gene Indy. *Proc. Natl. Acad. Sci U. S. A* **99:** 14315-14319.

Kopchick, J. J., Bellush, L. L., and Coschigano, K. T. (1999). Transgenic models of growth hormone action. *Annu. Rev. Nutr.* **19:** 437-461.

Kopito, R. R. (1997). ER quality control: the cytoplasmic connection. *Cell* **88:** 427-430.

Laffitte, B. A., Chao, L. C., Li, J., Walczak, R., Hummasti, S., Joseph, S. B., Castrillo, A., Wilpitz, D. C., Mangelsdorf, D. J., Collins, J. L., Saez, E., and Tontonoz, P. (2003). Activation of liver X receptor improves glucose tolerance through coordinate regulation of glucose metabolism in liver and adipose tissue. *PNAS* **100:** 5419-5424.

Lamberts, S. W., van den Beld, A. W., and van der Lely, A. J. (1997). The endocrinology of aging. *Science* **278:** 419-424.

Larsen, P. L. (1993). Aging and resistance to oxidative damage in Caenorhabditis elegans. *Proc. Natl. Acad. Sci. U. S. A* **90:** 8905-8909.

Larsen, P. L. (2001). Asking the age-old questions. *Nat. Genet.* **28:** 102-104.

Larsen, P. L., Albert, P. S., and Riddle, D. L. (1995). Genes that regulate both development and longevity in Caenorhabditis elegans. *Genetics* **139:** 1567-1583.

Larsen, P. L. and Clarke, C. F. (2002). Extension of life-span in Caenorhabditis elegans by a diet lacking coenzyme Q. *Science* **295:** 120-123.

Lee, C. H., Olson, P., and Evans, R. M. (2003a). Minireview: lipid metabolism, metabolic diseases, and peroxisome proliferator-activated receptors. *Endocrinology* **144:** 2201-2207.

Lee, C. K., Allison, D. B., Brand, J., Weindruch, R., and Prolla, T. A. (2002). Transcriptional profiles associated with aging and middle age-onset caloric restriction in mouse hearts. *Proc. Natl. Acad. Sci U. S. A* **99:** 14988-14993.

Lee, R. Y., Hench, J., and Ruvkun, G. (2001). Regulation of C. elegans DAF-16 and its human ortholog FKHRL1 by the daf-2 insulin-like signaling pathway. *Curr. Biol* **11:** 1950-1957.

Lee, S. S., Lee, R. Y., Fraser, A. G., Kamath, R. S., Ahringer, J., and Ruvkun, G. (2003b). A systematic RNAi screen identifies a critical role for mitochondria in C. elegans longevity. *Nat. Genet.* **33:** 40-48.

Levine, R. L. and Stadtman, E. R. (2001). Oxidative modification of proteins during aging. *Exp. Gerontol.* **36:** 1495-1502.

Levine, R. L., Wehr, N., Williams, J. A., Stadtman, E. R., and Shacter, E. (2000). Determination of carbonyl groups in oxidized proteins. *Methods Mol. Biol.* **99:** 15-24.

Liang, G., Yang, J., Horton, J. D., Hammer, R. E., Goldstein, J. L., and Brown, M. S. (2002). Diminished hepatic response to fasting/refeeding and liver X receptor agonists in mice with selective deficiency of sterol regulatory element-binding protein-1c. *J Biol Chem.* **277:** 9520-9528.

Liang, H., Masoro, E. J., Nelson, J. F., Strong, R., McMahan, C. A., and Richardson, A. (2003). Genetic mouse models of extended lifespan. *Exp. Gerontol.* **38:** 1353-1364.

Lin, J., Tarr, P. T., Yang, R., Rhee, J., Puigserver, P., Newgard, C. B., and Spiegelman, B. M. (2003). PGC-1beta in the regulation of hepatic glucose and energy metabolism. *J Biol Chem.*

Lin, S. S., Manchester, J. K., and Gordon, J. I. (2001). Enhanced gluconeogenesis and increased energy storage as hallmarks of aging in Saccharomyces cerevisiae. *J Biol Chem.* **276:** 36000-36007.

Liu, G., Loraine, A. E., Shigeta, R., Cline, M., Cheng, J., Valmeekam, V., Sun, S., Kulp, D., and Siani-Rose, M. A. (2003). NetAffx: Affymetrix probesets and annotations. *Nucleic Acids Res.* **31:** 82-86.

Longo, V. D. and Finch, C. E. (2003). Evolutionary Medicine: From Dwarf Model Systems to Healthy Centenarians? *Science* **299:** 1342-1346.

Lu, T. T., Repa, J. J., and Mangelsdorf, D. J. (2001). Orphan Nuclear Receptors as eLiXiRs and FiXeRs of Sterol Metabolism. *J. Biol. Chem.* **276:** 37735-37738.

Ludewig, A. H., Kober-Eisermann, C., Weitzel, C., Bethke, A., Neubert, K., Gerisch, B., Hutter, H., and Antebi, A. (2004). A novel nuclear receptor/coregulator complex controls C. elegans lipid metabolism, larval development, and aging. *Genes Dev.* **18:** 2120-2133.

Ma, Y., Brewer, J. W., Diehl, J. A., and Hendershot, L. M. (2002). Two distinct stress signaling pathways converge upon the CHOP promoter during the mammalian unfolded protein response. *J. Mol. Biol.* **318:** 1351-1365.

Ma, Y. and Hendershot, L. M. (2001). The unfolding tale of the unfolded protein response. *Cell* **107:** 827-830.

Ma, Y. and Hendershot, L. M. (2002). The mammalian endoplasmic reticulum as a sensor for cellular stress. *Cell Stress. Chaperones.* **7:** 222-229.

Mandavilli, B. S., Santos, J. H., and Van Houten, B. (2002). Mitochondrial DNA repair and aging. *Mutat. Res.* **509:** 127-151.

Martin, G. M. (2000). Some new directions for research on the biology of aging. *Ann. N. Y. Acad. Sci.* **908:** 1-13.

Martin, G. M., Austad, S. N., and Johnson, T. E. (1996). Genetic analysis of ageing: role of oxidative damage and environmental stresses. *Nat. Genet.* **13:** 25-34.

Matsuda, M., Korn, B. S., Hammer, R. E., Moon, Y. A., Komuro, R., Horton, J. D., Goldstein, J. L., Brown, M. S., and Shimomura, I. (2001). SREBP cleavage-activating protein (SCAP) is required for increased lipid synthesis in liver induced by cholesterol deprivation and insulin elevation. *Genes Dev.* **15:** 1206-1216.

Matsusue, K., Haluzik, M., Lambert, G., Yim, S. H., Gavrilova, O., Ward, J. M., Brewer, B., Jr., Reitman, M. L., and Gonzalez, F. J. (2003). Liver-specific disruption of PPARgamma in leptin-deficient mice improves fatty liver but aggravates diabetic phenotypes. *J Clin. Invest* **111:** 737-747.

Maxwell, K. N., Soccio, R. E., Duncan, E. M., Sehayek, E., and Breslow, J. L. (2003). Novel putative SREBP and LXR target genes identified by microarray analysis in liver of cholesterol-fed mice. *J Lipid Res.*

Melov, S. (2000). Mitochondrial oxidative stress. Physiologic consequences and potential for a role in aging. *Ann. N. Y. Acad. Sci.* **908:** 219-225.

Melov, S., Coskun, P., Patel, M., Tuinstra, R., Cottrell, B., Jun, A. S., Zastawny, T. H., Dizdaroglu, M., Goodman, S. I., Huang, T. T., Miziorko, H., Epstein, C. J., and Wallace, D. C. (1999). Mitochondrial disease in superoxide dismutase 2 mutant mice. *Proc. Natl. Acad. Sci. U. S. A* **96:** 846-851.

Merry, B. J. (2002). Molecular mechanisms linking calorie restriction and longevity. *Int. J Biochem. Cell Biol* **34:** 1340-1354.

Miller, R. A., Chang, Y., Galecki, A. T., Al Regaiey, K., Kopchick, J. J., and Bartke, A. (2002). Gene expression patterns in calorically restricted mice: partial overlap with long-lived mutant mice. *Mol. Endocrinol* **16:** 2657-2666.

116

Miyadera, H., Amino, H., Hiraishi, A., Taka, H., Murayama, K., Miyoshi, H., Sakamoto, K., Ishii, N., Hekimi, S., and Kita, K. (2001). Altered quinone biosynthesis in the long-lived clk-1 mutants of Caenorhabditis elegans. *J Biol Chem.* **276:** 7713-7716.

Mootha, V. K., Lindgren, C. M., Eriksson, K. F., Subramanian, A., Sihag, S., Lehar, J., Puigserver, P., Carlsson, E., Ridderstrale, M., Laurila, E., Houstis, N., Daly, M. J., Patterson, N., Mesirov, J. P., Golub, T. R., Tamayo, P., Spiegelman, B., Lander, E. S., Hirschhorn, J. N., Altshuler, D., and Groop, L. C. (2003). PGC-1alpha-responsive genes involved in oxidative phosphorylation are coordinately downregulated in human diabetes. *Nat. Genet.* **34:** 267-273.

Mouradian, M. M. (2002). Recent advances in the genetics and pathogenesis of Parkinson disease. *Neurology* **58:** 179-185.

Mueller, S., Weber, A., Fritz, R., Mutze, S., Rost, D., Walczak, H., Volkl, A., and Stremmel, W. (2002). Sensitive and real-time determination of H2O2 release from intact peroxisomes. *Biochem. J.* **363:** 483-491.

Murakami, S., Salmon, A., and Miller, R. A. (2003). Multiplex stress resistance in cells from long-lived dwarf mice. *FASEB J* **17:** 1565-1566.

Murakami, S., Tedesco, P. M., Cypser, J. R., and Johnson, T. E. (2000). Molecular genetic mechanisms of life span manipulation in Caenorhabditis elegans. *Ann. N. Y. Acad. Sci.* **908:** 40-49.

Murphy, C. T., McCarroll, S. A., Bargmann, C. I., Fraser, A., Kamath, R. S., Ahringer, J., Li, H., and Kenyon, C. (2003). Genes that act downstream of DAF-16 to influence the lifespan of Caenorhabditis elegans. *Nature* **424:** 277-283.

Nemoto, S. and Finkel, T. (2004). Ageing and the mystery at Arles. *Nature* **429:** 149-152.

Oberkofler, H., Esterbauer, H., Linnemayr, V., Strosberg, A. D., Krempler, F., and Patsch, W. (2002). Peroxisome Proliferator-activated Receptor (PPAR) gamma Coactivator-1 Recruitment Regulates PPAR Subtype Specificity. *J. Biol. Chem.* **277:** 16750.

117

Olsson, B., Bohlooly, Y., Brusehed, O., Isaksson, O. G., Ahren, B., Olofsson, S. O., Oscarsson, J., and Tornell, J. (2003). Bovine growth hormone-transgenic mice have major alterations in hepatic expression of metabolic genes. *Am J Physiol Endocrinol Metab* **285:** E504-E511.

Oscarsson, J., Ottosson, M., and Eden, S. (1999). Effects of growth hormone on lipoprotein lipase and hepatic lipase. *J Endocrinol Invest* **22:** 2-9.

Osiewacz, H. D. (2002). Mitochondrial functions and aging. *Gene* **286:** 65-71.

Parks, J. S., Brown, M. R., Hurley, D. L., Phelps, C. J., and Wajnrajch, M. P. (1999). Heritable disorders of pituitary development. *J Clin. Endocrinol Metab* **84:** 4362-4370.

Parodi, A. J. (2000). Protein glucosylation and its role in protein folding. *Annu. Rev. Biochem.* **69:** 69-93.

Partridge, L. and Gems, D. (2002a). Mechanisms of ageing: public or private? *Nat. Rev. Genet.* **3:** 165-175.

Partridge, L. and Gems, D. (2002b). The evolution of longevity. *Curr. Biol.* **12:** R544-R546.

Pedersen, W. A., Wan, R., and Mattson, M. P. (2001). Impact of aging on stress-responsive neuroendocrine systems. *Mech. Ageing Dev.* **122:** 963-983.

Pfaffl, M. W. (2001). A new mathematical model for relative quantification in real-time RT-PCR. *Nucleic Acids Res.* **29:** e45.

Pfaffl, M. W., Horgan, G. W., and Dempfle, L. (2002). Relative expression software tool (REST) for group-wise comparison and statistical analysis of relative expression results in real-time PCR. *Nucleic Acids Res.* **30:** e36.

Picard, F. and Auwerx, J. (2002). PPARgamma and Glucose Homeostasis. *Annu. Rev. Nutr.* **22:** 167-197.

118

Pletcher, S. D., Macdonald, S. J., Marguerie, R., Certa, U., Stearns, S. C., Goldstein, D. B., and Partridge, L. (2002). Genome-wide transcript profiles in aging and calorically restricted Drosophila melanogaster. *Curr. Biol* **12:** 712-723.

Preiss-Landl, K., Zimmermann, R., Hammerle, G., and Zechner, R. (2002). Lipoprotein lipase: the regulation of tissue specific expression and its role in lipid and energy metabolism. *Curr. Opin. Lipidol.* **13:** 471-481.

Prolla, T. A. (2002). DNA microarray analysis of the aging brain. *Chem. Senses* **27:** 299-306.

Rajapakse, N., Shimizu, K., Payne, M., and Busija, D. (2001). Isolation and characterization of intact mitochondria from neonatal rat brain. *Brain Res. Brain Res. Protoc.* **8:** 176-183.

Rakhit, R., Cunningham, P., Furtos-Matei, A., Dahan, S., Qi, X. F., Crow, J. P., Cashman, N. R., Kondejewski, L. H., and Chakrabartty, A. (2002). Oxidation-induced misfolding and aggregation of superoxide dismutase and its implications for amyotrophic lateral sclerosis. *J. Biol. Chem.* **277:** 47551-47556.

Rea, S. and Johnson, T. E. (2003). A metabolic model for life span determination in Caenorhabditis elegans. *Dev. Cell* **5:** 197-203.

Rhee, J., Inoue, Y., Yoon, J. C., Puigserver, P., Fan, M., Gonzalez, F. J., and Spiegelman, B. M. (2003). Regulation of hepatic fasting response by PPARgamma coactivator-1alpha (PGC-1): requirement for hepatocyte nuclear factor 4alpha in gluconeogenesis. *Proc. Natl. Acad. Sci U. S. A* **100:** 4012-4017.

Richardson, A., Liu, F., Adamo, M. L., Remmen, H. V., and Nelson, J. F. (2004). The role of insulin and insulin-like growth factor-I in mammalian ageing. *Best. Pract. Res. Clin. Endocrinol. Metab* **18:** 393-406.

Rogina, B., Helfand, S. L., and Frankel, S. (2002). Longevity regulation by Drosophila Rpd3 deacetylase and caloric restriction. *Science* **298:** 1745.

Roth, G. S., Lane, M. A., Ingram, D. K., Mattison, J. A., Elahi, D., Tobin, J. D., Muller, D., and Metter, E. J. (2002). Biomarkers of caloric restriction may predict longevity in humans. *Science* **297:** 811.

Russell-Jones, D. L., Watts, G. F., Weissberger, A., Naoumova, R., Myers, J., Thompson, G. R., and Sonksen, P. H. (1994). The effect of growth hormone replacement on serum lipids, lipoproteins, apolipoproteins and cholesterol precursors in adult growth hormone deficient patients. *Clin. Endocrinol (Oxf)* **41:** 345-350.

Seo, J., Bakay, M., Chen, Y. W., Hilmer, S., Shneiderman, B., and Hoffman, E. P. (2004). Optimizing signal/noise ratios in expression profiling: project-specific algorithm selection and detection p value weighting in affymetrix microarrays. *Bioinformatics.*

Shimomura, I., Bashmakov, Y., Ikemoto, S., Horton, J. D., Brown, M. S., and Goldstein, J. L. (1999). Insulin selectively increases SREBP-1c mRNA in the livers of rats with streptozotocin-induced diabetes. *Proc. Natl. Acad. Sci U. S. A* **96:** 13656-13661.

Shin, D. J. and Osborne, T. F. (2003). Thyroid Hormone Regulation and Cholesterol Metabolism Are Connected through Sterol Regulatory Element-binding Protein-2 (SREBP-2). *J Biol Chem.* **278:** 34114-34118.

Shostak, Y., Van Gilst, M. R., Antebi, A., and Yamamoto, K. R. (2004). Identification of C. elegans DAF-12-binding sites, response elements, and target genes. *Genes Dev.* **18:** 2529-2544.

Snow, M. I. and Larsen, P. L. (2000). Structure and expression of daf-12: a nuclear hormone receptor with three isoforms that are involved in development and aging in Caenorhabditis elegans. *Biochim. Biophys. Acta* **1494:** 104-116.

Sohal, R. S. (2002). Role of oxidative stress and protein oxidation in the aging process. *Free Radic. Biol. Med.* **33:** 37-44.

Sohal, R. S., Mockett, R. J., and Orr, W. C. (2002). Mechanisms of aging: an appraisal of the oxidative stress hypothesis. *Free Radic. Biol. Med.* **33:** 575-586.

Sreekumar, R., Unnikrishnan, J., Fu, A., Nygren, J., Short, K. R., Schimke, J., Barazzoni, R., and Nair, K. S. (2002). Effects of caloric restriction on mitochondrial function and gene transcripts in rat muscle. *AJP - Endocrinology and Metabolism* **283:** E38-E43.

Stadtman, E. R. (1992). Protein oxidation and aging. *Science* **257:** 1220-1224.

Stadtman, E. R. (2001). Protein oxidation in aging and age-related diseases. *Ann. N. Y. Acad. Sci.* **928:** 22-38.

Stadtman, E. R. and Levine, R. L. (2000). Protein oxidation. *Ann. N. Y. Acad. Sci.* **899:** 191-208.

Staels, B., van Tol, A., Chan, L., Will, H., Verhoeven, G., and Auwerx, J. (1990). Alterations in thyroid status modulate apolipoprotein, hepatic triglyceride lipase, and low density lipoprotein receptor in rats. *Endocrinology* **127:** 1144-1152.

Stenmark, P., Grunler, J., Mattsson, J., Sindelar, P. J., Nordlund, P., and Berthold, D. A. (2001). A new member of the family of di-iron carboxylate proteins. Coq7 (clk-1), a membrane-bound hydroxylase involved in ubiquinone biosynthesis. *J Biol Chem.* **276:** 33297-33300.

Tatar, M. and Rand, D. M. (2002). Aging. Dietary advice on Q. *Science* **295:** 54-55.

Tatar, M., Bartke, A., and Antebi, A. (2003). The Endocrine Regulation of Aging by Insulin-like Signals. *Science* **299:** 1346-1351.

Tien, M., Berlett, B. S., Levine, R. L., Chock, P. B., and Stadtman, E. R. (1999). Peroxynitrite-mediated modification of proteins at physiological carbon dioxide concentration: pH dependence of carbonyl formation, tyrosine nitration, and methionine oxidation. *Proc. Natl. Acad. Sci. U. S. A* **96:** 7809-7814.

Tobin, K. A., Ulven, S. M., Schuster, G. U., Steineger, H. H., Andresen, S. M., Gustafsson, J. A., and Nebb, H. I. (2002). Liver X receptors as insulin-mediating factors in fatty acid and cholesterol biosynthesis. *J Biol Chem.* **277:** 10691-10697.

Tollet-Egnell, P., Flores-Morales, A., Stahlberg, N., Malek, R. L., Lee, N., and Norstedt, G. (2001). Gene expression profile of the aging process in rat liver: normalizing effects of growth hormone replacement. *Mol. Endocrinol* **15:** 308-318.

Tollet-Egnell, P., Parini, P., Stahlberg, N., Lonnstedt, I., Lee, N., Rudling, M., Flores-Morales, A., and Norstedt, G. (2003). Growth hormone mediated alteration of fuel metabolism in the aged rat as determined from transcript profiles. *Physiol Genomics*.

Tu, B. P., Ho-Schleyer, S. C., Travers, K. J., and Weissman, J. S. (2000). Biochemical basis of oxidative protein folding in the endoplasmic reticulum. *Science* **290:** 1571-1574.

Tu, B. P. and Weissman, J. S. (2002). The FAD- and O(2)-dependent reaction cycle of Ero1-mediated oxidative protein folding in the endoplasmic reticulum. *Mol. Cell* **10:** 983-994.

Tusher, V. G., Tibshirani, R., and Chu, G. (2001). Significance analysis of microarrays applied to the ionizing radiation response. *PNAS* **98:** 5116-5121.

Van Voorhies, W. A. (2002a). Metabolism and aging in the nematode Caenorhabditis elegans. *Free Radic. Biol Med* **33:** 587-596.

Van Voorhies, W. A. (2002b). The influence of metabolic rate on longevity in the nematode Caenorhabditis elegans. *Aging Cell* **1:** 91-101.

Vandesompele, J., De Preter, K., Pattyn, F., Poppe, B., Van Roy, N., De Paepe, A., and Speleman, F. (2002). Accurate normalization of real-time quantitative RT-PCR data by geometric averaging of multiple internal control genes. *Genome Biol.* **3:** RESEARCH0034.

Viguerie, N. and Langin, D. (2003). Effect of thyroid hormone on gene expression. *Curr. Opin. Clin. Nutr. Metab Care* **6:** 377-381.

Weindruch, R., Kayo, T., Lee, C. K., and Prolla, T. A. (2001). Microarray profiling of gene expression in aging and its alteration by caloric restriction in mice. *J Nutr.* **131:** 918S-923S.

Williams, G. C. (1957). Pleitropy, natural selection and the evolution of senescence. *Evolution* **11:** 398-411.

Yamauchi, T., Waki, H., Kamon, J., Murakami, K., Motojima, K., Komeda, K., Miki, H., Kubota, N., Terauchi, Y., Tsuchida, A., Tsuboyama-Kasaoka, N., Yamauchi, N., Ide, T., Hori, W., Kato, S., Fukayama, M., Akanuma, Y., Ezaki, O., Itai, A., Nagai, R., Kimura, S., Tobe, K., Kagechika, H., Shudo, K., and Kadowaki, T. (2001). Inhibition of RXR and PPARgamma ameliorates diet-induced obesity and type 2 diabetes. *J Clin. Invest* **108:** 1001-1013.

Yan, L. J., Levine, R. L., and Sohal, R. S. (1997). Oxidative damage during aging targets mitochondrial aconitase. *Proc. Natl. Acad. Sci. U. S. A* **94:** 11168-11172.

Yan, L. J. and Sohal, R. S. (1998). Mitochondrial adenine nucleotide translocase is modified oxidatively during aging. *Proc. Natl. Acad. Sci. U. S. A* **95:** 12896-12901.

Yoshikawa, T., Ide, T., Shimano, H., Yahagi, N., Amemiya-Kudo, M., Matsuzaka, T., Yatoh, S., Kitamine, T., Okazaki, H., Tamura, Y., Sekiya, M., Takahashi, A., Hasty, A. H., Sato, R., Sone, H., Osuga, J., Ishibashi, S., and Yamada, N. (2003). Cross-talk between peroxisome proliferator-activated receptor (PPAR) alpha and liver X receptor (LXR) in nutritional regulation of fatty acid metabolism. I. PPARs suppress sterol regulatory element binding protein-1c promoter through inhibition of LXR signaling. *Mol. Endocrinol* **17:** 1240-1254.

Zhang, Y., Yin, L., and Hillgartner, F. B. (2003). SREBP-1 integrates the actions of thyroid hormone, insulin, cAMP, and medium-chain fatty acids on ACC{alpha} transcription in hepatocytes. *J. Lipid Res.* **44:** 356-368.

VITA

William H. Boylston, III was born on September 19, 1964 in Baltimore, Maryland to Barbara Fruge Boylston and Dr. William H. Boylston. Moving to Houston, Texas, William graduated cum laude from St. John's School in 1983. In 1985, he was selected for the DeBakey Summer Surgery Internship Program sponsored by the Baylor College of Medicine in Houston where he assisted in cardiovascular surgeries, was trained in autologous blood transfusion techniques, and collected data for a retrospective clinical study of post-operative diaphragmatic paralysis associated with coronary artery bypass surgery. He received a Bachelor of Arts in 1987, with a major in German Language and Literature and a minor in Chemistry from the University of Virginia.

Following graduation from U.Va., William worked for several years as a Legal Assistant in both the Tax and Corporate Litigation Departments at Vinson & Elkins law firm in Houston. He was subsequently employed in Portland, Oregon as a Cell Saver Technician, serving five major metropolitan hospitals in autologous blood and platelet salvage for trauma and vascular surgeries. Returning to Texas to pursue a career in biomedical research, William entered the University of Texas at San Antonio where he graduated summa cum laude in Neurobiology, receiving a Bachelor of Science in 1996. Thereafter, he continued his laboratory training in biochemistry and molecular biology as a Research Associate under Dr. James P. Chambers. Working on the rapid detection of bio-warfare agents, William developed a phage-displayed peptide recognition system to distinguish virulent B. anthracis from non-pathogenic strains of spore-forming bacteria. While in the laboratory, William also gained substantial teaching experience by supervising and training undergraduate and graduate students rotating or employed in the lab.

In 1998, William entered the Graduate School of Biomedical Science at UTMB in the Department of Human Biological Chemistry and Genetics, and was later married to Tina M. Havel. In 2001, William was awarded the HBC&G Graduate Student Award, and was also awarded the Sealy Center on Aging Graduate Student Award in both 2002 and 2003. His graduate work was supported by a Pre-doctoral Fellowship provided by the Claude D. Pepper Center at UTMB funded by the NIA. In the spring of 2004, William was awarded an NIA/NIH Training Grant by the Barshop Center for Aging and Longevity Studies to provide funding for his post-doctoral training with Dr. Pamela Larsen at the University of Texas Health Science Center San Antonio.

Permanent Address:

101 West Rosewood Avenue
San Antonio, Texas, 78212.

Education

B.S., *summa cum laude*, 1996, Biology, The University of Texas, San Antonio, Texas.

B.A., 1987, German (Chemistry), The University of Virginia, Charlottesville, Virginia.

Diploma, *cum laude*, 1983, St. John's School, Houston, Texas.

Published

Boylston, W.H.; Gerstner, A.; DeFord, J.H.; Madsen, M.; Flurkey, K.; Harrison, D.E.; and Papaconstantinou, J. 2004. Altered cholesterologenic and lipogenic transcriptional profile in livers of aging Snell dwarf ($Pit1^{dw/dwJ}$) mice. *Aging Cell.* **3**(5):283-296.

Madsen, M.A., Hsieh, C-C., Flurkey, K., Harrison, D.E., **Boylston, W.H.**, and Papconstantinou, J. 2004. Altered Oxidative Stress Response of the Long-lived Snell Dwarf Mouse. *Biochemical and Biophysical Research Communications*. **318** (3): 998-1005.

Choksi, K.B., **Boylston, W.H.,** Rabek, J. P. Widger, W.R. and Papaconstantinou, J. 2004. Oxidatively damaged proteins of heart mitochondrial electron transport complexes. *Biochimica et Biophysica Acta - Molecular Basis of Disease*. 1688(2): 95-101.

Rabek, J.P., **Boylston, W.H.**, and Papaconstantinou, J. 2003. Carbonylation of Endoplasmic Reticulum Chaperone Proteins in Aged Mouse Liver. *Biochemical and Biophysical Research Communications*. **305** (2): 998-1005.

Chambers, J.P. and **Boylston, W.H.** 1997. Taqman Technology: PCR Coupled with Fluorogenic Oligonucleotide Probes Provides a Sensitive and Rapid Detection System for Microbial Pathogens. US Army Research Office, ERDEC SCBRD-RTE. Final Research Report for Contract No. DAAD05-96-P-2940.

Chambers, J.P. and **Boylston, W.H.** 1996. Design of Species Specific Polymerase Chain Reaction Primers and Probes for the Rapid Detection of *Bacillus subtilis* var niger, *Bacillus cereus*, *Bacillus anthracis*, and *Bacillus thuringiensis.* Final Research Report for Contract No. DAAL03-91-C-0034.